

STUDY ON THE USE OF CELLULAR COFFERDAM FOR PERMANENT
HYDROPOWER USE

By

Soheyl Khademian

A thesis submitted to the Faculty and the Board of Trustees of the Colorado School of Mines in partial fulfillment of the requirements for the degree of Master of Science (Civil and Environmental Engineering)

Golden, Colorado

Date -----

Signed: _____

Soheyl Khademian

Signed: _____

Dr. Marte Gutierrez

Thesis Advisor

Golden, Colorado

Date -----

Signed: _____

Dr. Terri Hogue

Department Head of Civil
and Environmental Engineering

ABSTRACT

Cellular cofferdams are temporary constructions consisting of interlocking steel-sheet piling driven as a series of interconnecting cells. Cellular cofferdams have been employed mainly as provisional “water exclusion devices” for water diversion projects to permit dry construction of dams, locks, bridge footings and piers, hydroelectric power plants, and other in-water structures. This dissertation presents the results of a comprehensive study on the potential use of cellular cofferdams as basis for the design and construction of water retaining structures to sustainably and cost-effectively harness hydropower. Cellular cofferdams have been very rarely utilized as the main permanent structure for hydropower dams. Consequently, design and construction requirements for cellular cofferdams are less stringent than for hydropower dams. To make cellular cofferdams suitable for permanent hydropower use, one design concept that utilizes cellular cofferdams as the main or core element of the water-retaining dam structure is proposed. One particular key design concept is the so-called “dry construction technique” in which the granular fill in cofferdam cells and the downstream berm are permanently kept dry in contrast to the wet construction technique for temporary use of cellular cofferdams. The viability of the proposed permanent cellular cofferdam design concept for the construction and operation is demonstrated using well-established structural and geotechnical design procedures and computational modeling. Environmental and economic impacts of the proposed cellular cofferdam-based design are studied in comparison to traditional hydropower dam constructions. The improved performance of the proposed design concept, particularly in combination with the dry construction technique, shows cellular cofferdams have the potential to be used as basis for the construction of permanent hydropower dam structures that are versatile, with less impact on the environment, and will cost less to build than conventional hydropower dams.

TABLE OF CONTENTS

ABSTRACT.....	iii
LIST OF FIGURES.....	viii
LIST OF TABLES.....	xi
ACKNOWLEDGEMENT.....	xii
CHAPTER 1 GENERAL INTRODUCTION.....	1
1.1 Introduction.....	1
1.2 Background.....	2
1.3 Objectives of the Study.....	4
1.4 Thesis Organization	5
CHAPTER 2 DESIGN PROCEDURES FOR THE INSTALATION OF CELLULAR COFFERDAMS FOR PERMANENT HYDROPOWER USE.....	7
2.1 Proposed Design Concepts for Cellular Cofferdam.....	7
2.2 Wet and Dry Construction.....	9
2.3 Geotechnical and Structural Parameters.....	10
2.4 Loads on Cellular Cofferdam during Construction.....	13
2.4.1 Cell Geometry.....	13
2.4.2 Interlock Stiffness and Types.....	15
2.4.3 Cell Fill Densification and Lateral Loading.....	17
2.4.4 Foundation Stiffness.....	18
2.4.5 Cell Tensions.....	19
2.4.5.1 Main Cell Tensions.....	21
2.4.5.2 Arc Cell Tensions.....	22
2.4.5.3 Sheet Pile Tension through a Wye Pile.....	22
2.4.5.4 Common Wall Tensions	23
2.4.6 Lateral Eart Pressure Coefficient.....	23

2.4.7	Point of Maximum Sheet Pile Tension.	25
2.4.8	Depth of Pile Fixity.....	26
2.4.8.1	Matlock and Rees (1959) Method.....	26
2.4.8.2	Schroeder and Maitland (1979) Method.	26
2.4.8.3	TVA (1957) Method.	27
2.4.9	Depth of Embedment.	27
2.4.10	Interlock Tensions.....	27
2.4.11	Factor of Safety against Tensile Failure.	28
2.4.12	Earth Pressure Diagrams.....	29
2.4.13	Comparisons of Design Procedures with Computer Modeling Results.....	31
CHAPTER 3 DESIGN PROCEDURES FOR THE OPERATION OF CELLULAR COFFERDAMS FOR PERMANENT HYDROPOWER USE.....		
3.1	Geotechnical Hazards.	33
3.1.1	Sliding	33
3.1.2	Overtopping.....	38
3.1.3	Bearing Capacity Failure.	40
3.1.4	Slope Stability Failure.....	42
3.1.5	Seepage.	45
3.1.5.1	Seepage through the Cell Fill.....	46
3.1.5.2	Seepage through the Foundation.....	47
3.2	Geological Hazards.....	49
3.2.1	Overtopping and Emergency Spillway References.	49
3.2.1.1	Design of More Stable Cofferdam against Overtopping Failure. ...	53
3.2.1.2	Design of Emergency Spillway.	55
3.2.2	Earthquake Hazards.	56
3.3	Structural Hazards.....	58

3.3.1	Structural Design of Piles.	59
CHAPTER 4	ENVIRONMENTAL AND ECONOMIC IMPACTS OF PERMANENT CELLULAR COFFERDAMS FOR HYDROPOWER USE.	65
4.1	Reduction of Environmental and Economic Impacts.	65
4.1.1	In-water Construction.	66
4.1.2	Fast and Low-Cost Construction.	68
4.1.3	Easy to Reconfigure, Modify and Dismantle.....	69
4.1.4	Recycling of Construction Materials.	70
4.1.5	Reducing Footprint.	70
4.2	General Benefits of Cofferdams.	71
4.2.1	Less Impacts on Climate Change.....	71
4.2.2	Decreasing River Fragmentation.	72
4.2.3	Recreation.	72
4.2.4	Flood Control and Destruction.....	73
4.2.5	Water Storage.....	73
4.2.6	Sediment and Erosion Control.....	74
4.3	Hydropower Cellular Cofferdam Construction Procedure.	75
4.3.1	Pre-Dredging.....	76
4.3.2	Cell Template.....	76
4.3.3	Sheet Pile Driving.	77
4.3.4	Concrete Seal.	78
4.3.5	Cell Filling and Berm.....	79
4.3.6	Hydropower Generation.....	80
4.4	Construction Cost Analysis.	81
CHAPTER 5	GENERAL CONCLUSION.	85
5.1	Research Originality.	85

5.2	Summary of Accomplishments.....	85
	REFERENCES.	89
	APPENDIX A BASIC EQUATIONS USED IN THE MANUAL STABILITY CALCULATION OF CELLULAR COFFERDAM.....	94
	APPENDIX B MANUAL STABILITY CALCULATIONS BASED ON BOWLES, J.E. (1996).....	97

LIST OF FIGURES

Figure 1.1	In-water construction of a cellular cofferdam (photo from C.J. Mahan Construction Co).....	1
Figure 1.2	Willow Island Hydroelectric Project Cofferdam (Ciammaichella and Tantalla 2014).	3
Figure 2.1	Design concepts #1 and #2 for Kentucky cofferdam.....	7
Figure 2.2	Design concepts #3 and #4 for Kentucky cofferdam.....	8
Figure 2.3	Loading conditions for “wet construction”.....	9
Figure 2.4	Proposed “dry construction” modification for more permanent use of cellular cofferdam by the use of waterproof liner elements (e.g., asphalt) and a concrete cap.	10
Figure 2.5	Construction of Kentucky cellular cofferdam.....	11
Figure 2.6	Geometry of Kentucky cofferdam and its FLAC grids.	11
Figure 2.7	Equivalent 2D dimensions of cellular cofferdams.....	14
Figure 2.8	Sheet piling and connections used in cellular cofferdam construction (Bowles, 1996).	15
Figure 2.9	Interlock behavior (Wissman et., 2003).....	17
Figure 2.10	Influence of foundation stiffness on location of maximum sheet pile tension (Wissmann et al., 2003).	19
Figure 2.11	Typical cofferdam layout.....	20
Figure 2.12	Wye and Tee connections used in circular cofferdams (Bowles, 1996).....	21
Figure 2.13	Coefficient of lateral earth pressure at location of maximum sheet pile tension (Wissmann et al., 1995).	25
Figure 2.14	Hoop or interlock tensions according to TVA reproduced from USACE (1989).	28
Figure 2.15	Earth pressure diagram for piling seated on rock, no overburden or berm during cellular cofferdam installation.....	29
Figure 2.16	Earth pressure diagram for piling not seated on rock.	30
Figure 2.17	Earth pressure diagram for piling fully restrained by external passive and hydrostatic forces.	30

Figure 2.18	Earth pressure distribution along the walls of the Kentucky Cellular Cofferdam.	31
Figure 2.19	Magnified deformed mesh for Kentucky Cofferdam after placement of cellular fill.	32
Figure 3.1	Sliding stability of cellular cofferdams based on the TVA and Terzaghi Procedures.	35
Figure 3.2	Weights and horizontal forces acting on the cellular cofferdam.	36
Figure 3.3	“Manual” calculations of factor of safety against sliding $FS_{sliding}$	37
Figure 3.4	“Computational” calculations of factor of safety against sliding $FS_{sliding}$ (e.g. by averaging values of “state” along failure surfaces).	37
Figure 3.5	Overturning stability of cellular cofferdams based on the TVA and Terzaghi procedures.	38
Figure 3.6	Weights and forces acting on the cofferdam for overturning stability calculation.	39
Figure 3.7	Bearing capacity failure.	41
Figure 3.8	Slope stability diagram based on Improved Ordinary Method of Slices for design Concept #1.	42
Figure 3.9	Stability results for design concept #1 using the (a) asphaltic and (b) concrete liners.	43
Figure 3.10	Friction angles of gravelly soils based on different theories.	44
Figure 3.11	Factor of safety graphs against slope failure for design concept #1.	45
Figure 3.12	Typical pore pressure contours for the (a) wet and (b) dry construction practices used in the stability analysis of the proposed design concept in FLAC.	46
Figure 3.13	Typical pore pressure contours of the design concept #1 (wet).	47
Figure 3.14	Partial flow net beneath a cell on sand base on USACE (1989).	48
Figure 3.15	Illustration of overtopping and piping phenomena.	50
Figure 3.16	Increase in sheet pile deflection and subsequent decrease in FS of the cellular cofferdam in Lock and Dam No. 26 (Martin and Clough, 1990; Mosher, 1992).	51
Figure 3.17	Plot of (a) maximum cell deflection and (b) FS against overtopping loads for design concept #1.	52
Figure 3.18	Geometry of new design of cellular cofferdam.	54

Figure 3.19	Geometry of emergency spillway for cellular cofferdams.	56
Figure 3.20	Geometry and parameters of modified M-O method.....	57
Figure 3.21	Bending moment (in ft-lbs) diagrams along the length of both the upstream and downstream steel sheet piles during construction of the Kentucky cofferdam.	59
Figure 3.22	Bending moment (in ft-lbs) diagrams along the length of both the upstream and downstream steel piles due to water pressure from the reservoir.	60
Figure 3.23	Comparison of bending moments of the design concept #1 for a. “wet” and b. “dry” constructions.	61
Figure 3.24	Earth pressure diagrams acting on sheet piles of design concept #1 during operation in the “wet construction”.	63
Figure 3.25	Bending moment diagrams of design concept #1 during operation for “wet construction”.	63
Figure 4.1	Distribution of dams in the U.S.	65
Figure 4.2	The Hydropower Itaipu Dam located on border between Brazil and Paraguay. ...	66
Figure 4.3	Olmsted Locks and Dam project at Ohio River, Illinois, U.S.	67
Figure 4.4	A cofferdam on the Ohio River near Olmsted, Illinois, U.S.....	68
Figure 4.5	Dam Removal on the Elwha River in the Olympic Peninsula, Washington. U.S. ...	69
Figure 4.6	Hoover Dam in Utah, U.S.	71
Figure 4.7	Recreational facilities of dams.....	73
Figure 4.8	Aswan Dam, Egypt.	74
Figure 4.9	Austin Dam failure in Texas, 1911.....	75
Figure 4.10	Plan views of cofferdam structures formed with circular cells (Top), and diaphragm cells (Bottom).	76
Figure 4.11	Installation of wale and strut system and driving the sheet piles (Nemati, 2005). ...	77
Figure 4.12	Kentucky River Lock and Dam (Gilbert, 2011).	79
Figure 4.13	Components of Hydroelectric Power Plant (Irena, 2012).....	80
Figure A.1	Type of cofferdam failures for stability analysis (Bowles, 1996).	94
Figure A.2	Cell pressure profiles for stability analysis against cell shear (Bowles, 1996).....	95

LIST OF TABLES

Table 2.1	Properties of the cellular overburden, fill and berm sand used in the analysis and computational modeling for Kentucky cofferdam.	12
Table 2.2	Properties of the steel sheet pile walls.	13
Table 2.3	Dimensions for 2D equivalent geometry for Kentucky cellular cofferdam.	15
Table 2.4	Properties of cells and steel sheet piles for proposed design concept #1 of Kentucky cofferdam.....	16
Table 2.5	Increase in unloaded side sheet pile tensions during lateral loading in two cases of cellular cofferdam construction (Wissmann et al., 2003).....	18
Table 2.6	Different methods of estimating common wall tensions.	23
Table 2.7	Lateral earth pressure coefficients for calculating maximum earth pressure and cell hoop tension.	24
Table 2.8	Methods for estimating point of the location of the maximum sheet pile tensions from the mudline.....	25
Table 2.9	Recommended depth of pile embedment for cellular cofferdams.	27
Table 3.1	Summary of values of factor of safety against sliding for Kentucky cellular cofferdam.	37
Table 3.2	Summary of comparisson of values of factor of safety against sliding.	38
Table 3.3	Summary of values of factor of safety against slide for Kentucky cellular cofferdam.	40
Table 3.4	Numerical and Analytical results of $FS_{slope\ stability}$ for design concept #1 in “dry construction.”	44
Table 3.5	Various water level increments ΔH_w and their corresponding discharge loading q	54
Table 4.1	Per unit cost analysis of different hydropower dams.....	82
Table 4.2	Detailed approximation construction costs of different hydropower dams with same height and width.	83

ACKNOWLEDGEMENT

I would like to express my sincere gratitude to my advisor Dr. Marte Gutierrez for his continuous support of my Master, his patience, and his immense knowledge while treating me as his friend. I gratefully acknowledge the Department of Energy (DOE), Office of Energy Efficiency and Renewable Energy (EERE), for funding this research project. I would like to thank my committee members Dr. Reza Hedayat, and Dr. Shiling Pei who provided me with constructive comments from different perspectives.

To Esmat for her prayers

To Mohammad Mahdi for his support

To Zahedeh, Zoheir, and Ehsan for their help

CHAPTER 1

GENERAL INTRODUCTION

1.1 Introduction

Cellular cofferdams have been widely used as temporary water exclusion devices to permit dry construction of in-water structures such as dams, locks, bridge footings and piers, and hydroelectric power plants. Cellular cofferdams have been employed in a wide range of applications, geological and hydrological conditions, and with heights of up to 100 ft (30 m) and individual cell diameters of up 90 ft (27 m). They can be configured to any shapes by combinations of multiple cells. Steel sheet piling is one of the widely used method to construct cellular water retaining structures that are typically filled with granular fill (Figure 1.1). Steel sheet piling can be categorized into three shapes: circular, diaphragm, and cloverleaf. A circular shape (Figure 1.1) is commonly used for designing the cofferdam for the following main reasons: 1) it is stable as a single structure, 2) it can be filled as soon as it is constructed, and 3) it does not need various units of differential soil heights. Diaphragm cell might result in a failure of the entire cofferdam, but the collapse of a circular cell takes place locally. The circular cell is easier to form using templates as well as usually requiring less sheet piling (Bowles, 1996).



Figure 1.1. In-water construction of a cellular cofferdam (photo from C.J. Mahan Construction Co).

Cellular cofferdams have been very rarely utilized as the main permanent structure for hydropower dams. Consequently, design and construction requirements for cellular cofferdams are less stringent than for hydropower dams. In addition, there are risks and challenges associated with using cellular cofferdams as hydroelectric dams, particularly with respect to failure during flood events. The main hazard involves the potential that a flood exceeds the design flow and results in overtopping and failure of the dam. Other long-term design issues are failure of the foundation (i.e., sliding, overturning or bearing capacity), excessive seepage under the dam or through the cellular cofferdam fill, scouring of the foundation, corrosion of sheet piles, and structural failure of the sheet piles, supports and connections. For dams in seismically active areas, earthquake loads have to be considered. Historical record shows that a few cellular cofferdams have failed as temporary structures. The consequences of failure will be more severe if cellular cofferdams are used as permanent hydropower dams. To make cellular cofferdams suitable for permanent hydropower use, proposed design concepts that utilize cellular cofferdam as the main or core element of the water-retaining dam structure are proposed in this study. With their versatility in terms of speed of construction, low cost, ease of removal, and applicability to a wide range of conditions, cellular cofferdams have the potential to be adapted and used as the main component for the construction of future innovative hydropower dams.

1.2 Background

The circular-type cell with connecting cells was first implemented for the first steel pile cellular cofferdam built by TVA at Pickwick Dam in 1935. Then this type was used for the majority of the subsequent cofferdam constructions in the Tennessee River (Pile Buck, 1990). From the year 2001 to 2006, a newer temporary cellular cofferdam was built to provide for the future construction of a new 1,200 lock adjacent to the existing lock (Mahan, 2007). The following are notable examples of successful uses of cellular cofferdams:

- The St. Germans diaphragm cofferdam, with each cell measuring 20 ft (6 m) in height and 33 ft (10 m) by 50 ft (15 m) in area, and with the steel sheet piles embedded 40 ft (12 m) into the ground, is the second largest pumping station in the Europe (Iqbal 2009; Sheppard 2010).
- The Lock and Dam No. 26 located near Alton, Illinois in the Upper Mississippi was demolished in 1990 and replaced by the Melvin Price Locks and Dam. Part of the new lock

was built using cellular cofferdam (Mosher 1992). Each cell is 30x30 ft² (9x9 m²) in area, with a piling depth of 50 ft (15 m) and free height of 40 ft (9 m).

- The temporary cellular cofferdam at the Willow Island Hydroelectric Project (Figure 1.2) which required a 100 ft (30 m) excavation (Ciammaichella and Tantalla 2014).
- The Kentucky Dam Lock Addition Project consisted of construction of a temporary cellular cofferdam to provide for the future construction of a new 1,200 ft (365 m) lock adjacent to the existing lock (Weinmann et al. 2015). The work included construction of three 69 ft (21 m) diameter circular sheet pile cells, with three connecting arc cells and a sheet pile tie-in wall. Each cell required tremie concrete base plug, the largest of which required approximately 3,000 cubic yards (2,300 cu m) of concrete.
- The cofferdam for Belleville Hydroelectric Plant in West Virginia was designed to resist a 50 year flood or 65 ft (20 m) head while maintaining minimum navigation pools upstream and downstream during power plant construction (Meier et al. 2010).



Figure 1.2. Willow Island Hydroelectric Project Cofferdam (Ciammaichella and Tantalla 2014).

The most challenging applications of cellular cofferdams for hydropower use are when the dam has to be constructed and positioned in a narrow and steep section of the river, and when the foundation is hard rock. In both situations, it can be difficult to drive steel sheet piles into the ground. However, a recently completed project - the addition of a new powerhouse at the Tulloch Hydroelectric site on the Stanislaus River in the western foothills of the Sierras Nevada Mountains of central California - has shown that cellular cofferdam can be used to provide water exclusion structure even for very difficult environments. In this example, the cofferdam was constructed on a steeply fractured rock surface with a slope greater than 50° to isolate the powerhouse construction site excavation from the Goodwin Reservoir and the discharge from the existing powerhouse. (Bittner and Kirk 2014).

1.3 Objectives of the Study

The dissertation proposes the use of cellular cofferdams as the main component for the rapid, cost-effective and environmentally sustainable construction of water retaining structures for hydropower use. Specifically this study will:

- Present new design concepts of cellular cofferdams for permanent hydropower use and discuss main design issues of proposed design concepts for both wet and dry construction.
- Explain the main factors that control installation of design concepts for permanent cellular cofferdam and validate manual/analytical design procedures for interlock cell tensions against those obtained from computational modeling.
- Develop existing manual/analytical design procedures for the operation of cellular cofferdams and validate structural, geological and geotechnical calculations using results of computational model.
- Discuss the advantages and disadvantages of permanent hydropower cellular cofferdams in terms of environmental and economic impacts and analyze the construction cost of proposed design concepts to compare them with hydropower concrete dams and hydropower earth dams.

1.4 Thesis Organization

Conventional design methods for sheet-pile cellular cofferdams are based on empirical methods and limited field and experimental observations. Analytical techniques based on classical earth pressure theories and limit state design, which are used to analyze and design cellular cofferdams, are unable to account for several complex behaviors. Limitations include inability to account for nonlinear soil stress-strain behavior, soil-structure interaction, interface behavior between sheet pile and soil, three-dimensional geometry and loading conditions, interaction between seepage and soil deformation and effects of sequential loading. These limitations are overcome by numerical modeling using finite element or finite difference codes. The commercial code FLAC (Fast Lagrangian Analysis of Continua) version 8.0 developed by Itasca (2016), as a two-dimensional explicit finite difference program, which was initially built for geotechnical and seepage simulations (Coetzee et al., 1998), is employed in this study.

Chapter 2 presents different design concepts of cellular cofferdam based on Kentucky Cofferdam. It also proposes the design concept #1 of cellular cofferdam for the so called “dry” and “wet” construction. The main innovative component of the proposed design concept #1 is the envisioned advance in cellular cofferdam design towards more permanent and reliable application for hydropower generation while maintaining many of the beneficial features. This chapter presents the main factors that control installation and construction of cellular cofferdam. There are several design issues during construction and implementation of cellular cofferdams. Quantification of interlock and cell tensions is among the main issues that are tackled in this chapter by studying various design approaches and elaborating on their differences. The design methods are based on those proposed by Tennessee Valley Authority (1957), Terzaghi (1945), Schroeder and Maitland (1979), Swatek (1967), Matlock and Rees (1969), Wissmann et al. (2003), Cummings (1957), and Hansen (1953). The calculation procedures for interlock cell tension from the different design methods are compared with those computed by numerical modeling.

The main objective of chapter 3 is to present design procedures for the operation of cellular cofferdams for permanent hydropower use. Specifically, chapter 3 reviews the main design issues during operation of cellular cofferdams and develops existing manual/analytical design procedures for the operation of cellular cofferdams for permanent hydropower use. To demonstrate the

technical performance and feasibility of proposed design concept #1 during operation for permanent cofferdam, and the validity of the design procedures, numerical and analytical modeling are performed. Finite element and finite difference models using the FLAC (Fast Lagrangian Analysis of Continua) software, developed by Itasca (2016) are employed to simulate the structural response of proposed concept for cellular-cofferdam-based hydropower dams under realistic field conditions. The modeling simulates the response of the cellular cofferdam during operation, after the cellular wall is filled with fill material followed by loading hydrostatic loading from the reservoir. Representative properties for the foundation and berm soil or rock, cellular fill, and structural steel are used in the modeling. The analytical analyses are used to obtain detailed and accurate insights on the behavior and performance of the design schemes. To validate the FLAC simulation, the case of Kentucky cofferdam model is modeled and analyzed to demonstrate the capability of FLAC to model the cellular cofferdam stability and deformation. On the other hand, manual calculations of factor of safety of design issues during operation for proposed design concept #1 are developed for both “dry” and “wet” construction. These analytical and numerical calculations for structural, geological, and geotechnical analysis and design of permanent cellular cofferdams are used to identify potential failure modes and instability response of the dam.

Chapter 4 proposes the advantages and disadvantages of permanent cellular cofferdams for hydropower use in terms of environmental impact. Existing environmental concerns are studied for use in hydropower cellular cofferdams. Steps to mitigate any additional negative environmental impacts of hydropower cellular cofferdam constructions are proposed. The major generic sources of direct and indirect impacts of any hydropower project are expected and assumed to be the same, however, their relative importance will be site- and project-specific. Chapter 4 also lists and studies in detail the potential economic gains/losses from the use of cellular cofferdams in comparison to traditional methods for hydropower dam constructions. Steps of hydropower cellular cofferdam construction are proposed in order to estimate accurate construction costs. Moreover, existing economic analysis is modified for use in the hydropower cellular cofferdams. However, as mentioned in Changnon (2005), Schlenker et al. (2005), and Young (2005), efforts to quantify the economic impacts in water resources are hampered by the fact that the estimates are highly sensitive to different estimation methods and to different assumptions regarding how changes in water availability will be allocated across various types of water uses, e.g., between agricultural, urban, or in-stream uses. Finally, chapter 5 provides a comprehensive conclusion from this study.

CHAPTER 2

DESIGN PROCEDURES FOR THE INSTALATION OF CELLULAR COFFERDAMS FOR PERMANENT HYDROPOWER USE

2.1 Proposed Design Concepts for Cellular Cofferddam

Example extensions of cellular cofferdam that are studied in this dissertation are shown in Figures 2.1 and 2.2. The construction of the proposed design concept #1 is that of a granular material filled cellular cofferdam with concrete cap to prevent overtopping from the upstream water (Figure 2.1a). In design concept #2, the cofferdam cell is filled with dry concrete fill without capping the cell (Figure 2.1b). In the concrete-filled cellular cofferdam, dewatering of the cells can be avoided if the concrete is tremie-poured into the water-filled cell causing water to be displaced while simultaneously allowing the concrete to set (Yao et al. 1999). The main cells, which are evenly spaced, are constructed first followed by the arc cells in order to create a stable linear structure across the river channel. Berms maybe added downstream to increase the stability of the dam and reduce scouring. In design concept #2, the concrete filled cellular cofferdam is difficult to dismantle. However, the concrete filled cells provide a water-tight barrier. The main advantages of design concept #1 and #2 are that they are the simplest to build.

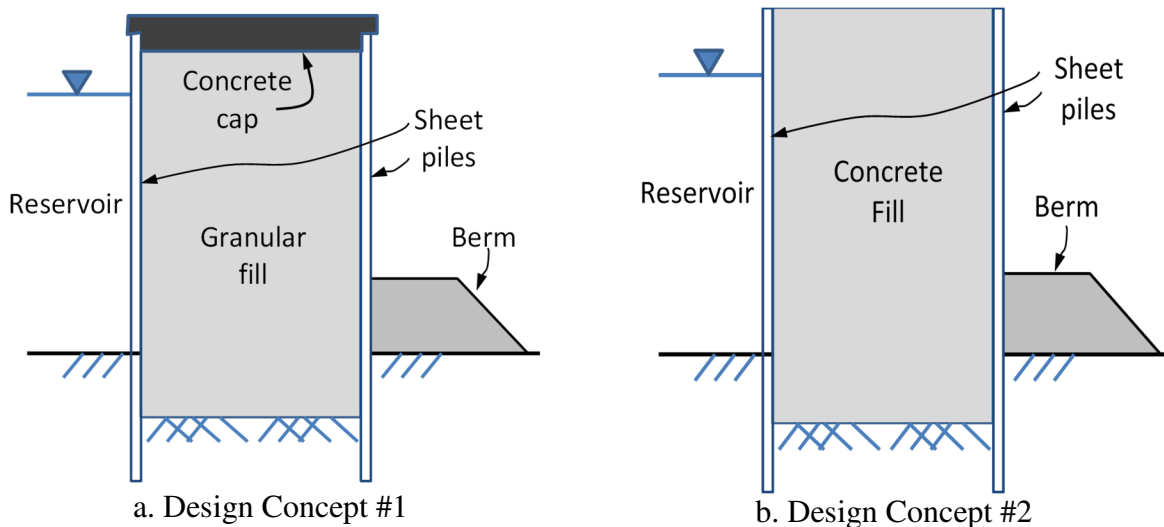


Figure 2.1. Design concepts #1 and #2 for Kentucky cofferdam.

In design concept #3, the cofferdam cell is filled with dry granular fill and overtopped with downstream concrete embankment (Figure 2.2a). Increased dam stability particularly due to overtopping can be also achieved by adding rock fill downstream of the cellular cofferdam as shown in Figure 2.2b. In addition to increasing stability, the downstream embankment reduces seepage through the dam and foundation. Of the two designs in Figure 2.2, the one which uses concrete or RCC (roller-compacted concrete) downstream embankment is more difficult to dismantle. The full dam can be constructed using cellular cofferdam with concrete or granular fill as the core structure. In contrast to traditional dam construction, the cellular cofferdam becomes the main core of the dam, and the additional embankment is built on top of it.

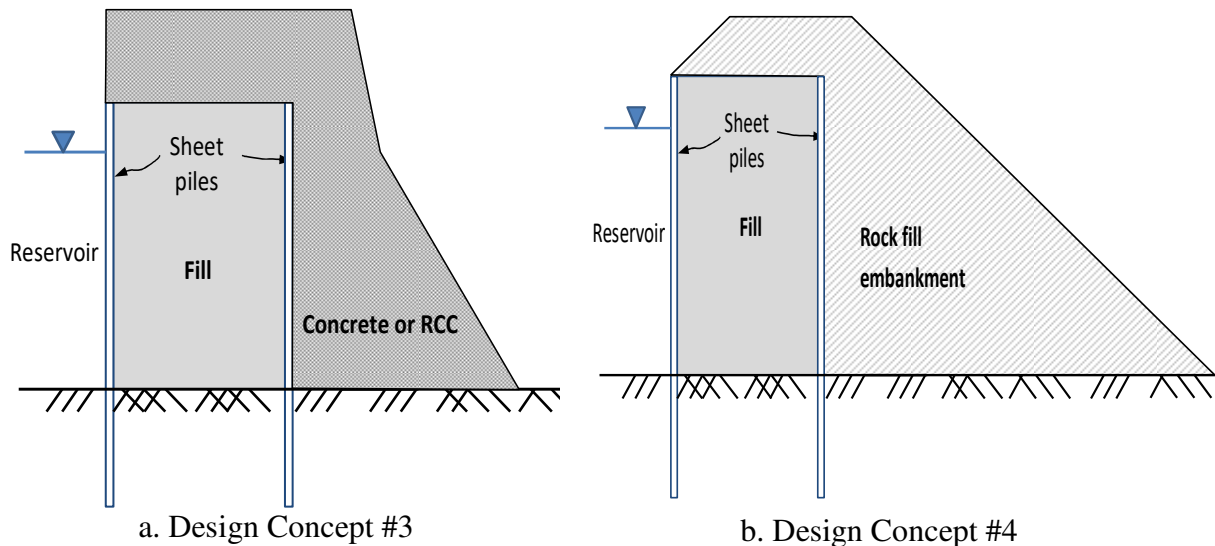


Figure 2.2. Design concepts #3 and #4 for Kentucky cofferdam.

The proposed design concepts for the cellular cofferdam can be built in water providing temporary water retaining structures for the construction of the downstream embankment. Numerical and analytical calculations that are studied in this dissertation are based on design concept #1. The main reason for choosing design concept #1 is that others can be simply achieved by modifying design concept #1 and changing the filling material and the size of downstream embankment. Therefore, the analysis of design concepts #2, #3 and #4 can be used in the case that structural and/or geotechnical failure for design concept #1 is possible.

In the design, the full dam can be constructed using cellular cofferdam with granular fill as the core structure and can be removed in water by dismantling the core cellular cofferdam last. This approach maintains the capability to rapidly and easily construct the dam in-water with less impact to the environment, and the adaptability to local conditions while maintaining low construction cost, ease of dismantling after its intended use.

2.2 Wet and Dry Construction

One of the drawbacks of cellular cofferdams for temporary use is that, due to the use of granular soil as cellular fill, seepage is allowed to happen across the dam. Such seepage occurs along the joints and connections of the sheet piles that form the cellular cofferdams. This type of construction is referred to as “wet construction” in this study as shown in Figure 2.3.

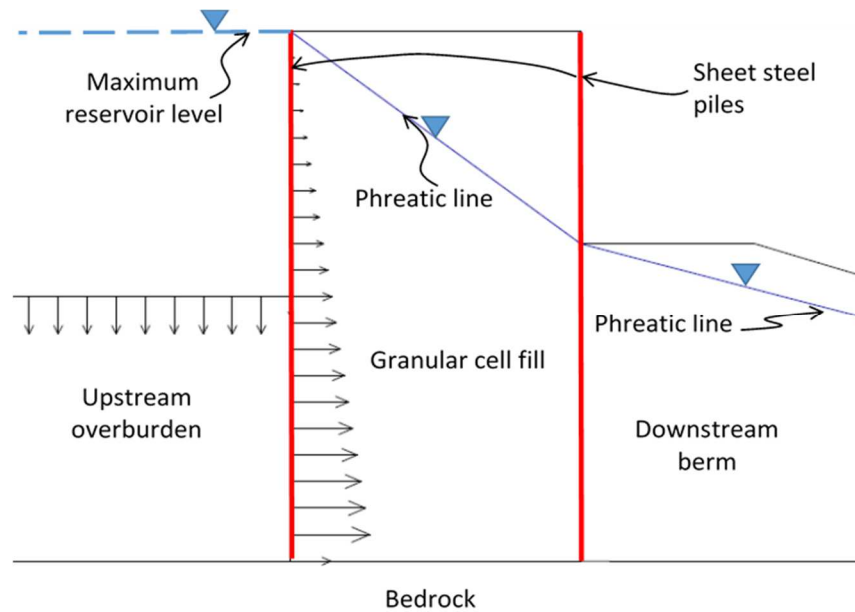


Figure 1.3. Loading conditions for “wet construction.”

There are several potential risks to long term and more permanent use of “wet construction” of cellular cofferdams. In general seepage, while normal for temporary water retaining structures, can be detrimental for permanent dam constructions. Seepage can lower the stability and safety of dams through increased buoyancy of the granular fill, and cause seepage-induced piping downstream of the dam. Though this seepage is allowed for temporary use of cellular cofferdam due to cost savings and shorter construction times, the “wet construction” may not be suited for the use of cellular cofferdam for more permanent and more long-term use.

A concept that is proposed in this study is the so-called “dry construction” of cellular cofferdam with granular fill. This can be achieved by adding a waterproof seal inside the cell and bellow the cellular fill material (Figure 2.4). One potential seal material is asphalt that is easy to install, and very flexible resulting in low potential for cracking when loaded and bent. Asphaltic core is already widely used as barrier against seepage for earth embankment dams. Another potential seal material is concrete that is highly impermeable. The advantage of “dry construction” in terms of increased stability and safety is demonstrated in this study using the original and unmodified design configuration, and material properties used in the Kentucky cofferdam construction.

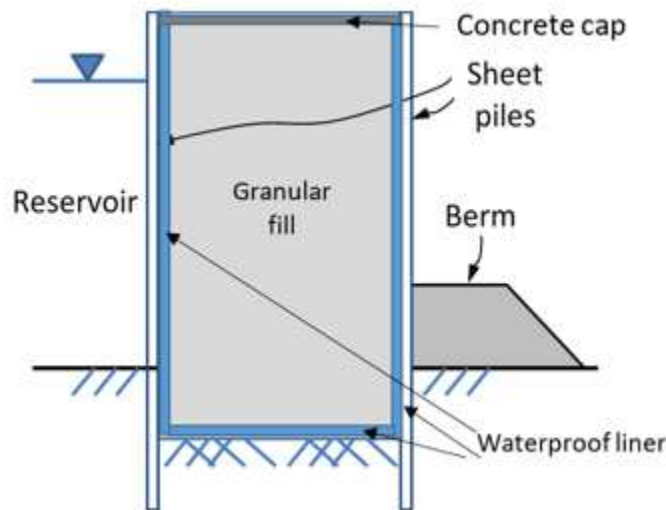


Figure 2.4. Proposed “dry construction” modification for more permanent use of cellular cofferdam by the use of waterproof liner elements (e.g., asphalt) and a concrete cap.

2.3 Geotechnical and Structural Parameters

To demonstrate the technical performance and feasibility of the proposed design concept #1, and the validity of the design procedures, numerical modeling is performed. The FLAC (Fast Lagrangian Analysis of Continua) developed by Itasca (2014), which has the ability to create complex meshes and built-in stress calculation and simulate staged construction, is used in the modeling. Kentucky Cellular Cofferdam (Figure 2.5) is used in the study to provide realistic conditions and parameters using data and information from a cofferdam that has already been designed and built. By showing the validity of the methodologies used in the study to an actual case, it can be argued that the methodology can be applied to other conditions and situations in the field. It is noted that the Kentucky cofferdam shown in Figure 2.5 was designed and built based

on the most common types of cellular cofferdam that are used of temporary structure. As said before, this type of design consists of cells of steel sheet piles driven into the foundation then filled in by granular soil.



Figure 2.5. Construction of Kentucky cellular cofferdam.

The geometry and FLAC grid of the cofferdam that are used in the numerical modeling is shown in Figure 2.6. In this study, the imperial unit is used to ease constructing the model from its original design that appeared in the literature (Pile Buck, 1990).

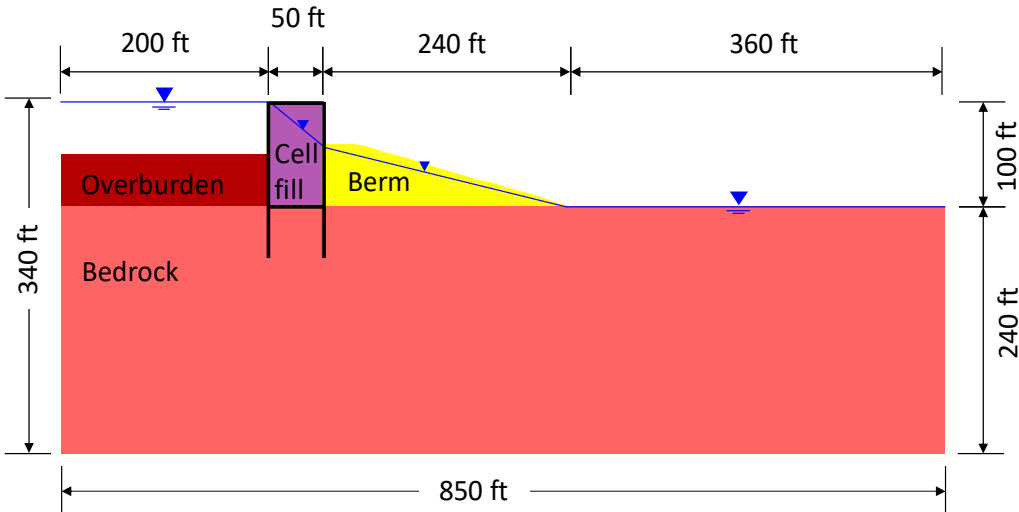


Figure 2.6. Geometry of Kentucky cofferdam and its FLAC grids.

The main material used in the construction of the Kentucky cellular cofferdam is sand. The bedrock is not included in the modeling as it is assumed to be impermeable and much stiffer and stronger than the sand. The properties for the sand (overburden, cellular fill and berm) are given in Table 2.1. The sand is modeled as an elastoplastic non-associated Mohr-Coulomb material with linear elastic Young's modulus E , Poisson's ratio, friction and dilation angles and zero cohesive strength. The parameters are obtained from Duncan et al. (1987), and Virginia Department of Transportation (2013) based on the typical values from the description of the soil types.

Table 2.1. Properties of the cellular overburden, fill and berm sand used in the analysis and computational modeling for Kentucky cofferdam.

Parameter	Soil type				Unit
	Overburden	Bedrock	Fill/berm	Concrete	
Dry unit weight, γ_d	110	170	139	139	lb/ft ³
Young's modulus, E	$5.8 \cdot 10^4$	$7.3 \cdot 10^6$	$4.4 \cdot 10^4$	$2.0 \cdot 10^6$	psi
Poisson's ratio, ν	0.30	0.30	0.27	0.20	-
Cohesion, c	0	$1.5 \cdot 10^3$	0	$4.6 \cdot 10^2$	psi
Friction angle, ϕ	30	45	30	55	...°
Porosity, n	0.3	0.3	0.3	0.3	-
Permeability, k	$9.3 \cdot 10^{-5}$	$9.3 \cdot 10^{-7}$	$9.3 \cdot 10^{-5}$	$3.3 \cdot 10^{-12}$	ft/s

The friction angle of 30° in Table 2.1 is lower than the 34° expected from the specifications of the degree of compaction of the cellular fill material as reported in Pile Buck (1990) and Marold (2012). However, there were no indications if the required degree of compaction was actually achieved, and thus, friction angle of 30° appears to be reasonable if not conservative. As mentioned, above the bedrock is not included in the modeling. The beam elements representing the steel sheet piles are given in Table 2.2.

Table 2.2. Properties of the steel sheet pile walls.

	Imperial Units	SI Units
Density	490 pcf	8050 kg/m ³
Young's modulus	4.32 · 10 ⁹ psf	207 GPa
Poisson's ratio	0.2	

2.4 Loads on Cellular Cofferdam during Construction

In this section, the influence of cell geometry, interlock stiffness, foundation stiffness, cell fill densification, sheet pile penetration depth, and interlock tensions on the sheet pile tensions are reviewed and discussed. After studying all of these parameters, earth pressure diagrams of proposed design concept #1 for Kentucky cellular cofferdam are studied analytically and numerically (based on FLAC computer modeling).

2.4.1 Cell Geometry

Figure 2.7 shows the equivalent 2D dimensions of cellular cofferdam. From Figure 2.7, the total area of the soil fill A_{soil} in all cells that are connected to each other can be calculated as:

$$A_{soil} = N\pi r_i^2. \quad (2.1)$$

where r_i = inner radius of each cell = area of soil fill and N = number of cells. The total length of the wall L is calculated as:

$$L = 2Nr_i. \quad (1.2)$$

The equivalent area of rectangular wall $A_{rectangle}$ made up of several cells is calculated as:

$$A_{rectangle} = B \cdot L = N\pi r_i^2. \quad (2.3)$$

$$B = \frac{N\pi r_i^2}{2Nr_i} = \frac{\pi}{2} r_i = \frac{\pi}{4} D = 0.785D \quad (2.4)$$

where B equivalent width of a rectangular wall. As can be seen, the equivalent width of $B = 0.785D$ is only slightly smaller than maximum the $B = 0.818D$ from Bowles (1996).

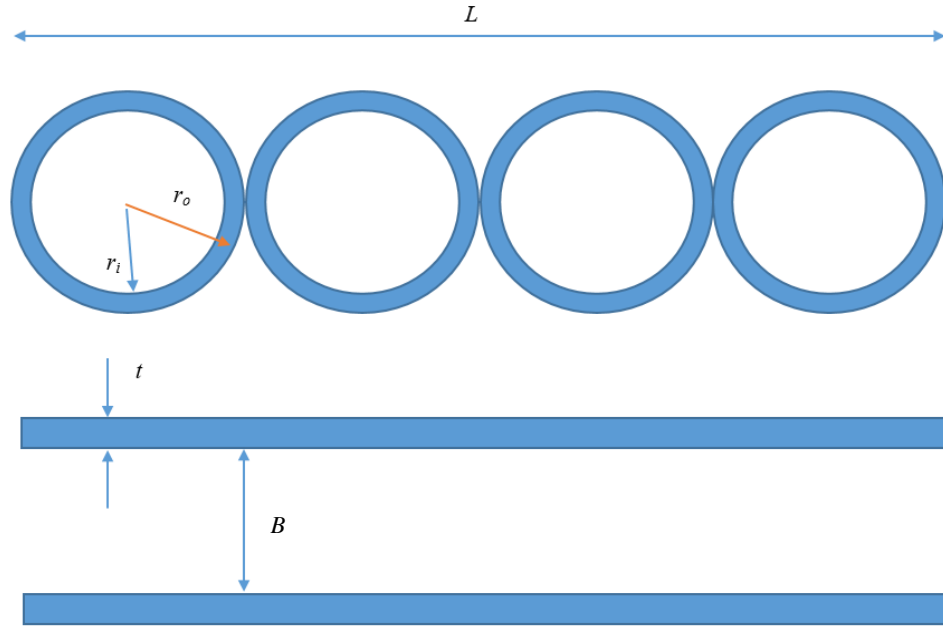


Figure 2.7. Equivalent 2D dimensions of cellular cofferdams.

Equivalent 2D dimensions of cellular cofferdams defines the area of the cofferdam. In addition to the equivalent width of the 2D model, it is necessary to find an equivalent 2D thickness of the steel sheet piles from the actual circular cells. This can be obtained from the moment of inertia of all steel cells, which is calculated as:

$$I_{cell} = N \frac{\pi}{4} (r_o^4 - r_i^4) \quad (2.2)$$

Then with the equations (2.1) to (2.5), the thickness of equivalent rectangular 2D wall can be derived, which are shown in the below calculations (approximating the width of the dam is measured from the center to the mid-thickness of the steel pile).

$$2 \left(\frac{B}{2} \right)^2 L \cdot t = I_{cell} \quad (2.3)$$

$$t = \frac{2I_{cell}}{B^2 L} \quad (2.4)$$

Using the above calculations yields the dimensions that are utilized in the equivalent 2D modeling of the Kentucky cellular cofferdam listed in Table 2.3.

Table 2.3. Dimensions for 2D equivalent geometry for Kentucky cellular cofferdam.

Parameter	Value		Description
r_i	58.83 ft	17.94 m	Inner diameter of each cell
r_o	58.89 ft	17.95 m	Outer diameter of each cell
A_{soil}	78,820.88 ft ²	24,030.76 m ²	Total area of soil fill
N	29		Number of cells
L	1,705.98 ft	520.12 m	Length of wall
B	46.20 ft	14.09 m	Equivalent width of 2D wall
T	0.26 ft	0.08 m	Thickness of 2D wall
I_{cell}	40,356.93 ft ⁴	348.68 m ⁴	Moment of inertia of a steel cell

2.4.2 Interlock Stiffness and Types

In general, there are two types of interlock web sections used for cellular cofferdams: 1) straight piles interlock, and 2) Z-piles interlock. Of the two sections, Z piles interlock develops larger moments and very high bending stresses from cell-bursting forces. Also, tension forces would produce large pile distortions in Z-piles (Bowles, 1996). Because of the issues that Z piles have, straight pile interlocks are more stable and commonly used than Z piles for permanent cofferdam structures. In Figure 2.8, a typical circular cell using straight web sections is shown with three different kinds of interlocks which are used for circular cofferdams based on the thumb-and-finger joint.

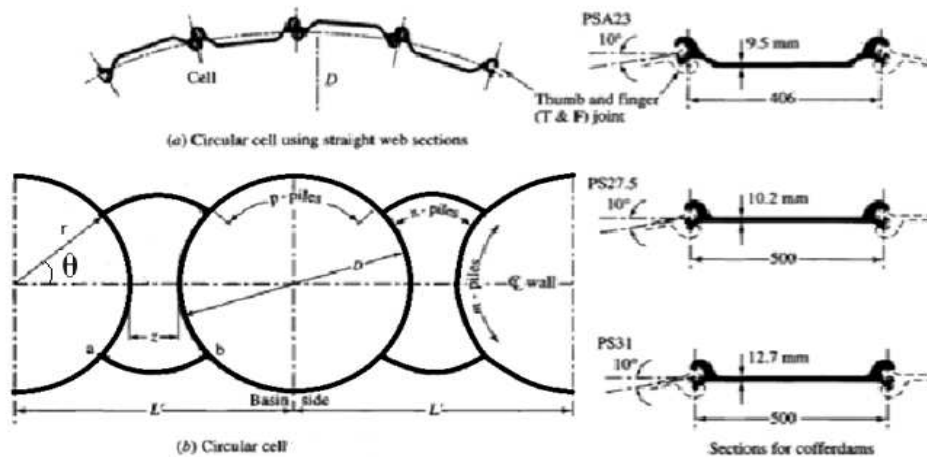


Figure 2.8. Sheet piling and connections used in cellular cofferdam construction (Bowles, 1996).

According to Bowles (1996), sheet piling interlocks allow a maximum of about 10-degree deviation between two interlocking piles. Therefore, the following minimum cell radius r is required to prevent interlock failure:

$$r_{\min} = \frac{\text{Driving Distance}}{2 \sin 10^\circ} \quad (2.8)$$

where “driving distance” is the width of the interlock, which can be obtained from handbooks of standard steel sections. For example, for interlocking PS31 steel pile sections, the driving distance is 500 mm as shown in Figure 2.8. Equation (2.8) ensures the cell radius is large enough and ensure proper connectivity between sections. Knowing the cell radius and interlock length gives the number piles needed to form a circular cell using straight web sections using the following equation:

$$N_s = \frac{2\pi r}{\text{Driving Distance}} \quad (2.9)$$

where N_s is the number of piles for each cell. Based on the equations (2.8) and (2.9), the dimensions in Table 2.4 for the case of the Kentucky Cellular Cofferdam can be obtained as an example.

Table 2.4. Properties of cells and steel sheet piles for proposed design concept #1 of Kentucky cofferdam.

Parameter	Value		Description
r_{\min}	4.72 ft	1.44 m	Minimum cell radius
N_s	226		Number of piles

Interlock stiffness, which affects cellular pile deformation and, in turn, loads has two major types: low stiffness and high stiffness. A low interlock stiffness is useful for removal of slack in connection between piles, while a high stiffness leg permits only elastic response of interlocks. Slack results in gap between two interlocks when they install on the field. When the gap between interlocks is large enough, interlocks can deflect easily and is called loose interlocks. If interlock slacks increase, sheet piles deflect radially outward more and lateral earth pressure will decrease, so sheet pile tensions will decrease. For high stiffness leg, the slack between interlocks is often

small and is called “tight interlocks” which produce lower deflection and higher sheet pile tensions. Figure 2.9 demonstrates the differences in loose and tight interlock load-displacement responses, which are approximately bilinear in the load range of interest. The results shown are based on laboratory pull-out tests collected by Wissmann et al. (2003). As can be seen, a wide range of sheet pile tension is obtained which vary by about 25 kN/cm for the same interlock displacements.

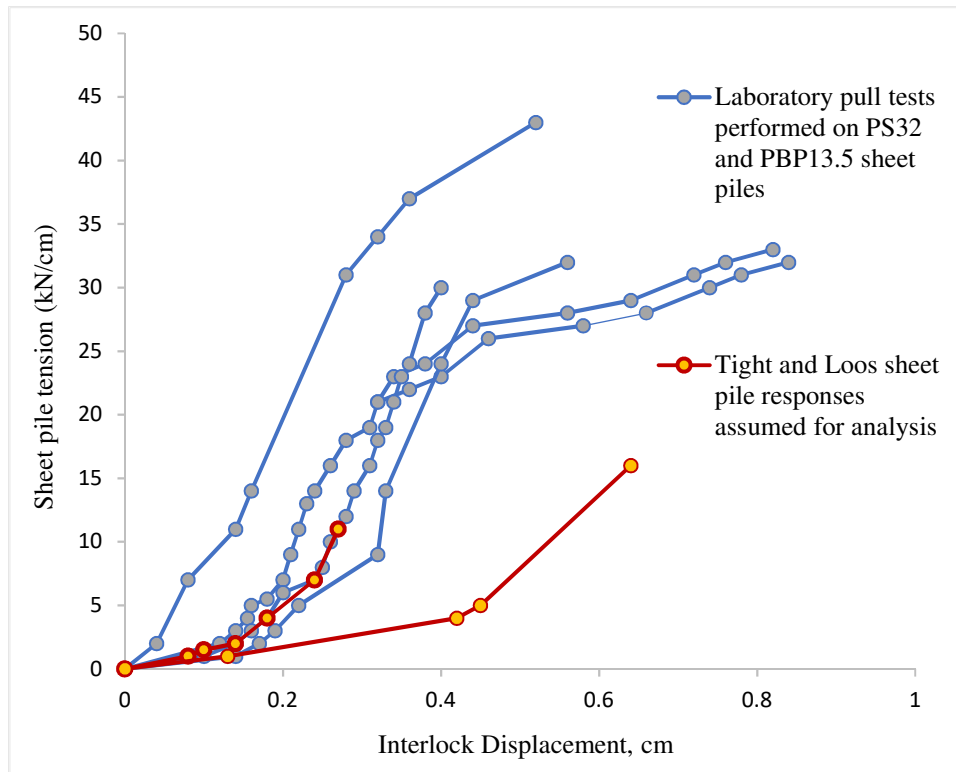


Figure 2.9. Interlock behavior (Wissmann et al., 2003).

2.4.3 Cell Fill Densification and Lateral Loading

The granular fill placed inside cells are densified with vibratory probes in conjunction with the de-watering of the cell. During densification, hoop tension in the piles along the cell circumference increases by additionally an average of 1.33 kN/mm near the location of maximum sheet pile bulge (Point p). After densification, tensile load returns to values close to those before densification and due to water pressure. During cell filling, tension decreases on the loaded side, increases on the unloaded side, and remains the same over the common walls (Wissmann et al., 2003). As an example, Table 2.5 shows how tensions increase in unloaded side during lateral

loading of two examples of cellular cofferdam structures, namely, the Trident and Long Beach cellular cofferdams.

Table 2.5. Increase in unloaded side sheet pile tensions during lateral loading in two cases of cellular cofferdam construction (Wissmann et al., 2003).

Structure	Maximum tension	Average incremental tension increase	Increase relative to end of filling (%)
Trident	0.32	0.18	27
Long Beach	0.56	0.33	0.54

In the Trident and Long Beach cellular cofferdams, the unloaded side sheet piles were designed to withstand an additional average tension of 0.56 kN/mm during lateral loading from densification.

2.4.4 Foundation Stiffness

Circular cofferdams are on hydrostatic conditions because the pressure increases linearly with the height of cell, and then the distance of maximum sheet pile tension from mudline decreases. As the cell becomes more slender (increase in value of height/cell diameter), the relative significance of foundation restraint decreases, so the foundation becomes less stable. When it happens, the value of relative location of maximum sheet pile tension Z with respect to pile height H decreases, and then modulus number decreases because the modulus number highly depends on foundation restraint (Figure 2.10). As expected, foundation on hard (bedrock) offers resistance to outward sheet pile deflection more than soft foundation.

Stability of foundation stiffness also depends on the type of interlock. If the interlock is loose (high stiffness), interlocks can deflect more and it reduces lateral earth pressure on foundation which produces less sheet piles tension. Therefore, the best option for having more stability is, if possible, using loose interlocks on hard foundation.

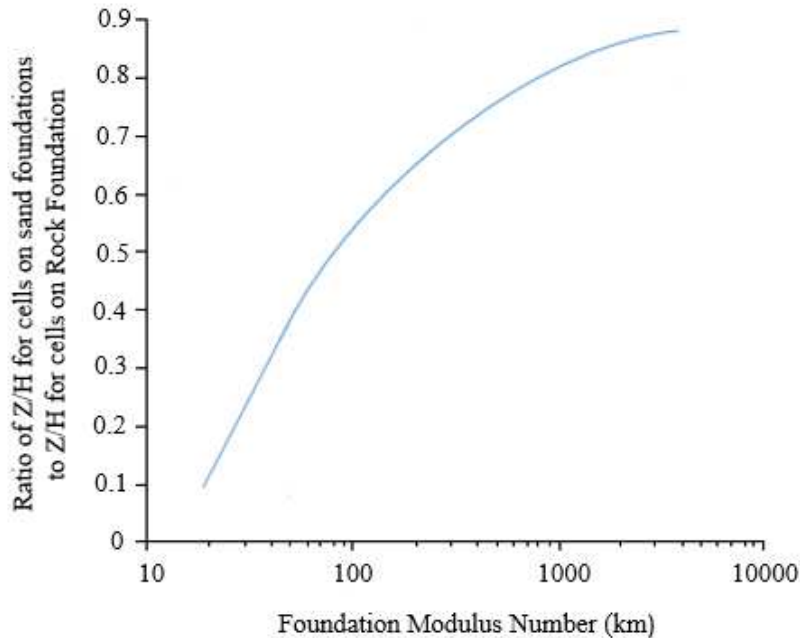


Figure 2.10. Influence of foundation stiffness on location of maximum sheet pile tension (Wissmann et al., 2003).

2.4.5 Cell Tensions

There are several methods to estimate interlock and cell tensions in circular cofferdams. In order to explain all approaches, there is a need to know what the similarities and differences are between these ways. The methods are: Tennessee Valley Authority (1957), Terzaghi (1945), Schroeder and Maitland (1979), Swatek (1967), Matlock and Rees (1969), Wissmann et al. (2003). Cummings (1957), and Hansen (1953). This section does not go through Hansen's method, because it is based on the DAS (Double Axisymmetric Superposition) computer program to get results. Instead, numerical results on FLAC modeling will be used in the validation of existing methods. Cummings (1957) proposed a method of analysis of cellular cofferdams based on model studies for the tilting of a cofferdam on rock. The method provides a simple analysis, however, the physical models used to establish the method are constructed of relatively stiff material for the size of the model, which may not be realistic when related to the flexible sheet piling sections and dimensions of a field structure.

Cells in circular cofferdams have three different parts. They are divided into the main cell, the common wall, and the arc cell as shown in Figure 2.11. Main cells are bigger continuous circular cofferdam cells and arc cells are smaller circles which connect main cells together.

Common walls are mutual cells between main and arc cells. Main cell filling, which is placement of interior fill material, results in radial pressures and sheet pile bulging, so it increases cell tensions. During filling of the arc cells, the fill material pushes the common cell to center of main cell, causes reduction of the net deflection, and reduces the common wall tension. At the same time, tensions in the arc cell are transmitted to the piles, and increases tension in common wall. At the end, total net deflection increases in common walls because tension produced in the common walls are greater than reduction in net outward radial pressures. These observations are based on instrumentation data and numerical results of cofferdam structures made by Wissmann, et al. (2003).

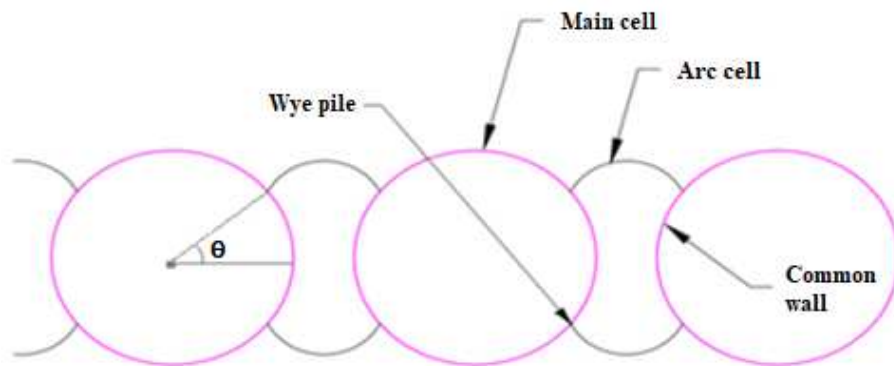
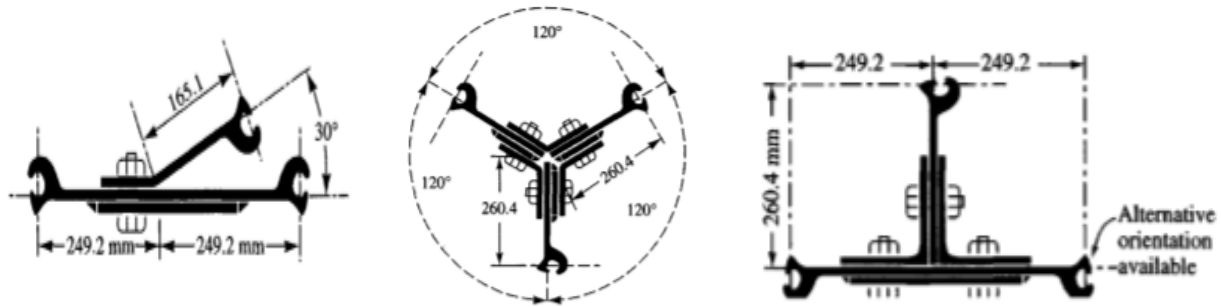


Figure 2.11. Typical cofferdam layout.

In Figure 2.11, θ is the angle between axis of cellular structure and main cell radius that extends through Wye pile. This angle can be 30-degree or 45-degree in circular cofferdams, but the design of more permanent circular cofferdams Wye cell connections requires use of θ equal to 30-degrees due to structure of Wye cell connections.

There are also cell connections which make connections between arc and main cell piles. Cell connections are designed in two major types called Wyes cell connections and Tees cell connections as shown in Figure 2.12. Wye cell connections used with two different angles which are 30-degree and 120-degree (Figures 2.12a and b). The Tee pile sections are just used with 90-degree (Figure 2.12c). The Wye and Tee pile sections belong to key piles which connect arc cells and main cells together. Because of the unusual depth of penetration of the piling for cellular cofferdams, which ranges from 50 to 95 ft (15 to 29.0 m), and the high stresses that may develop during cell filling, the 30-degree wye type of cell offers a longer connecting arc and provides more flexibility during the pile driving.



a. 30° Y cell connections

b. 120° Y cell connections

c. 90° T cell connections

Figure 2.12. Wye and Tee connections used in circular cofferdams (Bowls, 1996).

2.4.5.1 Main Cell Tensions

The main design issue for the installation and construction of cellular cofferdams is the cell tension that develops during the filling of the main cells with granular material. The maximum cell tension that develops must not exceed the tensile strength of the steel piling and the connections between the piles. There are different methods to calculate the cell tensions, and the main formula for main cell tension is based on hoop tension equation which is:

$$T_m = pr_m \quad (2.10)$$

where T_m is main cell sheet pile tensions, p is effective lateral earth pressure at point of maximum sheet pile tensions, and r_m is main cell radius. According to the TVA (Tennessee Valley Authority, 1957) method the hoop tension p is estimated as:

$$p = \sigma'_v K \quad (2.11)$$

where K is the coefficient of lateral earth pressure, which can be determined in several ways as explained below, and σ'_v is the equivalent earth pressure at the base of the fill, which can be estimated from:

$$\sigma'_v = \frac{1}{2} \gamma H^2 \quad (2.12)$$

where γ is unit weight of cell fill (that can be dry or buyout), and H is the height of top of the cell fill.

2.4.5.2 Arc Cell Tensions

For estimating Arc cell tensions, there are two methods. One of the methods are defined by TVA (1957), and Schroeder and Maitland (1959) who suggested that the Arc cell tension is exactly same as the Main cell tension, and equations (2.10)-(2.12) can be used. The other method is proposed by Wissman et al., (1995) who proposed the equation (2.13), which accounts for the increase in net deflection during arc cell filling. Wissmann suggests that $T_{arc\ fill}$ can be estimated using a modified form of equations (2.10) and (2.11) to include a 0.03 reduction in the net lateral earth pressure coefficient based on model studies of earth pressure in cofferdam structures:

$$T_{arc\ fill} = r_m \sigma'_v (K_\phi - 0.3) \quad (2.13)$$

where $T_{arc\ fill}$ is the Arc cell fill tension, and K_ϕ is the coefficient of lateral earth pressure coefficient in Wissman et al.'s method as explained below.

2.4.5.3 Sheet Pile Tension through a Wye Pile

There is just one method to calculate sheet pile tensions through a Wye pile which is that of Wissman et al. (1995). Sheet pile tension is transmitted to Wye piles during arc cell filling and it results in more tensions in the common walls. Wissman et al. tried to find Wye pile tension to find common wall tension which is the sum of the arc cell tensions and the Wye pile tension. According to their method, the common wall tension decreases and Wye pile tension increases during Arc cell filling. In contrast, TVA and Maitland and Schroeder assumed that Main cell tension is equal to the arc cell tension. The Wissman equation for the Wye pile tension T_{wye} is:

$$T_{wye} = r_a K_a \cos \theta \quad (2.14)$$

where r_a is the radius of arc cell, K_a is the active earth pressure coefficient (discussed in next sections), and θ is Wye pile angle.

2.4.5.4 Common Wall Tensions

There are three methods for finding common wall tensions as shown in Table 2.6. As explained in Section 2.4.5, the effect of loading generally results in a net increase in cofferdam common wall tension following arc cell filling. Both methods by TVA (1957) and Swatek (1967) are based on the maximum earth or cell fill pressure. The method of Wissmann et al. (1995) assumes that the common wall tension T_{cw} as the sum of the arc cell and Wye pile tensions.

Table 2.6. Different methods of estimating common wall tensions.

Method	Common Wall Tension T_{cw}
TVA (1957)	$T_{cw} = p L \secant\theta$
Swatek (1967)	$T_{cw} = pL$
Wissman et al. (1995)	$T_{cw} = T_{arc,fill} + T_{wye}$

where L is distance between center of the main and the arc cells. The Swatek method can be as much as 30% less conservative than the TVA method depending on the value of θ .

2.3.6 Lateral Earth Pressure Coefficient

The coefficient of lateral earth pressure K is required to calculate the maximum earth pressure in Equations. (2.11), (2.13) and (2.14). It depends on many factors including: cell height, cell aspect ratio, and interlock stiffness. According to cofferdam studies, there are four different methods for estimating coefficient of lateral earth pressure at point of maximum sheet pile tension, and these are all shown in Table 2.7. Knowing the proper coefficient number is very important in design of cellular cofferdams, because K is used in almost tension equations. In Table 2.7, K is the coefficient of lateral earth pressure, K_a is the Rankine active earth pressure coefficient, K_ϕ is the coefficient of the lateral earth pressure at the location of maximum sheet pile tension, K_{35} is the K value for soils with a friction angle of 35° , ϕ is the friction angle of soil and δ is the interface friction angle between soil and the steel sheet pile wall, which is assumed to be $2\phi/3$.

Table 2.7. Lateral earth pressure coefficients for calculating maximum earth pressure and cell hoop tension.

Method	K	Lateral Earth Pressure K
Terzaghi (1945)	0.4	0.4
TVA (1957)	K_a	$K_a = \tan^2(45^\circ - \frac{\phi}{2})$
Maitland & Schroeder (1979)	1.2 K_a to 1.6 K_a	$K_a = \frac{\cos^2 \phi}{\cos \delta (1 + \sqrt{\frac{\sin(\delta + \phi) \sin \phi}{\cos \delta}})^2}$
Wissmann et al. (1995)	K_ϕ	$K_\phi = K_{35} ((1 - \sin \phi) / 0.43)$

Of the different methods, the lateral earth pressure coefficients from Schroeder and Maitland (1979), and Wissmann et al. (1995) are probably the most appropriate in designing cellular cofferdams. Schroeder and Maitland's method more accurately accounts for the interface friction between soil and pile. Wissman et al.'s method is based on real scale model results of cofferdam structures (Figure 2.13). According to this method, the results are for cell fill with friction angle of 35°, so estimating K_ϕ for other friction angles need a proper equation (Table 2.7). Using K_ϕ equation needs to have K_{35} for new structures. At this step, knowing cell height and type of interlock (loose or tight) helps to find an estimate of K_{35} using Figure 2.13.

Two trend lines A and B are shown in Figure 2.13. Trend line A is for cells with loosely connected sheet pile and for cells below 16 m in height. Trend line B is for tightly connected sheet piles and is usually used for cells above 12 m in height. Contours for different cell height to diameter ratios H/D and interlock tightness are provided between the two trendlines. Transitional cases occur as the cell size increases and slack is taken out of the sheet pile assemblage. During transition from trend lines A to B, the value of K increases because the effect of high stiffness leg of interface response is felt. For example, a tight sheet pile with cell height of 30 m has a coefficient K_{35} of 0.31 using Figure 2.13.

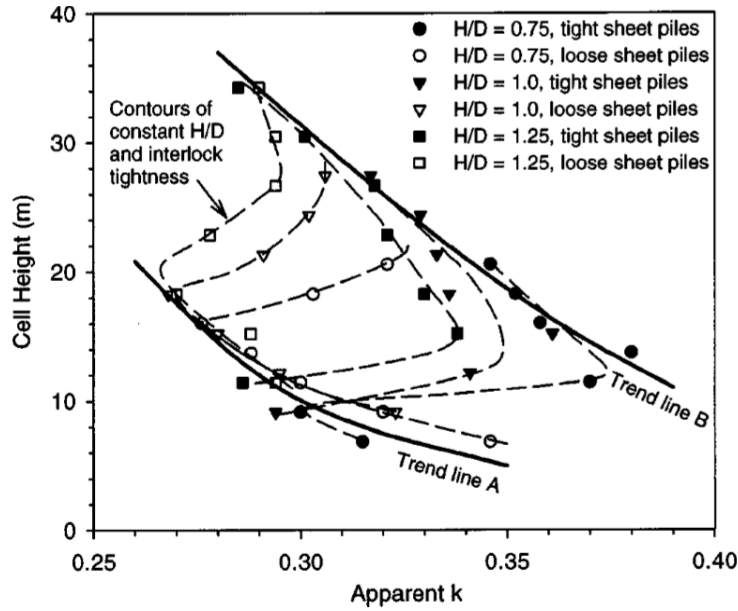


Figure 2.13. “Coefficient of lateral earth pressure at location of maximum sheet pile tension reported in Wissmann et al., 1995.”

2.4.7 Point of Maximum Sheet Pile Tension

Another important factor in the design of cellular cofferdam during construction is determining the location of the maximum earth pressure and correspondingly the maximum sheet pile tension. This location is referred by the symbol Z or ρ and is measured from the mudline. There are three different methods for finding maximum sheet pile tensions point as shown in Table 2.8. In this table H_b is the distance from the top of the cell to mudline, and H_c is the distance from the top of the cell to the location of sheet pile fixity in the foundation soils. Only in Schroeder and Maitland’s method, is Z measured from the location of sheet pile fixity (explained below in Section 2.4.8).

Table 2.8. Methods for estimating point of the location of the maximum sheet pile tensions from the mudline.

Method	Location Z
Terzaghi (1945)	0
TVA (1957)	$H_b/4$
Schroeder and Maitland (1979)	$H_c/3$

2.4.8 Depth of Pile Fixity

The point of pile fixity is where the pile is fixed and does not deflect horizontally. Estimating depth of fixity is one of the important parts of cellular cofferdam design because it is required for finding the location of the maximum cell tension p_{max} , distance of point of maximum sheet p from mudline Z , and the effective cell height H . There are three methods for finding the point of fixity, which are: Matlock and Rees (1969), Schroeder and Maitland (1979), and TVA (1957) as part of the different methods explained above. All of these methods calculate the depth of point of pile fixity D from the mudline to find the distance of top of the cell to the point of pile fixity (cell height) H_c using:

$$H_c = H_b + D \quad (2.15)$$

where H_b is the distance of top of the cell to mudline (i.e., the free cell height).

2.4.8.1 Matlock and Rees (1959) Method

In this method, the point of fixity is calculated as:

$$D = 3.1T \quad (2.16)$$

$$T = 5\sqrt{\frac{EI}{N}} \quad (2.17)$$

where E is the Young's modulus of elasticity of the pile which is 207 GPa for steel in the SI unit shown in Table 2.2, I is the moment of inertia of the pile, and N is the constant of horizontal subgrade reaction.

2.4.8.2 Schroeder and Maitland (1979) Method

According to Schroeder and Maitland's method, the location of fixity at depth below the mudline is where the passive earth pressure acting outside the sheet pile walls balances the active earth pressure acting on the inside of cell:

$$D = \frac{\sigma'_v}{\gamma'(K_p - K_a)} \quad (2.18)$$

where σ'_v is the effective vertical stress at the mudline due to the weight of the cellular fill, γ' is effective unit weight below the mudline, and K_p and K_a are the Rankine passive and active earth-pressure coefficients for the soil below the dredge line. If the dredge line soil has $\phi = 0^\circ$, using D between 0.3 to 0.5 m is suitable.

2.4.8.3 TVA (1957) Method

According to the TVA (1957) method, the depth of pile fixity D varies from $H_b/3$ or $H_b/4$, where H_b is the distance from the top of the cell to mudline. There is not a significant difference in the design whether $H_b/3$ or $H_b/4$ is used. Instead of finding D , it is also possible to use H_b equal to H_c .

2.4.9 Depth of Embedment

Depth of embedment is the dimension of pile from mudline to the depth of required penetration into the foundation. Currently, there two methods are used to define the depth of embedment of piles d_f which are shown in Table 2.9.

Table 2.9. Recommended depth of pile embedment for cellular cofferdams.

Method	Depth of embedment, d_f
Terzaghi (1945)	$d_f = 2D/3$
Matlock and Rees (1969)	$d_f > 5T$

where T is defined in equation (2.17), and D is depth of pile fixity.

2.4.10 Interlock Tensions

Determination of interlock tension is based on the hoop tension equation and the maximum tension occurs in the interlock web sections (Figure 2.14). The maximum computed interlock tension t_{max} according to USACE (1989) is simply equal to;

$$t_{max} = q_t r \quad (2.19)$$

where r is cell radius and q_t is the maximum earth pressure at the point of maximum interlock tension calculated from:

$$q_t = \gamma H K_a \quad (2.20)$$

where γ is unit weight of soils, H is height of cell, and K_a is active earth pressure coefficient of cell fill. One may obtain the maximum tension force from a free body diagram that considers hoop tension in both the main and connecting cells.

Internal horizontal pressure at any depth in the cell fill is the sum of the earth pressure and water pressures. Earth pressure is equal to effective weight of the cell fill above that depth multiple by coefficient of horizontal earth pressure K .

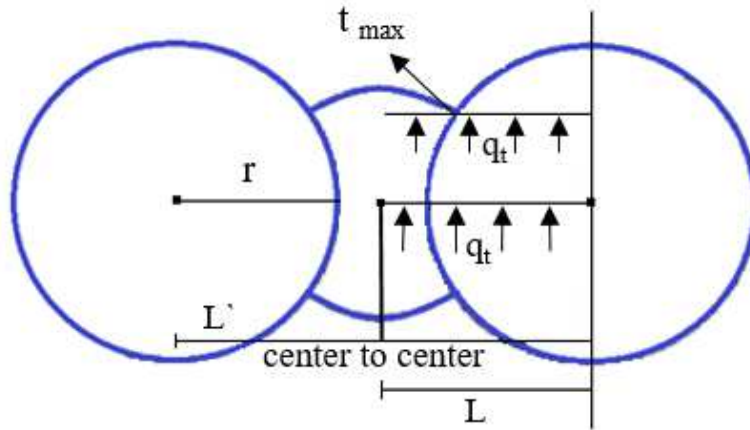


Figure 2.14. Hoop or interlock tensions according to TVA reproduced from USACE (1989).

2.4.11 Factor of Safety against Tensile Failure

After estimating maximum cell and interlock tension loads, it is necessary to apply a Factor of Safety FS against tensile failure to account for uncertainties in the design procedures, material properties used, and potential deficiencies in the construction. Factor of safety FS for tensile loading is simply:

$$FS = \frac{T_f}{T_{max}} \quad (2.21)$$

where T_f is the tensile strength of the sheet pile or the interlock, both of which are specified by the pile manufacturer for the most commonly used sheet pile sections in cellular cofferdam construction, and T_{max} is the maximum tensile load on the pile or the interlock. The minimum Factor of Safety FS for tensile failure should be at least 2.0.

2.4.12 Earth Pressure Diagrams

Three main interlock pressure diagrams to design cellular cofferdam for installation load are available and they are based on type of foundation and the assumed point of maximum horizontal pressure p . These diagrams show us how earth pressure diagram estimates in different situations. Three figures are shown below according to USACE (1989).

In Figure 2.15, H_1 is the average height of level of the saturated soil, H_2 is the height if saturation line at inboard face, H is height of cell, p is point of maximum sheet pile tension measure from the bottom of the cell fill, and C is the point of pile fixity where the pile does not move laterally. The maximum potential height of the maximum pile tension p_{max} is at $H/4$.

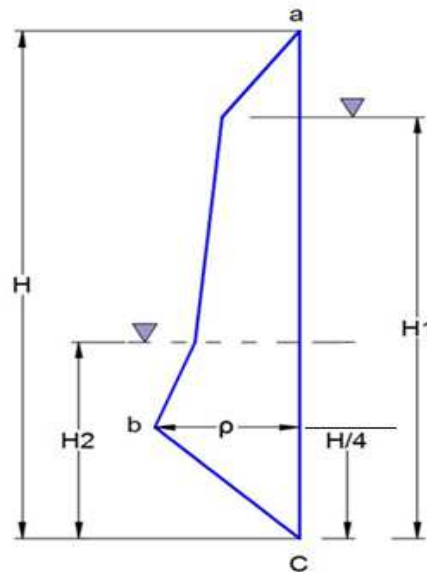


Figure 2.15. Earth pressure diagram for piling seated on rock, no overburden or berm during cellular cofferdam installation.

In Figure 2.16, ρ_{max} is at the base of cell if there is no berm. If there is berm, ρ_{max} is at top of berm or overburden.

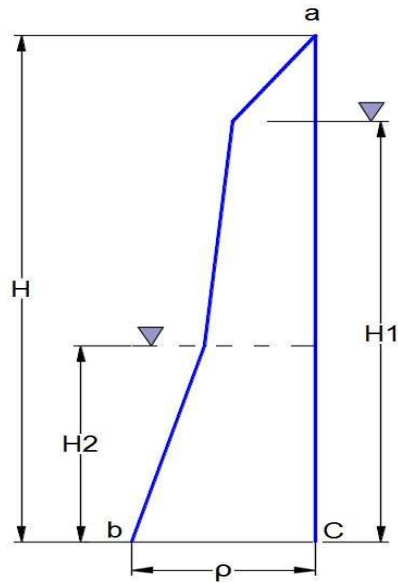


Figure 2.16. Earth pressure diagram for piling not seated on rock.

In Figure 2.17, H_b is the height of the downstream berm or overburden, H_{pf} is distance from top of berm or overburden to point of fixity, and H' is height of cell above C which point of fixity. As before, ρ_{max} is at $H'/4$ or at the top of berm or overburden.

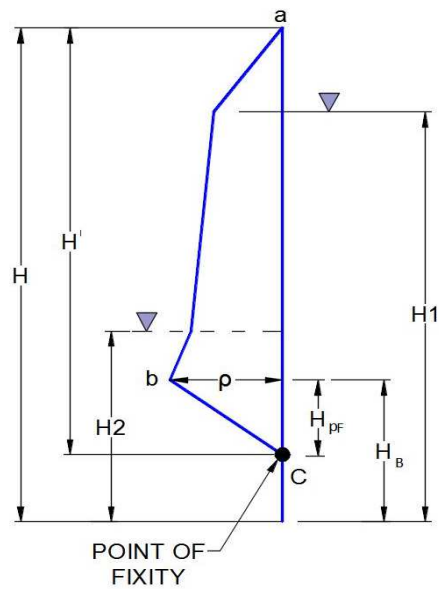


Figure 2.17. Earth pressure diagram for piling fully restrained by external passive and hydrostatic forces.

2.4.13 Comparisons of Design Procedures with Computer Modeling Results

Computer modeling of typical Kentucky cellular cofferdams and their modifications can be used for permanent hydropower application. Results from these computer modeling are used to qualitatively validate the design procedures presented in this chapter. Two aspects of the design procedures can be easily verified: 1) the distribution of earth pressure against the cellular cell walls which determines the maximum cell and interlock tensions and their locations, and 2) the point of pile fixity which will determine required depth of pile penetration.

The computer simulations are carried out based on one case history of Kentucky cellular cofferdam construction. The FLAC simulation of the wet construction involves two stages: cell filling and water loading. Figure 2.18 shows the distribution of earth pressure against the cellular cell walls for construction. With the exception of the upstream and downstream sides of the Kentucky Cofferdam, it can be seen that the earth pressure decreases almost linearly with depth all the way below the mudline. This holds true for the downstream and upstream sides of Kentucky cofferdam where there is a berm. The linear distribution extends all the way down to the bottom of the model which is assumed to correspond to a rock foundation. The results shown in Figure 2.18 suggest that the linear distribution shown in Figure 2.15 is appropriate for the case studied.

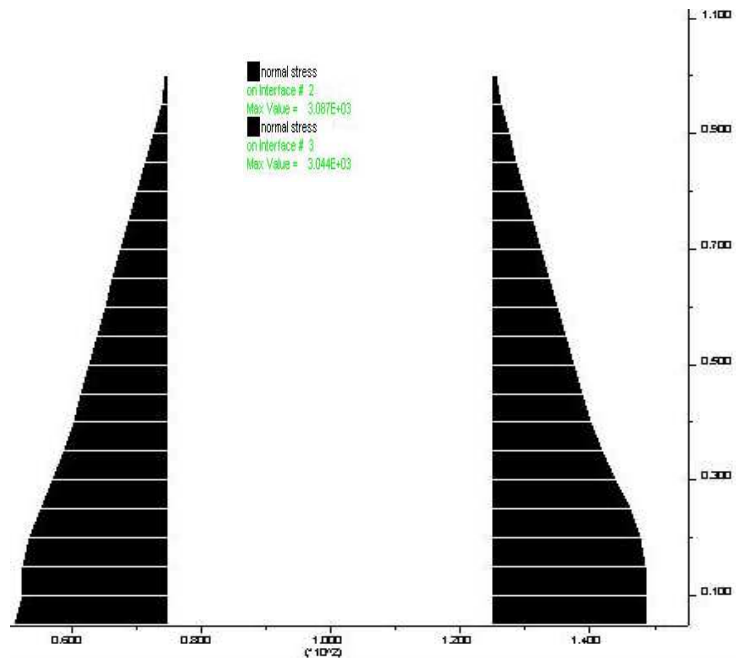


Figure 2.18. Earth pressure distribution along the walls of the Kentucky Cellular Cofferdam.

Figure 2.19 shows the exaggerated deformed mesh of Kentucky Cofferdam. For this case, it can be seen that the piles continue to expand outwards and as a result the pile fixities occur at the base of the model which are assumed to be the location of the rock foundations. The results shown in Figure 2.19 indicate that the stiffness of the pile and the foundation, and the presence of a downstream berm significantly affect the deformation of the pile and the location of the pile fixity. Thus, methods that account for soil-structure interaction such as the one proposed by Matlock and Rees (1969) in equations (2.16) and (2.17), which are expressed in terms of pile stiffness and ground reaction coefficient should be preferred in determining pile fixity and depth of penetration.

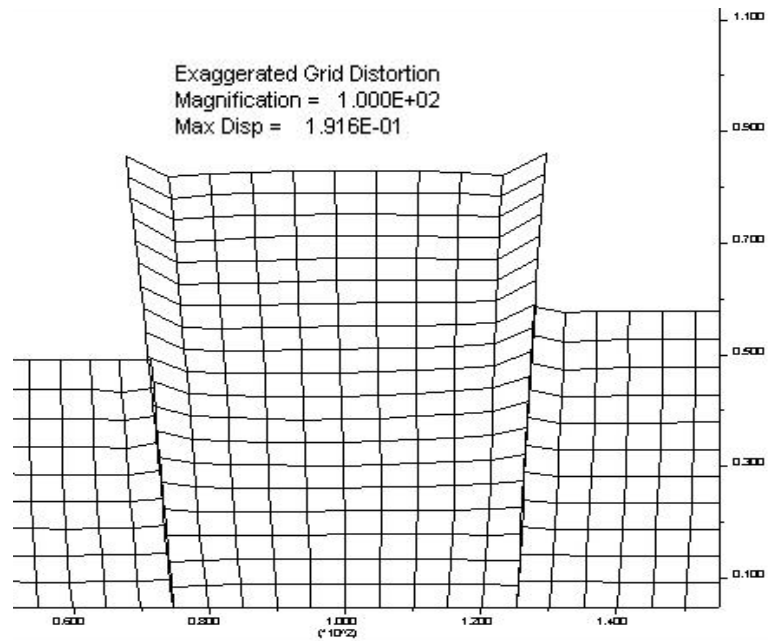


Figure 2.19. Magnified deformed mesh for Kentucky Cofferdam after placement of cellular fill.

CHAPTER 3

DESIGN PROCEDURES FOR THE OPERATION OF CELLULAR COFFERDAMS FOR PERMANENT HYDROPOWER USE

3.1. Geotechnical Hazards

There are several criteria and considerations for considering ensuring the safe and reliable design of permanent hydropower cellular cofferdams during operation. These considerations include geotechnical, geological, and structural hazards. Though there are no general solutions for some of these conditions because of the complexity of the cell geometry, sheet piles, and material fill, specific factor of safety estimates must be developed. Owing to the uncertainties in the river environments, the current analytical methods for the cofferdam design are semi-empirical. Examples are the Tennessee Valley Authority (1957), also called Terzaghi (1945), which was used for the Kentucky cofferdam design as illustrated in chapter 2. Manual factor of safety calculations and formulas for the proposed design concept #1 of Kentucky cofferdam are illustrated in Appendix A and B.

Section 3.1 studies geotechnical hazards which include stability against sliding, overturning, bearing capacity failure, slope failure of the downstream berm, and seepage induced failure.

3.1.1 Sliding

Analytical calculations are performed to obtain estimates of the stability and safety of the Kentucky cofferdam. In order to calculate stability and factor of safety, knowing horizontal earth pressures are necessary. Horizontal earth pressures are calculated using Poncelet's Earth Pressure equations which give active, and passive earth pressures equal to:

$$P_a = \frac{1}{2} \gamma H^2 K_a \quad ; \quad K_a = \frac{\cos^2 \phi}{\cos(\delta) \left[1 + \sqrt{\frac{\sin(\phi + \delta) \sin \phi}{\cos \delta}} \right]^2} \quad (3.1)$$

$$P_p = \frac{1}{2} \gamma H^2 K_p \quad ; \quad K_p = \frac{\cos^2 \phi}{\cos \delta \left[1 - \sqrt{\frac{\sin(\phi + \delta) \sin \phi}{\sin \delta}} \right]^2} \quad (3.2)$$

where P_a is the active pressure, P_p is the passive earth pressure, K_a is the coefficient of active earth pressure, K_p is the passive earth pressure, γ is the dry or buoyant unit weight of the soil, H is the height of the soil or wall, ϕ is the angle of friction of the soil, and δ is the interface friction angle between soil and the steel sheet pile wall, which is assumed to be $2\phi/3$.

In general, a cell on rock will very rarely fail on its base, probably because of friction of the fill and anchoring of the sheet pile penetrated to some distance into the rock. However, in alluvial soils excess hydrostatic pressure reduces the effective stress and, subsequently, reduces shearing resistance to a very small value.

A cellular cofferdam design needs a detailed study of the subsurface below the design bottom of the cell and an adequate sliding analysis. Adequate measures to prevent such failure should be incorporated in the cell design, if any potential for sliding failure exists. The subsurface investigation should be extended to at least 15 to 20 feet below the design base level of the cell. The presence of any cracks or joint pattern in the apparently competent rock mass below the base should be carefully investigated. If soft seams or presheared surfaces due to faulting are found, extremely low shear strengths approaching the residual strengths should be used in the analysis (USACE, 1989).

The method of TVA (1957) for sliding is also called Approximate method of sliding. This method is used to discuss and calculate sliding stability as shown in Figure 3.1. The factor of the safety of 1.25 is considered to be the typical lowest minimum value against failure due to foundation against sliding and shear for temporary structures. Higher factor of safety values are often used.

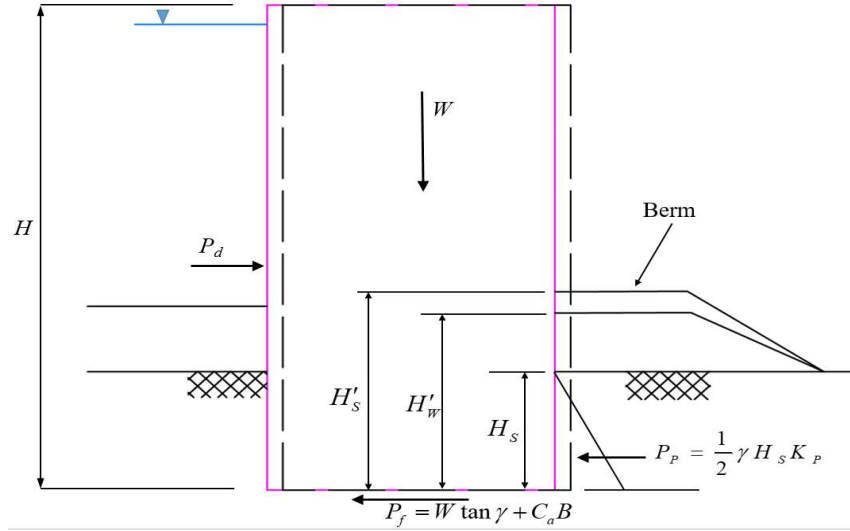


Figure 3.1. Sliding stability of cellular cofferdams based on the TVA and Terzaghi procedures.

The base and the berm of the cellular sheet pile cofferdam resist the cell from sliding by friction against the horizontal hydrostatic forces, and active and passive earth pressure. However, given the large magnitude of forces from the earth and water pressures, the shear resistance provided by the steel sheet pile is often neglected. Considering the forces given in Figure 3.2, the factor of safety against sliding $FS_{sliding}$ can be calculated assuming two potential failure modes of the downstream berm:

- Sliding below the cellular cofferdam and downstream berm:

$$FS_{sliding} = \frac{\text{Resisting}}{\text{Driving}} = \frac{P_{f,wall} + P_{f,berm} + P_{wall}}{P_w + P_a} \quad (3.3)$$

- Sliding below the cellular cofferdam and passive failure of the berm:

$$FS_{sliding} = \frac{\text{Resisting}}{\text{Driving}} = \frac{P_{f,wall} + P_p + P_{wall}}{P_w + P_a} \quad (3.4)$$

where P_w is the pressure from the water in the reservoir upstream of the cofferdam, and P_a is the active earth pressure from the sand behind the cofferdam, $P_{f,wall}$ friction force resistance below the cellular wall, $P_{f,berm}$ friction force resistance below the berm, P_p is the passive earth pressure resistance from the sand behind the cofferdam, and P_{wall} the resistance from any wall built in the

berm (assumed zero in the case of Kentucky cellular cofferdam). Note that the shearing resistance from the steel sheet piles forming the cells are neglected.

In the calculation of the $FS_{sliding}$, two assumptions of the unit weight of sand can be made in the calculation of the weights of the cellular wall and the berm (or the passive earth pressure resistance from the berm):

- 1) Bouyant unit weights of the sand for “wet construction,” and
- 2) Dry unit weights of the sand for “dry construction.”

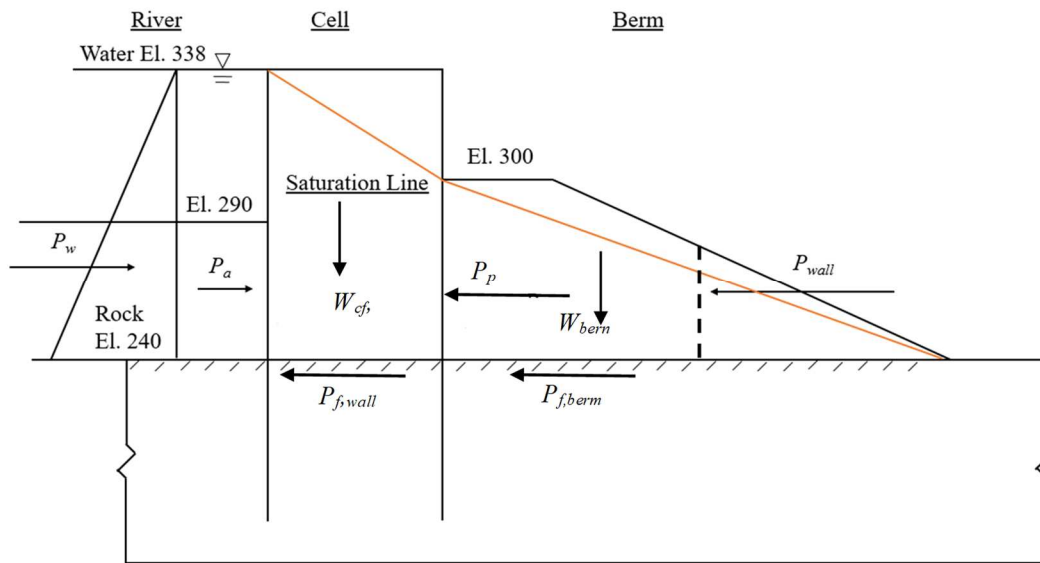


Figure.3.2. Weights and horizontal forces acting on the cellular cofferdam.

For “wet construction,” as is the case for the Kentucky cellular cofferdam, the seepage of water through the cellular fill must be accounted for to obtain a more reliable estimate of the factors of safety, and in this case, the procedure shown in Figure 3.2 is more appropriate. In Figure 3.2, the orange lines represent the approximate and idealized location of the phreatic or water saturation lines due to seepage from upstream to downstream.

Given the dimensions of cells and cofferdam in Figure 2.5, and the properties of sand in Table 2.1, the $FS_{sliding}$ for the “wet” and “dry” constructions are summarized in Table 3.1.

Table 3.1. Summary of values of factor of safety against sliding for Kentucky cellular cofferdam.

Factor of safety against sliding, $FS_{sliding}$	Wet construction	Dry construction
Sliding below berm	1.18	2.38
Passive failure of berm	1.31	2.74

As can be seen, the lowest factor of safety against sliding is 1.18 in the case of passive failure of the berm and assuming “wet” conditions. This is the reason why constructing a wall in the berm is deemed to be needed to increase the factor of safety as was the case, for example, for the temporary cellular cofferdam in the Willow Island Hydroelectric Project (Ciammaichella and Tantalla, 2014). Also, the table shows significant increase in factor of safety in the case of “dry construction.” The next step is Comparison of numerical and analytical results of sliding stability analysis. Figure 3.3 and 3.4 show the manual and computational calculations of factor of safety against sliding in “wet construction” of Kentucky cofferdam.

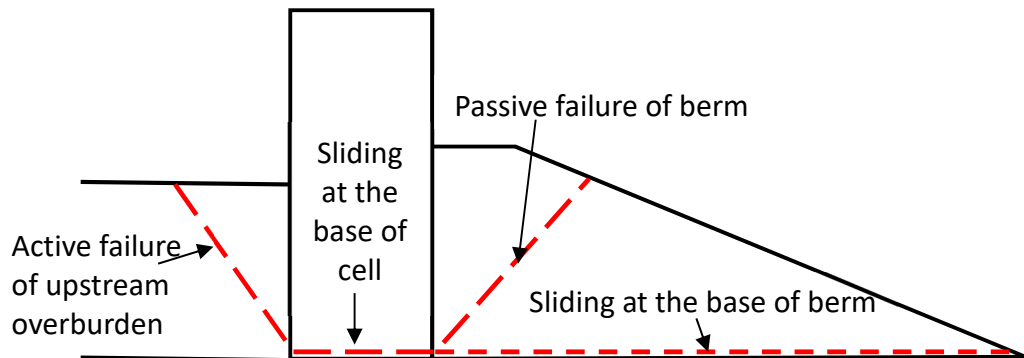


Figure 3.3. “Manual” calculations of factors of safety against sliding $FS_{sliding}$.

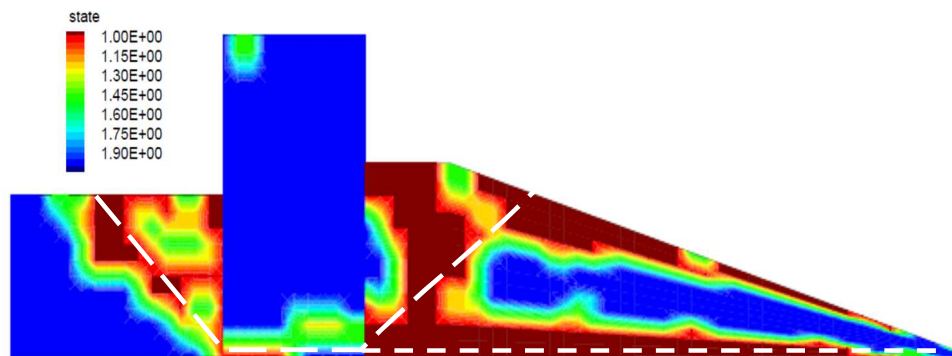


Figure 3.4. “Computational” calculations of factors of safety against sliding $FS_{sliding}$ (e.g. by averaging values of “state” along failure surfaces).

Using numerical and analytical calculations for wet construction, gives the factor of safety against sliding for both manual and computational results as shown in Table 3.2. Note that manual calculations are based on Kentucky cellular cofferdams as shown in Table 3.1.

Table 3.2. Summary of comparison of values of factor of safety against sliding.

	Manual	Computational	Difference
Sliding below berm	1.18	1.15	2.5%
Passive failure of berm	1.31	1.25	4.6%

Factors of safety against sliding $FS_{sliding}$ from “computational” calculations are within 95% of “manual” calculations. This accuracy shows that manual calculations of design concepts are correct and reliable. Therefore, other design issues during operation are calculated analytically and/or numerically. If $FS_{sliding}$ is not high enough, the general solutions to reduce the potential for sliding stability failure are based on adopting the measures of seepage control below cell, dissipation of excess hydrostatic pressure, and berm construction on the downstream side.

3.1.2 Overturning

A cofferdam must be stable against overturning. Analysis and tests on sheet pile cells driven into sand indicated that failure by tilting due to overturning moment should occur long before the maximum sliding resistance is reached. Figure 3.5, shows the overturning stability geometry based on TVA (1957) theory.

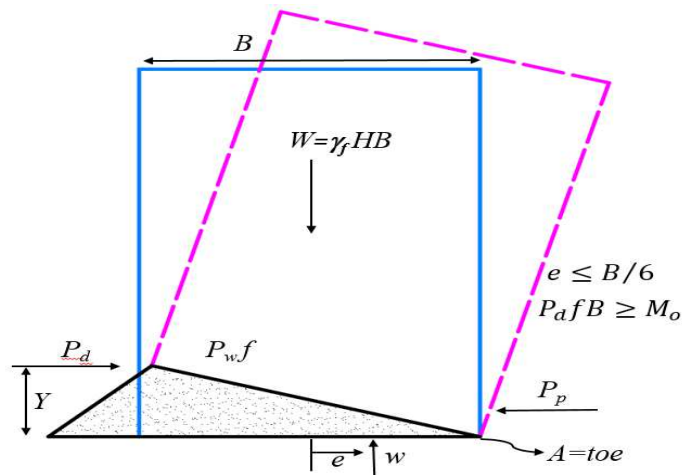


Figure 3.5. Overturning stability of cellular cofferdams based on the TVA and Terzaghi procedures.

Overtuning stability can be achieved by ensuring that the resultant vertical force at the base of the cellular cofferdam W should be located within the middle one-third of the base of the wall. The distance \bar{x} of the resultant weight is calculated from the summation of moments from the toe of the wall:

$$\bar{x} = \frac{\sum M_{\text{overtuning}} - \sum M_{\text{resisting}}}{W} \quad (3.5)$$

where $\sum M_{\text{overtuning}}$ is the summation of all overturning (clockwise) moments and $\sum M_{\text{resisting}}$ is the summation of all resisting (counter clockwise) moments from the toe as shown in equations (3.6) and (3.7):

$$\sum M_{\text{overtuning}} = P_{\text{berm}} \left(\frac{H_{\text{berm}}}{3} \right) + w \left(\frac{B}{2} \right) \quad (3.6)$$

$$\sum M_{\text{Resisting}} = P_w \left(\frac{H_w}{3} \right) + P_{\text{overburden}} \left(\frac{H_{\text{overburden}}}{3} \right) \quad (3.7)$$

In Figure 3.6, the forces acting on cofferdam and heights of berm and overburden for overturning stability analysis are shown.

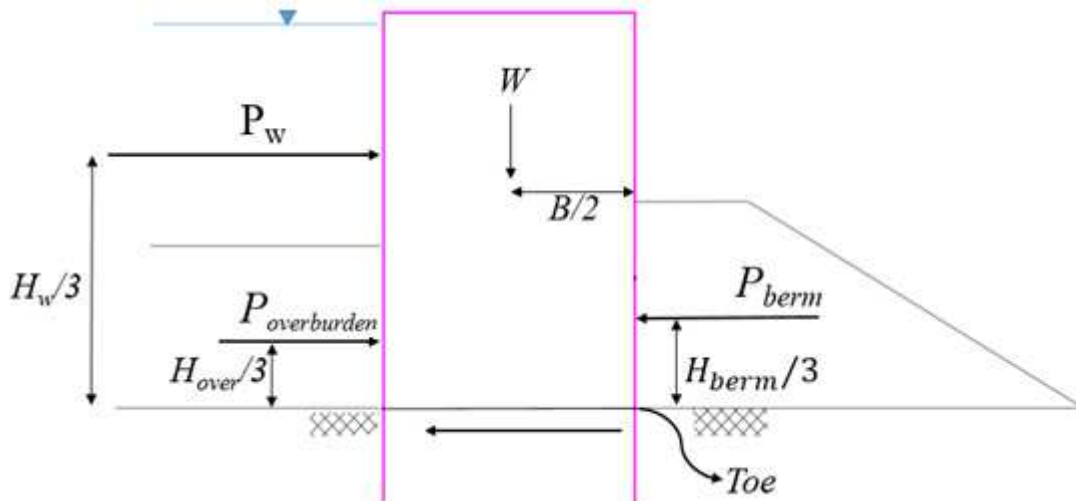


Figure 3.6. Weights and forces acting on the cofferdam for overturning stability calculation.

In the calculation of the weight of cellular cofferdam, W , two values can be used: 1) saturated unit weight of the sand for the case of “wet construction,” and 2) dry unit weight of the sand for the case of “dry construction.” Table 3.3 summarizes the distance \bar{x} of the resultant weight for the case of “wet” and “dry” constructions of Kentucky cofferdam.

Table 3.3. Summary of values of factor of safety against slide for Kentucky cellular cofferdam.

	Wet construction	Dry construction
Distance of resultant vertical force from the toe of the wall, \bar{x} (ft)	16.1	27.4
$\frac{B}{3} \leq \bar{x} \leq \frac{2B}{3}$?	Barely	Yes

As can be seen, for the wet construction, \bar{x} is barely within the middle third of the base of the wall. Significant increase in stability against overturning is achieved with the dry construction.

3.1.3 Bearing Capacity Failure

As the foundation of design in “wet” and “dry” construction is rock, it is assumed that the cellular cofferdam is safe from bearing capacity failure because the bearing capacity of rock is usually controlled by the defects in the rock structure rather than the strength alone. If the penetration of the sheet piles into the overburden is adequate and seepage of water underneath the cell base is controlled, the bearing capacity of granular soil is generally good. The seepage which reduces the shear strength of the soil on the downstream side of the cofferdam and thus reduces the bearing capacity can be controlled by using an adequate berm on the downstream side.

As can be seen in Figure 3.7, Terzaghi boundary condition theory can be used for both cohesive and granular soils supporting cellular structures. The FS against bearing capacity failure should be determined by the maximum pressure at the base of the cellular structures.

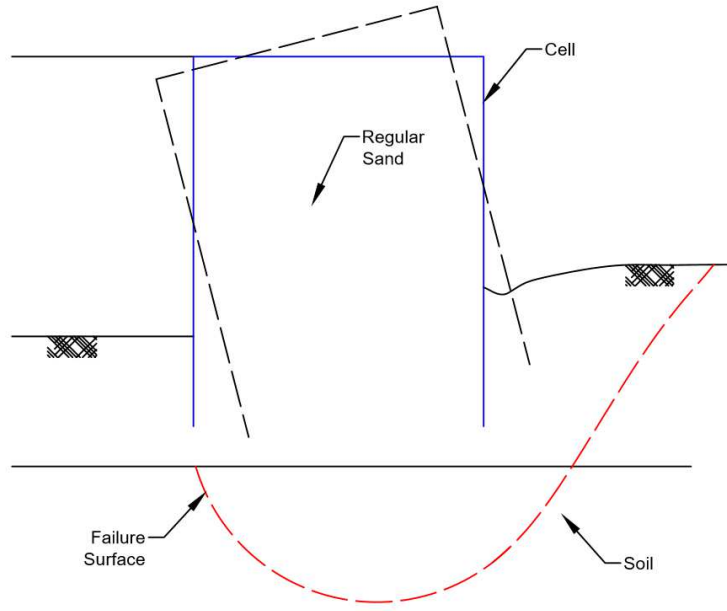


Figure 3.7. Bearing capacity failure.

The minimum factor of safety against bearing capacity is 1.5 but usually more than that is considered for permanent structures. FS against bearing capacity based on Terzaghi theory is:

$$FS_{bearing\ capacity} = \frac{q_{ult}}{q_a} \quad (3.8)$$

where q_{ult} is ultimate bearing capacity and q_a is applied load on the foundation. Estimating ultimate bearing capacity is given by two formulas for:

1) Strip loaded area:
$$q_{ult} = \frac{1}{2} \gamma B N_\gamma + C N_c + \gamma D_F N_q \quad (3.9)$$

2) Circular loaded area:
$$q_{ult} = 0.6 \gamma B N_\gamma + 1.3 C N_c + \gamma D_F N_q \quad (3.10)$$

where γ is unit weight of soil around cell B is equivalent cell width, and N_q, N_c, N_γ are the Terzaghi bearing capacity factors depending on the angle of shearing resistance of the soil, C is cohesion of soil, and D_F is distance from the ground surface to the toe of the cell.

Applied load on the foundation (q_a) is equal to weight of the cell fill divided by the total area of soil fill as shown below:

$$q_a = \frac{W}{A} \tag{3.11}$$

Using equations (3.8) and (3.10), and cell fill properties, factor of safety against bearing capacity failure in “dry construction” is equal to:

$$FS_{\text{bearing capacity}} = \frac{845.7}{284.1} = 2.98$$

This factor of safety shows that even if the foundation is not rock for design concept # 1, it is still stable against bearing capacity failure.

3.1.4 Slope Stability Failure

The main aim of slope stability is to determine the factor of safety against slope failure. Failure in the soil is governed by the Mohr-Coulomb criterion. There are several methods which use different assumptions in order to determine the FS_{slope} .

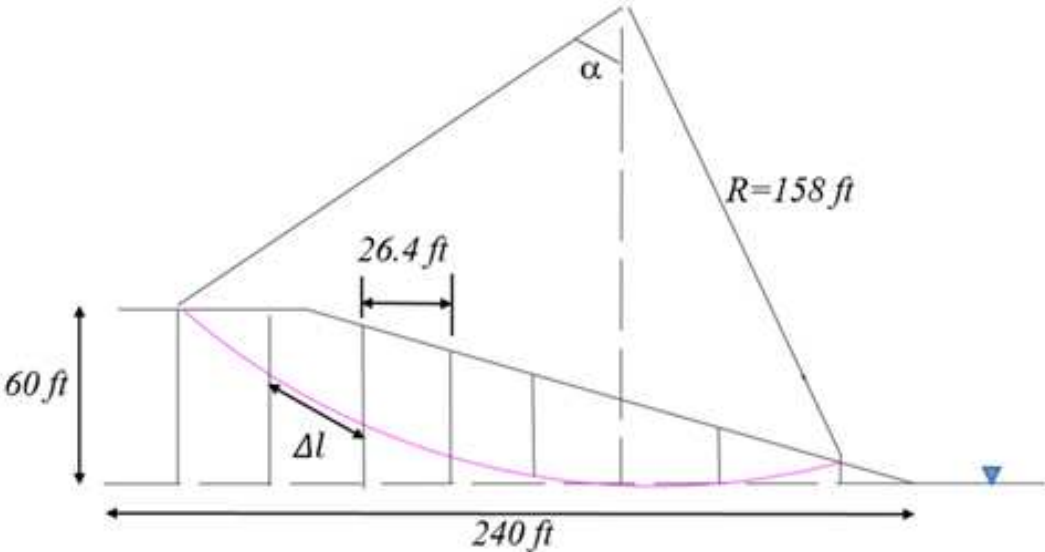


Figure 3.8. Slope stability diagram based on Improved Ordinary Method of Slices for design concept #1.

One of the simplest and most commonly used assumptions is Improved Ordinary Method of Slices (IOMS). The method requires that the geometry be sub-divided into slices, and to delineate the forces on each of the slice as shown in Figure 3.8. Note that the red line shows boundary of slope failure. The FS against slope failure in IOMS is equal to:

$$FS_{slope} = \frac{\text{Resisting Moment}}{\text{Overturning Moment}} = \sum_{i=1}^n \frac{[c_i \Delta l_i + (w_i + u_i) \cos \alpha_i \tan \phi_i]}{w_i \sin \alpha_i} \quad (3.12)$$

where n is number of slices, c_i is cohesion force of the soil, Δl_i is width of the i^{th} slice, W_i is the weight of the rotating body of i^{th} slice, U_i is hydraulic force of i^{th} slice, α_i the angle subtended by the failure circle at its center of the i^{th} , and ϕ is the friction angle of the soil. Manual calculations of factor of safety of design concept #1 in “dry construction” have been done based on IOMS theory. The FLAC results of factor of safety for design concept #1 is also calculated as shown in Figure 3.9.

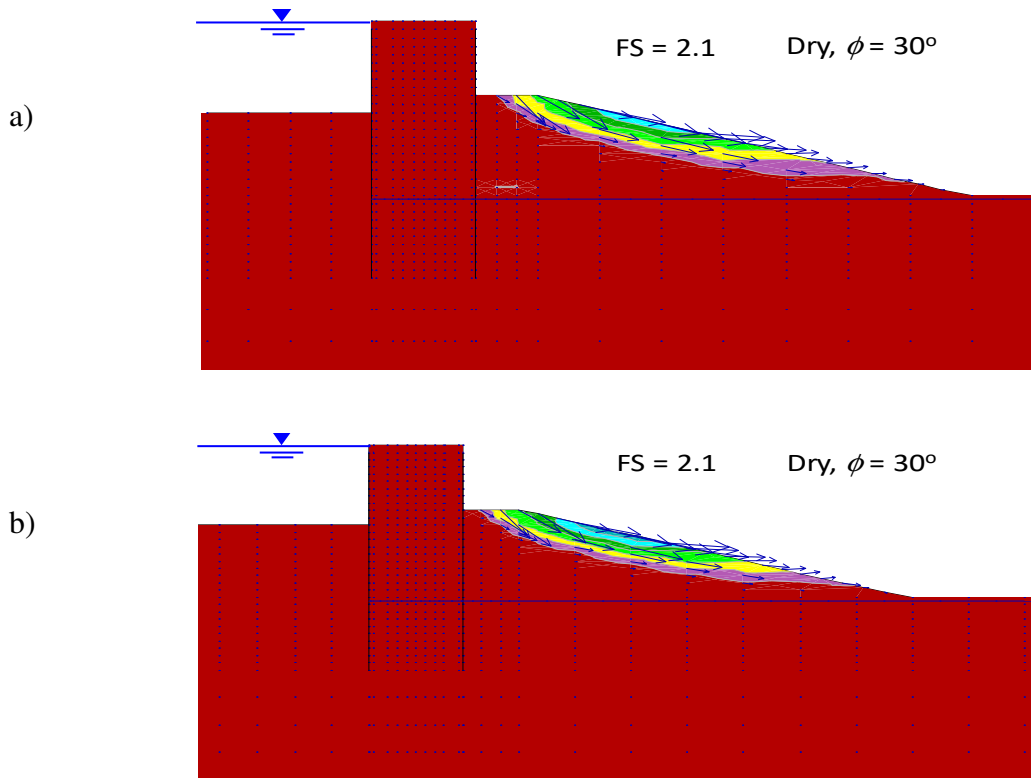


Figure 3.9. Stability results for design concept #1 using the (a) asphaltic and (b) concrete liners.

Computational results of “dry construction” shows that there is no difference in the stability of the cofferdam when either the asphaltic liner (Figure 3.9a) or the concrete liner (Figure 3.9b) is used. This is because, in both cases, failure by sliding occurs in the downstream berm. Hence, the strengthening effect from the concrete liner in the inner cell is not fully in use.

Table 3.4 shows manual and computational calculations of slope stability analysis and the difference between them. This accuracy proves that both finite element procedure and manual calculation of design concept #1 are accurate.

Table 3.4. Numerical and Analytical results of $FS_{slope\ stability}$ for design concept #1 in “dry construction.”

	Computational	Manual	Difference
$FS_{slope\ stability}$	2.10	2.19	4.2%

As can be seen from Table 2.1, the berm and cell fill are the same material. Using different friction angles of soils for calculations of FS_{slope} , is a reliable way to achieve the highest factor of safety. Therefore, in the stability analysis of the proposed design concept of the Kentucky cofferdam, their friction angle (ϕ) values are varied from $\phi = 60^\circ$ to $\phi = 30^\circ$. This different ranges of friction angle are based on various theories and methods of gravelly soils as shown in Figure 3.10.

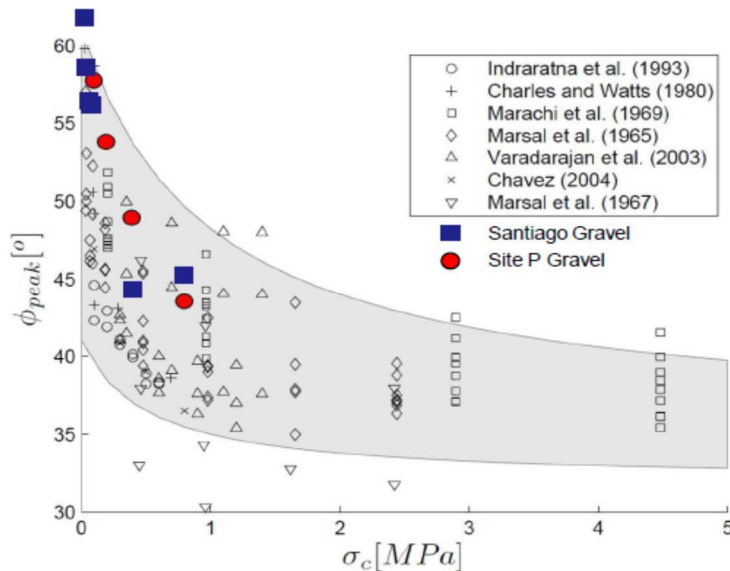


Figure 3.10. Friction angles of gravelly soils based on different theories.

The FS from each simulation of reduced ϕ is then plotted into a graph of FS vs. ϕ to observe at what ϕ that the cofferdam will have FS > 3.0, which is the assumed FS value for permanent structure. The results are shown in Figure 3.11 for both “dry” and “wet” constructions for asphaltic liner and concrete liner. As expected, the “wet construction” in each case results in lower FS values than the “dry construction” does. In both cases, FS = 3.0 is resulted when $\phi = 40^\circ$ for “dry construction” and $\phi = 50^\circ$ for “wet construction.”

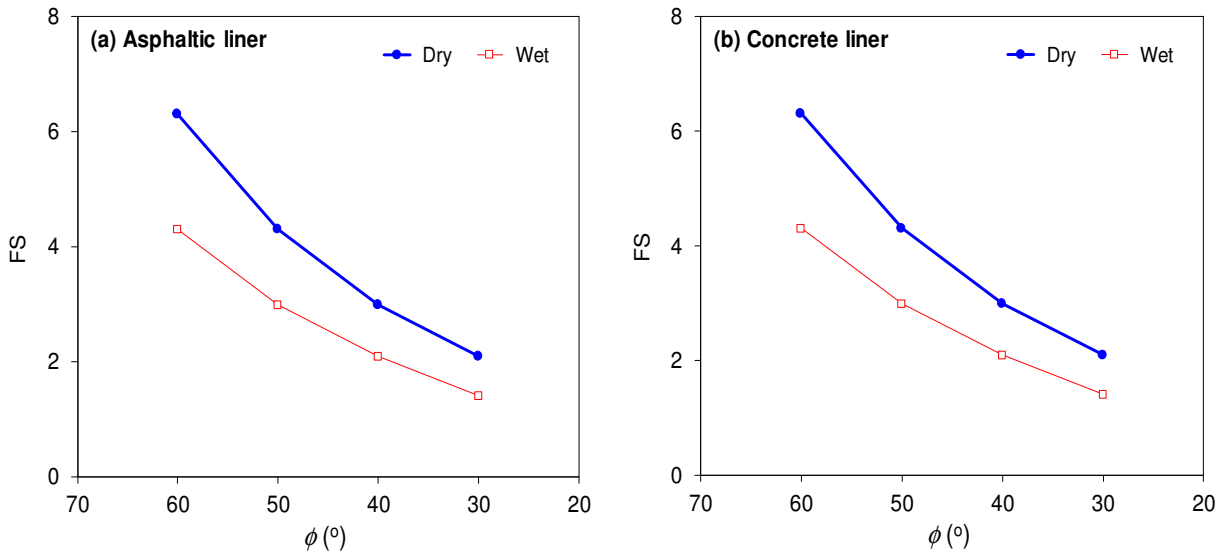


Figure 3.11 Factor of safety graphs against slope failure for design concept #1.

3.1.5 Seepage

Generally, two types of seepage are to be considered for designing a cellular cofferdam: 1) Seepage through the cell fill, and 2) Seepage through foundation under seepage. Demonstrating the typical pore pressure contours for the “wet” and “dry” construction, is the first step of this chapter for analyzing seepage response of Kentucky cofferdams. In Figure 3.12, “wet construction” only uses the buoyant densities for the cellular fill material and the berm without explicitly assigning pore pressure distribution in the cofferdam model. In addition to simplify the analysis, this approach is done to rigorously demonstrate the difference in the mechanical response of the cofferdam between the “dry construction” that uses dry material density and the “wet construction” that uses the buoyant material density. In practice, the “wet construction” means the water from the upstream reservoir is continuously allowed to seep into the cofferdam cell and then flow toward the downstream berm. In the long term, this “leakage” through the cell sheet piles will

establish the steady state pore pressure distribution indicated by the shape of the phreatic line that will appear like the assumed one in Figure 3.12.

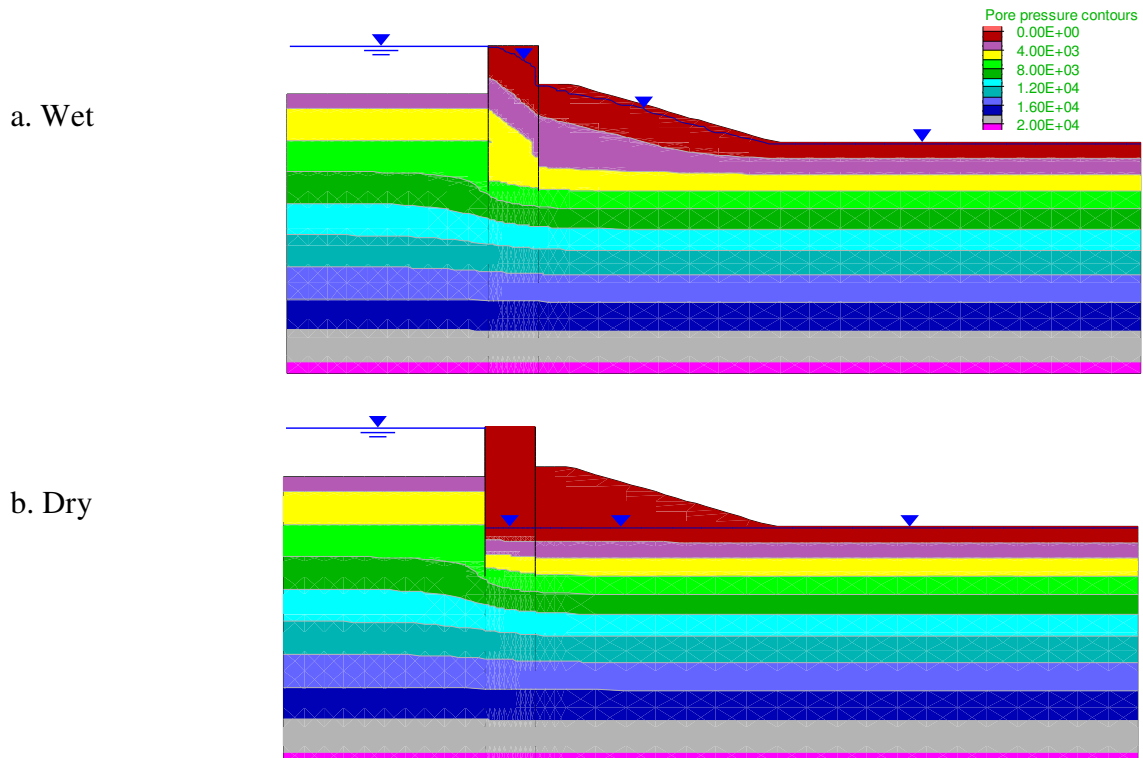


Figure 3.12. Typical pore pressure contours for the (a) wet and (b) dry construction practices used in the stability analysis of the proposed design concept in FLAC.

There are several potential risks of seepage to long term and more permanent use of “wet construction” of cellular cofferdams such as seepage-induced piping and erosion downstream of the dam.

3.1.5.1 Seepage through the Cell Fill

As said before, for “wet construction,” as is the case for the Kentucky cellular cofferdam, the seepage of water through the cellular fill must be accounted for to obtain an estimate of the factors of safety. There is no seepage through cell fill for “dry” conditions as it is designed to keep cell fill dry during operation using asphalt liner or concret liner. Therefore, seepage response of the cell fill for design concept #1 in “wet construction” has been calculated.

According to USACE (1989), The zone of saturation within the cell fill is influenced by the following factors: Leakage of water into the cell through the outboard piles, drainage of water from the cell through the inboard piles, lower permeability than expected of the cell fill, flood overtopping the outboard piles or wave splash, and possible leakage of water into the cell fill from any pipeline crossing the cells.

Figure 3.13 shows the typical seepage response (i.e., pore pressure field) of design concept #1 when the “wet construction” is simulated. In practice, the “wet construction” means the water from the upstream reservoir is allowed to seep into the cofferdam cell and to flow toward the downstream berm. In the long term, the fluid flow will reach the steady state pore pressure distribution as indicated by the shape of the saturation lines as appear in Figure 3.13.

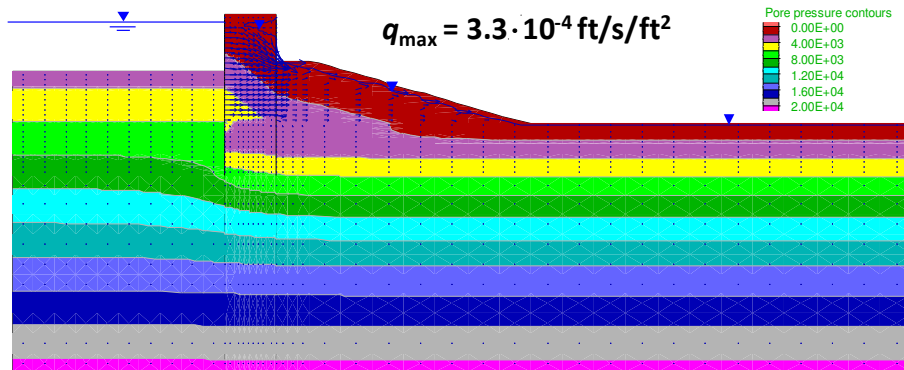


Figure 3.13. Typical pore pressure contours of the design concept # 1 (wet).

Figure 3.13 shows that if the wet construction is used, there is no significant difference in the maximum outflow rate in the cofferdam. FLAC simulation shows that the maximum flow rate is averagely around $q_{\max} = 3.0 \cdot 10^{-4}$ ft/s/ft². However, it is the corresponding mechanical response that matters.

3.1.5.2 Seepage through the Foundation

Cofferdams are primarily used for dewatering of construction areas and must sometimes withstand very high differential heads of water. Since, the foundation of design concept #1 is bedrock, seepage through foundation is less likely to happen, but if the cofferdam is supported on sand, seepage of water from the upstream to the downstream side will occur through the sand underneath the sheet piles as shown in Figure 3.14.

The possibilities of different types of failures due to seepage through granular soils can be studied by flow net analysis. In Figure 3.14, H_w is the height of water from top of the cell to location of pile fixity, H_s is height from top of overburden to location of pile fixity, h is height from top of the cell to bottom of berm (Ground water table), H_b is the height from top of the berm to location of pile fixity, and B is width of the cell.

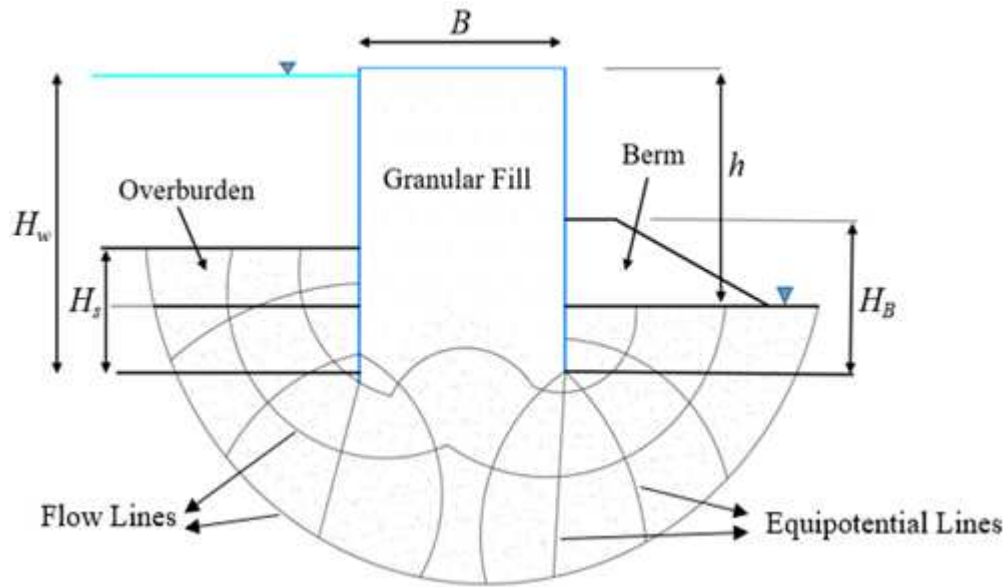


Figure 3.14. Partial flow net beneath a cell on sand base on USACE (1989).

In the Figure 3.14, the upstream and downstream surfaces of the permeable layer are equipotential lines, and all flow lines intersect them at right angles. Also, the boundary of the impervious layer and surfaces of the sheet pile are flow lines. The equipotential lines intersect the sheet pile at 90° .

In this theory, total discharge through all channels, per unit width of the structure, is equal to:

$$q = \frac{N_F}{N_d} K \Delta H \quad (3.13)$$

where N_F is number of flow channels, N_d is number of potential drops, K is coefficient of permeability of foundation, and ΔH is the difference between height of water upstream and downstream of the cellular cofferdam. Using equation (3.13), the total discharge beneath a cell on sand can be calculated.

If total discharge is too high, there are some solutions for seepage reduction to reduce water pressures and seepage forces in the critical exit area downstream of the cofferdam. The methods used include: impervious cutoffs, grout curtains, upstream impervious blankets, and drainage to reduce water pressures in the embankment and foundation soils.

3.2 Geological Hazards

In order to study the main design issues during operation of cellular cofferdams, the geological hazards are taken into considerations. Geological hazards include extreme flooding leading to overtopping of the dam, and earthquakes.

3.2.1 Overtopping and Emergency Spillway

One of the loadings that makes the cofferdam vulnerable is the overtopping loading from the increase of the upstream water level. Cofferdams are sensitive to overtopping depending on the materials and configuration and even environmental conditions. Failure mechanisms of overtopping is usually the consequence of an extreme flood and often the cause of partial or complete failure. In addition to creating additional lateral pressure on the upstream sheet pile, the overtopping flow will cause hydro-dynamic forces to act on the rockfill part in the downstream berm, dragging the rockfill materials and causing instability of the entire cofferdam (Larese et al., 2009).

Figure 3.15 illustrates an overtopping phenomenon in which there is an overflow from the increment of the upstream water level (ΔH_w) relative to its existing depth (H_w). This overflow may eventually induce cofferdam failure due to the continuous erosion process on the face of the downstream berm or piping through the embankment. Statistical analysis has shown that overtopping failure due to erosion or piping accounts for more than 30% of dam failures (Costa, 1985; Foster et al., 2000; Jandora and Říha, 2008; USBR, 2012). Nevertheless, the failure is less likely to facilitate breaching in rockfill dams than in earthfill dams due to the inherent cohesion of rockfill materials.

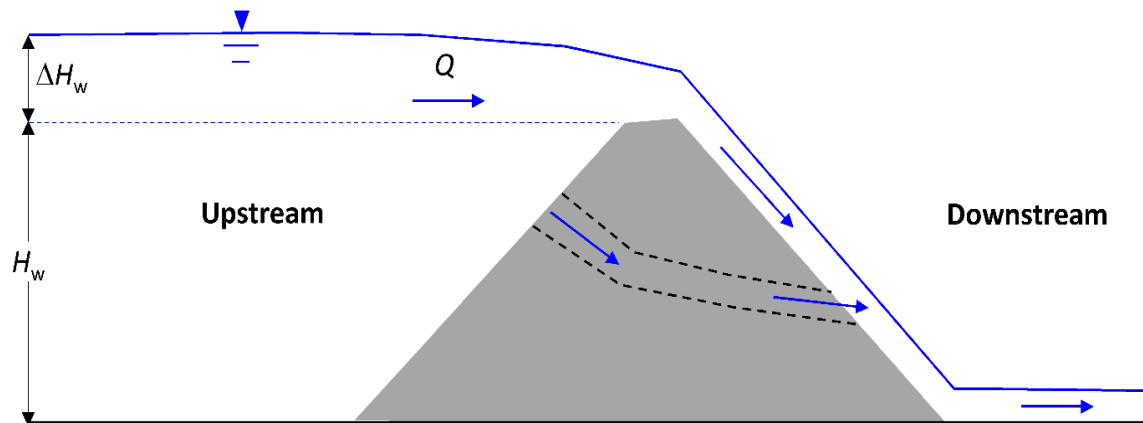


Figure 3.15. Illustration of overtopping and piping phenomena.

Various researchers in geotechnical engineering have performed a number of numerical simulations of dam instability due to flow overtopping. Among others, Martin and Clough (1990) and Mosher (1992) performed three-dimensional finite element analysis to investigate the effect of extreme differential loadings on the response of Lock and Dam No. 26. Simulated as a multiplication of flood load (corresponds to the maximum upstream water level, H_w), the overtopping load caused an increase in sheet pile deflection and subsequent decrease of the factor of safety (FS) of the cofferdam (Figure 3.16). In addition to being simple, their technique provides an insight for how to approximate the uncertainties in the amount of discharge flow, Q , that is overtopping the cofferdam.

The load-deflection and load-factor of safety (FS) responses for design concept #1, are now summarized. This is done to reconfirm that the general trend of the results from the overtopping analysis in this study corresponds to that in the previous research (Martin and Clough, 1990; Mosher, 1992).

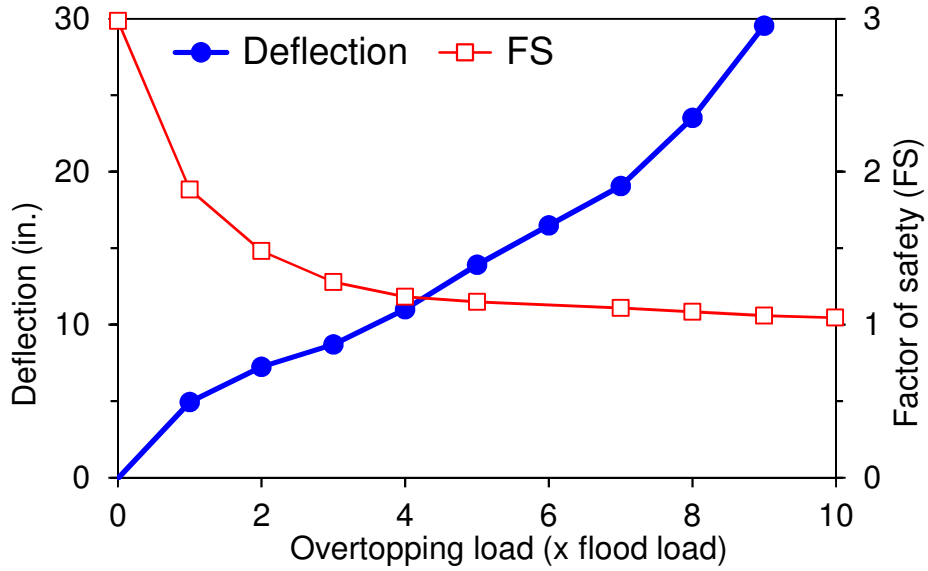
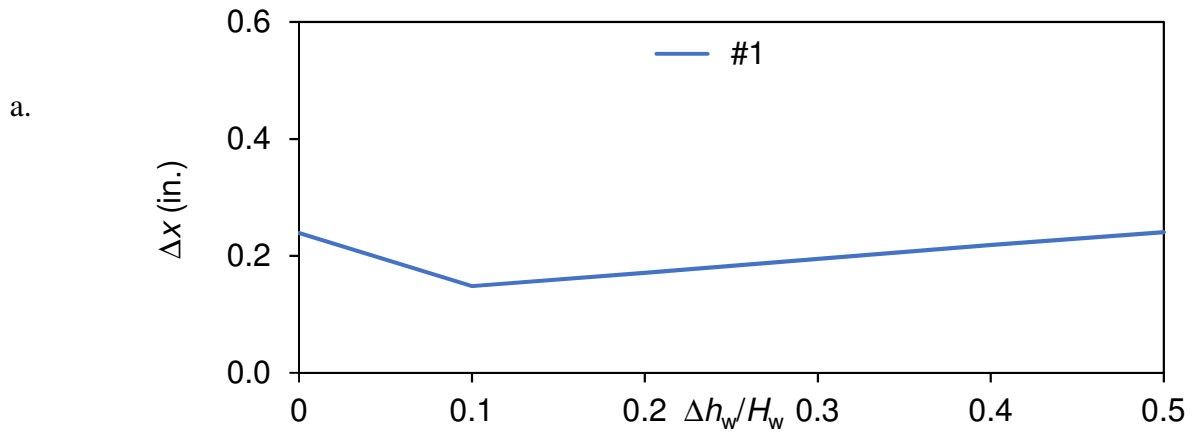


Figure 3.16. Increase in sheet pile deflection and subsequent decrease in FS of the cellular cofferdam in Lock and Dam No. 26 (Martin and Clough, 1990; Mosher, 1992).

Figure 3.17a plots the maximum deflections of the upstream pile tip for different overtopping loads for design concept #1. As has been seen in the preceding results, greater pile tip deflections are observed with the increase of $\Delta H_w/H_w$ ratios. Correspondingly, the FS of proposed design concept decreases with the increase of $\Delta H_w/H_w$ ratios (Figure 3.17b). This trend is similar to that for Lock and Dam No. 26 as plotted in Figure 3.16.



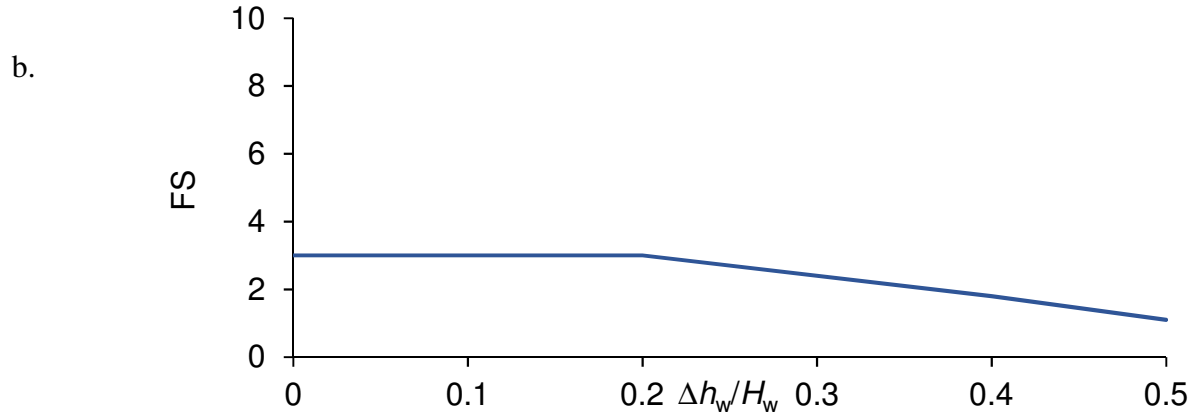


Figure 3.17. Plot of (a) maximum cell deflection and (b) FS against overtopping loads for design concept #1.

In particular, an increase in the degree of compression and tension experienced by the upstream pile and a deflection of the pile toward the downstream side is observed. Consequently, the factor of safety for the design concept decreases with the increase of the overtopping loads. The increase in $\Delta H_w/H_w$ ratios also causes an increase in the saturation value and distribution in the downstream berm. Consequently, an increase in the induced displacement in the berm will be observed, reducing the stability of the berm. Due to the overtopping loads, the stability of the cofferdam designs would be largely controlled by the stability of the downstream berm.

Manual calculations of $FS_{\text{overtopping}}$ are based on different overtopping loads and resisting force. During overtopping, construction of cofferdam becomes wet that gives the lowest factor of safety against overtopping. Factor of safety against overtopping is equal to:

$$FS_{\text{overtopping}} = \frac{\text{Resisting}}{\text{Overtopping Load}} \quad (3.14)$$

The range of factor of safety starts from 3 to 1.1 which are not very reliable and stable. Therefore, a proper emergency spillway and a new design of cofferdam can be considered to reduce overtopping and to prevent construction failure.

3.2.1.1 Design of More Stable Cofferdam against Overtopping Failure

There should be a design procedure for situations that overtopping occurs. There are two parts that should be taken into consideration for making cellular cofferdams more stable:

1) Design of “dry” concept during construction.

Significant increases in factors of safety are obtained when seepage was prevented and the cellular fill material and the downstream berm were kept dry, which is to be accomplished through the use of waterproof elements inside the cofferdam. The numerical modeling using FLAC also show the potential increased stability and performance of “dry construction” of cellular cofferdams. “Dry construction” can be achieved by adding a waterproof seal inside the cell to encapsulate the cellular fill material. The seal will prevent seepage and keep the cellular soil fill dry. One potential seal material is asphalt, which is highly impermeable. Moreover, top of the cells can be covered with concrete or asphalt cap to keep cell fill dry as discussed in chapter 1. The performance of the “dry construction” of cellular cofferdam as analytically and numerically demonstrates that with the “dry construction” modification, cellular cofferdams can be potentially used as more stable permanent structures especially for improving stability against overtopping.

2) New design of the berm.

In general, foundation and downstream slope are believed to be potential locations at risk in terms of overtopping failure. Using computational results of FLAC, a new design of a high berm with fill materials that have large number of permeability is shown in Fig. In this design, the berm material is rockfill that have large number of permeability due to have ability to allow water to pass through it. Moreover, because of the height of the berm, overtopping is less likely to occur on downstream of the cofferdam.

Figure 3.18 illustrates the overtopping loadings that are applied to proposed design concept #1 of the Kentucky cellular cofferdam. In the upstream side, the increase of water level is represented by the increase in hydrostatic pressure due to the increment of water level ΔH_w . In the downstream side, the overtopping flow Q is represented by applying the discharge flow q that acts normal to the downstream berm. In this part, only the “dry construction” technique is used for the overtopping analysis. This simplified but realistic approach combines that proposed by previous researchers to assess the effect of extreme differential loadings on cofferdam and slope stabilities

in weak ground (Acharya et al., 2016; Chinkulkijniwat et al., 2016; Martin and Clough, 1990; Mosher, 1992; Wu and Xia, 2014).

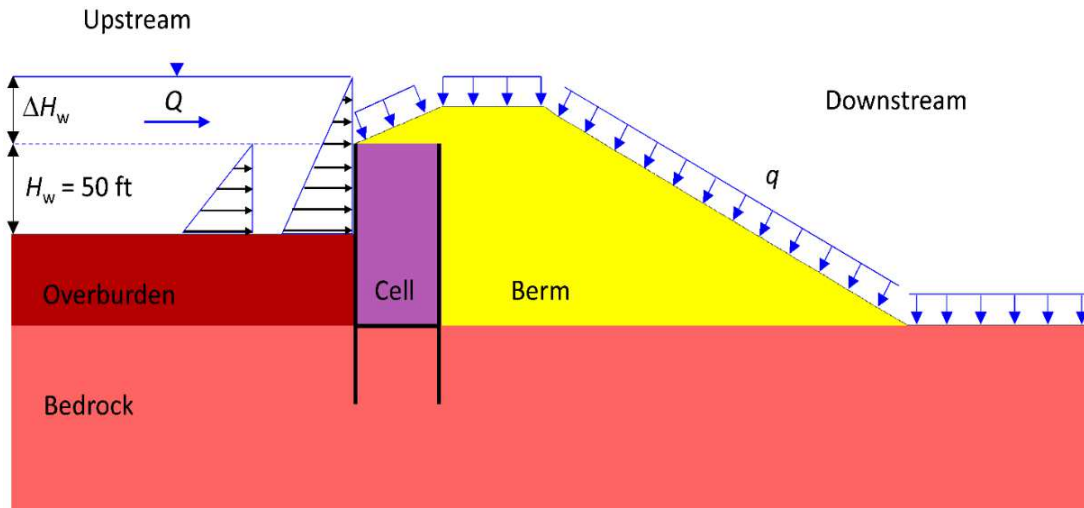


Figure 3.18. Geometry of new design of cellular cofferdam.

To accommodate uncertainties in the degree of overtopping loads, a parametric study is performed to observe the mechanical response of the cofferdam and its stability under various $\Delta H_w/H_w$. Table 3.5 presents various water level increments ΔH_w to be applied as hydrostatic pressure in the upstream side and its corresponding overtopping flow Q to be applied as discharge flow q in the downstream side. The ratio $\Delta H_w/H_w = 0.0$ corresponds to the flooding load that has been applied to each design concept for the Kentucky cofferdam, i.e., $\Delta H_w = 0$ ft and $H_w = 50$ ft.

Table 3.5. Various water level increments ΔH_w and their corresponding discharge loading q .

$\Delta H_w/H_w$	Water level increment ΔH_w (ft)	Discharge flow q (ft/s)
0.0	0	0.0
0.1	5	$2.9 \cdot 10^{-6}$
0.2	10	$5.8 \cdot 10^{-6}$
0.4	20	$1.2 \cdot 10^{-5}$
0.5	25	$1.5 \cdot 10^{-5}$

For each ΔH_w in Table 3.5, the discharge flow q is applied normal to the downstream berm and is assumed to accumulate over a period of twenty days. This is done to represent the circumstance of overtopping flow that is occurring at moderate intensity and duration.

A gradual increase of upstream water level was also reported during December 1982 and April 1983 in which the increased depth of the Mississippi River threatened to overtop Lock and Dam No. 26 (Martin II and Clough, 1990; Mosher, 1992). The model is then run to mechanical equilibrium and factor of safety calculation is subsequently performed to investigate the effect of the overtopping loadings on the mechanical response and stability of each of the cofferdam design concepts, respectively. Further, for overtopping analysis, the friction angle ϕ of the rockfill for the fill/berm material has been set to 40° . This value is taken from the section 3.1.4 as the minimum friction angle that gives $FS \geq 3.0$ in design concept #1. The material and sheet pile properties used for overtopping analysis are listed in Tables 2.1 and 2.2.

These two ways together can increase the factor of safety against overtopping, but for stability analysis new calculation should be used due to have different height and material of downstream berm and different height of upstream water. Due to the new design of the berm and water level, manual calculation of factor of safety against design issues should be modified using buoyant unit weight (γ_b) instead of dry unit weight (γ_{dry}) for the berm material and different height of upstream water ($H_w + \Delta H_w$).

3.2.1.2 Design of Emergency Spillway

Spillway is an important relationship between the storage capacity of a reservoir and the discharge capacity of hydraulic structures. A spillway is a structure used to provide the controlled release of flows from a dam into a downstream area. An emergency spillway is designed to provide additional protection against overtopping of a dam and is intended for use under unusual or extreme conditions. Having an emergency spillway is necessary for more permanent cofferdams to induce overtopping through downstream of the cofferdam. Figure 3.19 shows a design concept of emergency spillway for cellular cofferdams. A spillway can be located on rock or soil foundations, but if available, it is highly recommended that a spillway be located on a rock

foundation. More robust design and construction considerations will be needed for a soil foundation.

The emergency spillway should be located where the overtopping is most likely to happen. The size and width of a spillway depends on the size of cells and cofferdam. The emergency spillway can be located at the first or middle, or end of cellular cofferdam. Figure 3.19 shows the emergency spillways that are located at the middle and the end of the cellular cofferdam. It is very important to understand that a spillway is a key feature of a dam, and its location and size are critical to ensure reliable and safe reservoir operations that meet project operational needs.

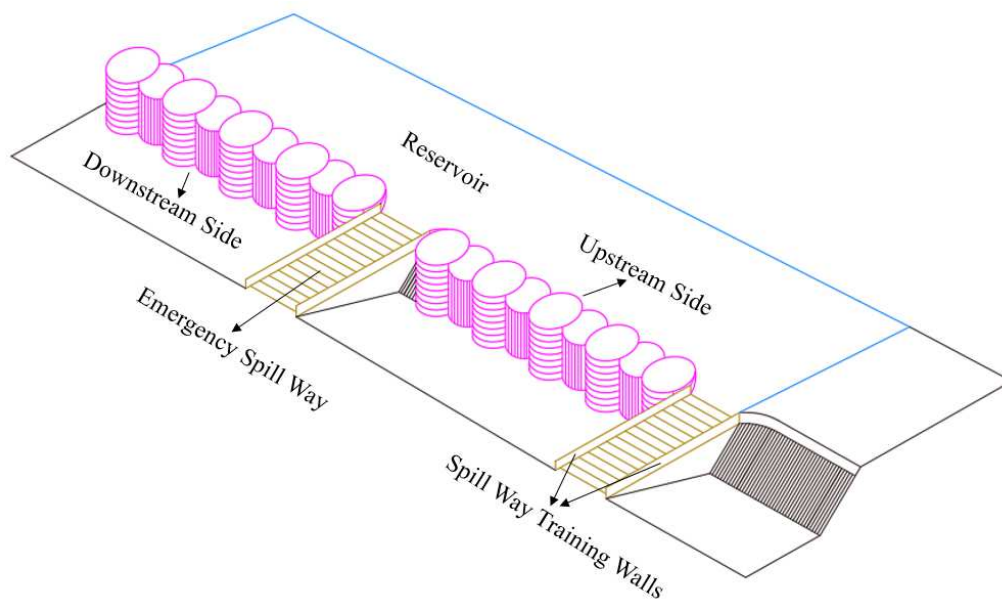


Figure 3.19. Geometry of emergency spillway for cellular cofferdams.

3.2.2 Earthquake Hazards

One of the most commonly hazards that can fail a cofferdam is earthquake. As earthquake ground shaking affects the cofferdam body and structures and all hydromechanical components of a cofferdam project at the same time. All these elements have to be able to resist some degree of earthquake action. Stability analysis against earthquake failure can be done using manual calculations. Theory of Mononobe-Okabe is the one that is used.

Mononobe-Okabe (M-O) method is still employed as the first option to estimate lateral earth pressures during earthquakes by geotechnical engineers. Considering some simple

assumptions and using a closed form method, M-O solves the equations of equilibrium and suggests seismic active and passive lateral earth pressures. Mononobe and Matsuo (1929) and Okabe (1927) proposed a method to determine lateral earth pressure of granular cohesionless soils during earthquake. The method was a modified version of Coulomb theory (1977), in which earthquake forces are applied to the failure mass by pseudo-static method. To get a final simple formulation like other closed form solutions in geotechnical engineering, M-O uses exact form solution with simple assumption such as simplicity in geometry, material behavior, or dynamic loading to make the equations solvable (Yazdani et al., 2013).

The original M-O method, uses retaining wall angle (α) and backfill angle (β) which are irrelevant to design of Kentucky cofferdams. It is because the berm and overburden in cellular cofferdams, are designed to be perpendicular to the ground surface. Therefore, the original M-O method should be modified. Figure 3.20 shows the parameters and characteristics of Modified M-O method. In M-O method, static force equilibrium is satisfied for a rigid wedge placed on a failure plane with elastic-perfectly plastic behavior based on Mohr-Coulomb failure criteria.

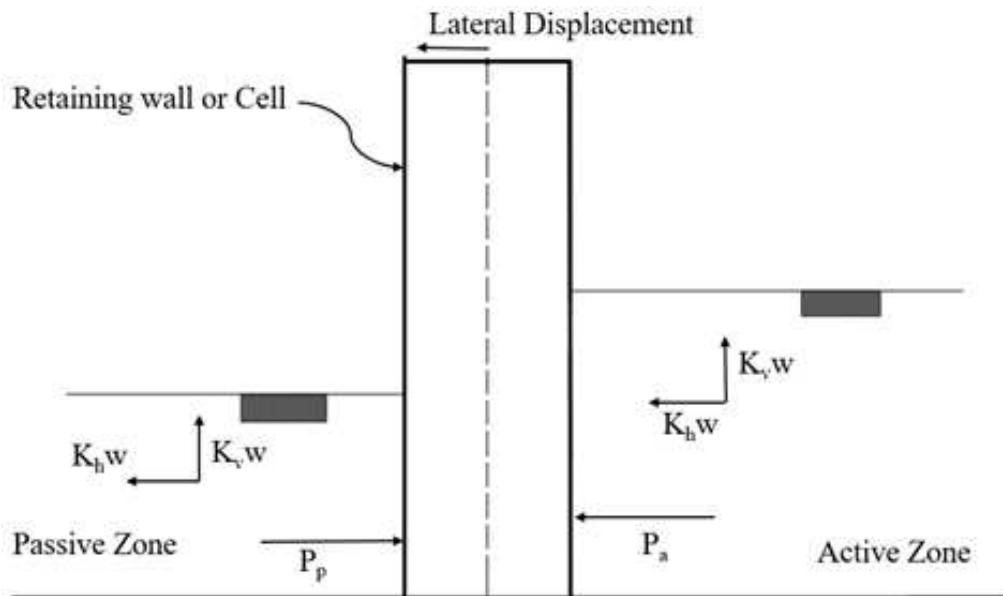


Figure 3.20. Geometry and parameters of modified M-O method.

In Figure 3.20, K_h and K_v are horizontal and vertical acceleration coefficients. Active and passive forces of Modified M-O method, can be calculated using the following equations:

$$\begin{pmatrix} P_a \\ P_p \end{pmatrix} = \frac{1}{2} \gamma H^2 (1 - K_v) \begin{pmatrix} K_a \\ K_p \end{pmatrix} \quad (3.15)$$

$$\begin{pmatrix} K_a \\ K_p \end{pmatrix} = \left[\cos^2(\phi - \theta) \right] \times \left\{ \cos \theta \times \cos(\delta + \theta) \times \left[1 \pm \left(\frac{\sin(\phi + \delta) \times \sin(\phi - \theta)}{\cos(\delta + \theta)} \right)^{1/2} \right]^2 \right\}^{-1} \quad (3.16)$$

$$\theta = \tan^{-1} \left(\frac{K_h}{1 - K_v} \right) \quad (3.17)$$

where H is wall height, δ is soil-wall friction angle, γ is soil unit weight, ϕ is soil interaction friction angle, K_h is horizontal earthquake coefficient, K_v is vertical earthquake coefficient, P_a is active forces, P_p is passive forces, K_a is Rankine active earth pressure coefficient, and K_p is Rankine passive earth pressure coefficient.

In the original M-O method, water table is not considered directly in the model, and the earth pressure is given only for the “dry construction.” Using this method instead of equations (3.1) and (3.2), gives different earth pressure coefficients and different earth pressures. Therefore, different earth pressure diagrams and bending moment diagrams will be used. Mononobe-Okabe (M-O) is a reliable way to design a more stable cofferdam against earthquake hazards in “dry construction.”

3.3 Structural Hazards

In order to study the structural hazard of cellular cofferdam, analytical and numerical calculations are performed based on the design of piles. The structural failure of sheet piles forming the cofferdam walls happens when proper calculations of bending moment of piles are not considered in the design.

3.3.1 Structural Design of Piles

Structural failure of piles can occur during construction (installation) and during operation due to water pressure from the reservoir. Estimating and analyzing bending moments of steel sheet piles of Kentucky cofferdams during construction and operation, is the first step of this chapter.

Figure 3.21 shows the bending moment (in ft-lbs) diagrams along the length of both the upstream and downstream steel piles during construction. The maximum bending moment for the left pile is $1.06 \cdot 10^6$ ft-lbs and occurs at about 15 ft below the dredge line. For the downstream pile, the maximum bending moment is $5.56 \cdot 10^5$ ft-lbs and occurs at about 15 ft below the top of the berm. These bending moments can be divided by the section modulus of the steel pile to obtain the maximum bending stresses along the piles. It is expected that the bending stress are much smaller than the allowable strength of steel, and consequently, bending failures are not expected. The bending moment diagrams are similar to the behavior of steel sheet piles embedded in sand with sand backfill as used for retaining walls.

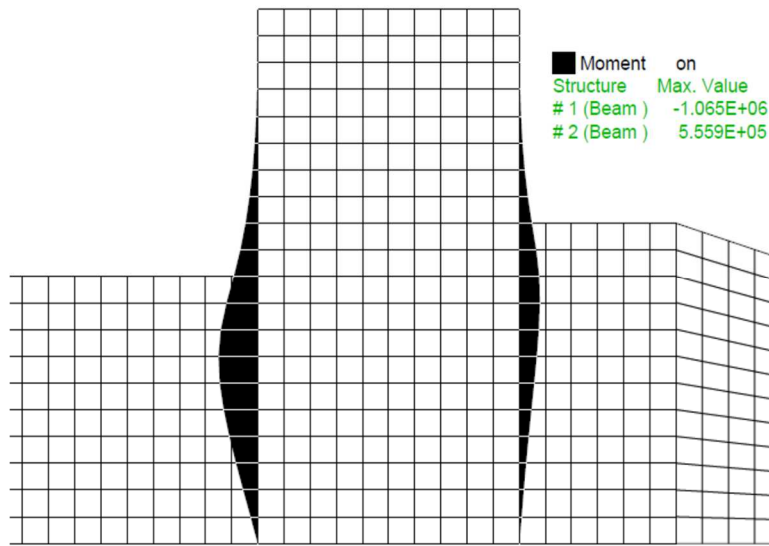


Figure 3.21. Bending moment (in ft-lbs) diagrams along the length of both the upstream and downstream steel sheet piles during construction of the Kentucky cofferdam.

Figure 3.22 shows the bending moment (in ft-lbs) diagrams along the length for both the upstream and downstream steel piles after the application of the water pressure from the reservoir. The maximum bending moment for the left pile is $1.6 \cdot 10^6$ ft-lbs and occurs at about 15 ft below

the dredge line. The bending moment in the upstream pile increased by $540 \cdot 10^3$ ft-lbs due to the applied reservoir water pressure. For the downstream pile, the maximum bending moment is $1.24 \cdot 10^6$ ft-lbs and occurs at about 15 ft below the top of the berm. The bending moment increased by $680 \cdot 10^3$ ft-lbs due to the applied reservoir water pressure. As said before, these bending moments can be divided by the section modulus of the steel pile to obtain the maximum bending stresses along the piles.

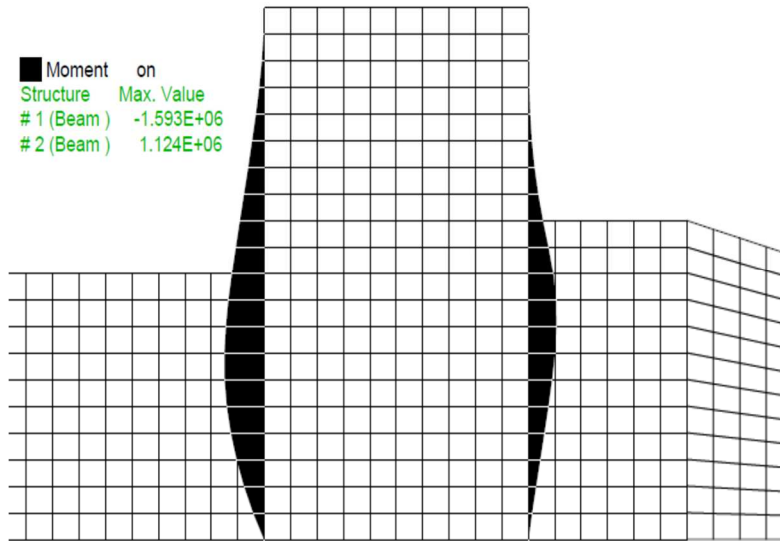


Figure 3.22. Bending moment (in ft-lbs) diagrams along the length of both the upstream and downstream steel piles due to water pressure from the reservoir.

It is also of interest to observe the structural response of the sheet piles of the proposed design concept # 1 based on numerical results. Figure 3.23 shows the distribution of the induced bending moment in both piles for the “wet” and “dry” construction. The bending moment is considered positive when the pile’s face towards the upstream side experience tension.

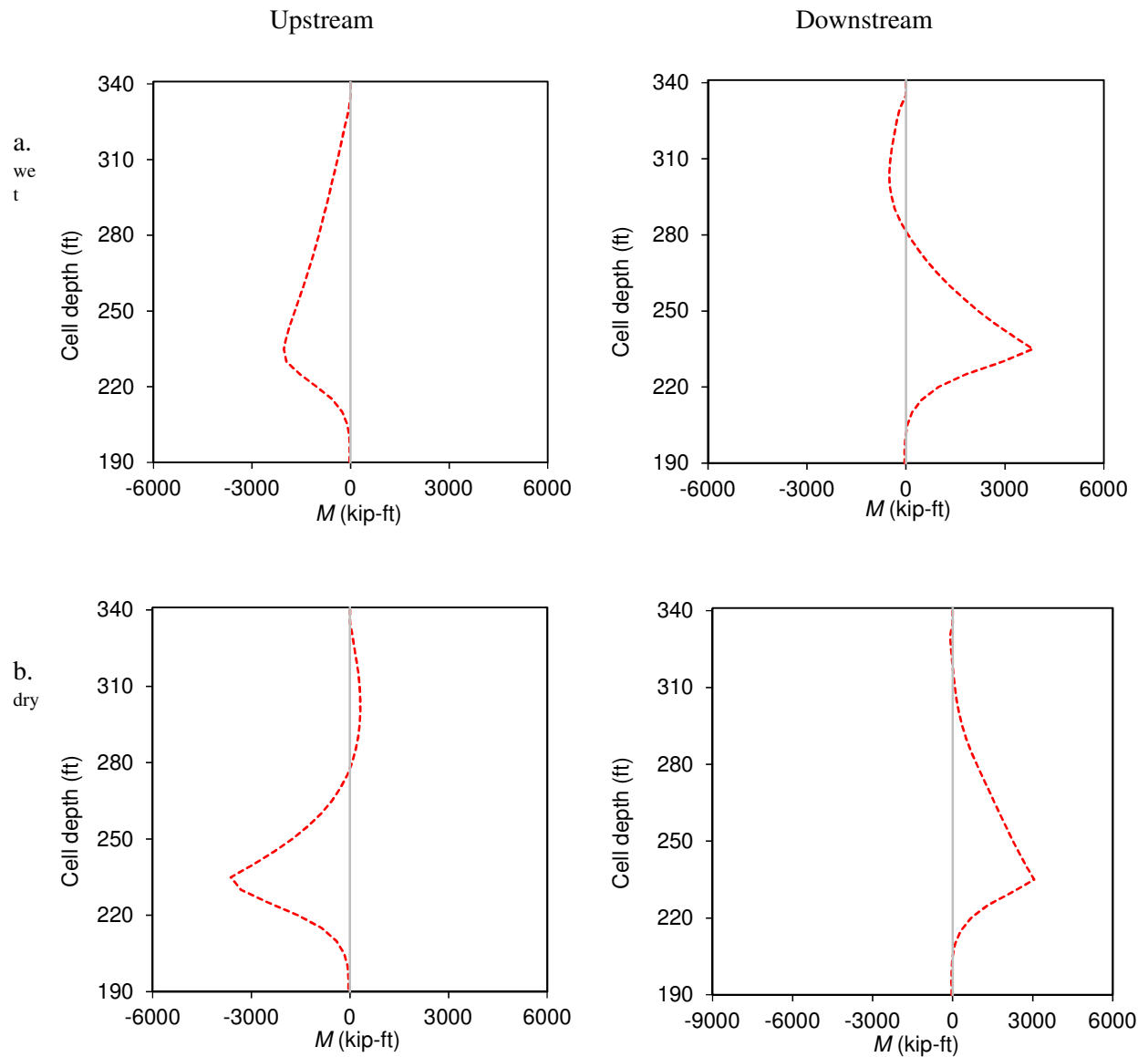


Figure 3.23. Comparison of bending moments of the design concept #1 for a. “wet” and b. “dry” constructions.

Of all computational results, with the “wet construction,” most of the inner side of the upstream cell experiences compression while that of the downstream cell experiences tension. Only the upstream cell experiences tension in the inner side of the cell. With the “dry construction,” both cells in design concept #1, experience tension in the inner side of the cell. This bending moment response corresponds to that appears in Iqbal (2009). The “wet construction” has less influence in the structural response of the upstream pile. The degree of the induced moment, in the

“dry construction” is superior in the upstream pile than those in the downstream pile. Current study assumes the piles to behave elastically (i.e., the piles have infinite yield strength).

Manual calculations of bending moments and earth pressure forces acting on the sheet piles during operation have been done in order to compare and validate numerical and analytical results. There is just a difference between the calculations of bending moments in analytical and numerical ways. As said before, the bedrock is not included in the numerical modeling as it is assumed to be impermeable and much stiffer and stronger than the sand, but the bedrock is included in the manual calculations of bending moments based on bedrock properties shown in Table 2.1. It has been done in order to see the difference of diagrams with and without bedrock properties.

Earth pressure calculations are necessary for estimating maximum bending moments in upstream and downstream sides of the cofferdam. The first step is to find and calculate active and passive forces acting on both sides of cofferdam. Using retaining wall calculations, active and passive earth pressures (in lbs/ft²) and the points that they act on the sheet piles can be determined. According to the geometry of design concept #1, and the soil properties shown in Table 2.1, earth pressure diagrams are plotted as shown in Figure 3.24. As can be seen, forces acting on the upstream and downstream of the sheet piles are different based on different active and passive earth pressures and various layers and properties of the soils.

After calculations of the earth pressures, bending moment diagrams are plotted. Figure 3.25 shows the bending moment (in ft-lbs) diagrams along the length for both the upstream and downstream steel piles in “wet construction” for design concept # 1 after the application of the water pressure from the reservoir. The maximum bending moment for the left pile is $1.3 \cdot 10^6$ ft-lbs and occurs at about 35 ft below the top of the overburden. For the downstream pile, the maximum bending moment is $7.1 \cdot 10^6$ ft-lbs and occurs at about 3 ft below the dredge line.

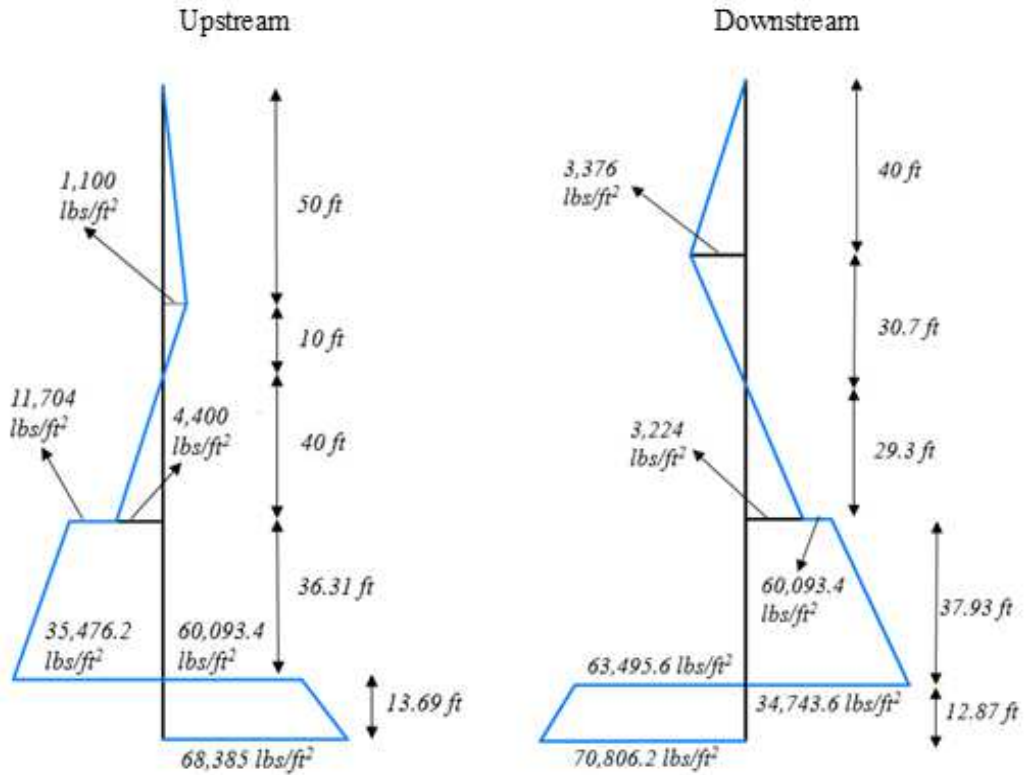


Figure 3.24. Earth pressure diagrams acting on sheet piles of design concept #1 during operation in the “wet construction”.

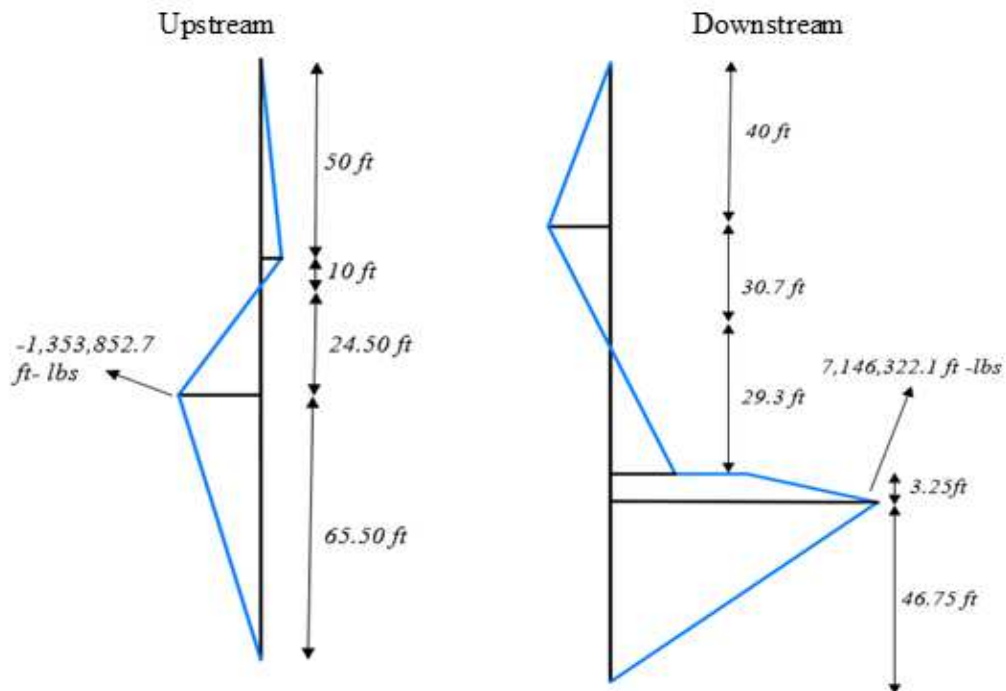


Figure 3.25. Bending moment diagrams of design concept #1 during operation for “wet construction”.

In the manual calculations, the buoyant unit weights are used for all properties of soils because it is assumed that all soils are saturated in overburden, cell fill, berm, and bedrock. Comparing bending moment diagrams of “wet construction” in Figures 3.23a and 3.24, shows that diagrams are very similar to each other, but the maximum bending moments are different. It is because of differences between bedrock properties in the numerical and analytical calculations. Moreover, there are jumps in the bending moment and earth pressure diagrams that occur in boundary of layers.

CHAPTER 4

ENVIRONMENTAL AND ECONOMIC IMPACTS OF PERMANENT CELLULAR COFFERDAMS FOR HYDROPOWER USE

4.1 Reduction of Environmental and Economic Impacts

The World Commission on Dams estimates that 40-80 million people have been displaced by dam construction in living memory. The building of dams often brings unintended social consequences. It is estimated that almost a quarter of a million square kilometers of land have been inundated by the impoundment of river waters over the last century, as can be seen in Figure 4.1, for instance, in distribution of dams in the U.S (KDNG, 2007).



Figure 4.1. Distribution of dams in the U.S.

One of the main environmental risks posed by the construction of large dams is the disturbance of the natural ecologies. Major of impacts altered ecologies include the destruction of the habitat of local living organisms including potentially endangered species, and the growth of other species including potentially waterborne disease vectors (Baba and Hirose, 1998). The use of cellular cofferdams as proposed in this study is meant to reduce environmental impacts of hydropower dam constructions.

The aim of this project is to develop technologies that will allow construction of hydropower dams within a maximum time of two years. The construction cost and time of hydropower cellular cofferdam will be much less than conventional earthfill or concrete hydropower dams due to less amount of foundation work required in the cellular cofferdams. One of the most important problems of traditional hydropower dams is the huge costs of construction and the long time it takes to build them. For example, Itaipu Dam (Figure 4.2) cost \$20 billion and took 18 years to build. Actual costs for hydropower dams are almost always far higher than estimated costs on average around 30 percent higher. Internationally private investors in power projects are largely avoiding large dams and prefer to invest in cheaper and less risky gas-fired power plants (Kundzewicz et al., 2007).



Figure 4.2. The Hydropower Itaipu Dam located on border between Brazil and Paraguay.

The manner to which the reduction in environmental and economic consequences will be achieved in conjunction with advantages of the proposed cellular cofferdam design concept #1 are listed and explained in following sections.

4.1.1 In-Water Construction

One of the major negative consequences of constructing dams is the need to divert river flow during construction. This requires the construction of diversion tunnels or channels which modifies the river environment, alters river flow already at the construction stage, and increases significantly the construction expenses due to instalment of additional equipment as well as

construction time. Figure 4.3 shows Olmsted hydropower dam that has cost three billion dollars to construct. One of the biggest contributors to this price was in-water construction problem which emphasizes the important advantages of cellular cofferdams (States and Accountability, 2017).



Figure 4.3. Olmsted Locks and Dam project at Ohio River, Illinois, U.S.

The proposed cellular cofferdam design can be constructed in water which avoids the need to divert water flow during construction. The overall environmental footprint is reduced by avoiding diversion of the river during construction, and by the ability to completely remove the dam from the site. Cellular cofferdams also allow excavation and construction of structures in otherwise poor environment.

One of the most significant savings of the proposed design concept in terms of construction time and expenses accrue from avoiding the need for two construction stages with a temporary structure to divert water and a final dam structure. In the case of cellular cofferdams, the temporary structure becomes part of the final structure. Moreover, the cofferdam can be decommissioned more easily than conventional dams and while the main cofferdam structure is in water. Shorter construction time and ease of removal reduce the construction cost. In almost all existing old hydropower dams, decommissioning and removal have not been fully considered.

4.1.2 Fast and Low-Cost Construction

Hydropower dams are usually very expensive and complex structures that require major investments and several years to plan and construct. Using cellular cofferdams, it is envisioned that medium-sized 10 to 50 ft hydropower dams can be rapidly built and deployed in a maximum of two years, which is longer than typical time it takes to build temporary cellular cofferdam structures but much shorter than typical construction times for conventional concrete and earthfill dams. Cellular cofferdams require only several weeks to a few months to complete a single cell, and several cells can be constructed simultaneously. It is projected that hydropower dams based on cellular cofferdam design and construction will be versatile and have less impact on the environment based on faster construction time than conventional hydropower dams.

During construction, time is of great importance to the owner. Less time results in less money being spent. It is because of less expenses in labor and equipment using in the construction process. Figure 4.4 shows a cellular cofferdam which was built very fast for the purpose of constructing the Olmsted Lock and Dam (Schneider, 2014).



Figure 4.4. A cofferdam on the Ohio River near Olmsted, Illinois, U.S.

In contrast to traditional dams which require specialized and heavy-duty construction equipment, cellular cofferdams require only standard construction equipment which contribute to reduced construction time and cost. This standard type allows any average-sized contractors with minimal fleet of equipment to construct the dam. The ability to engage contractors with different

levels of capability allows for more competitive bids thereby lowering the construction cost. Also, smaller size of cellular cofferdam results in lower construction cost due to the less amount of equipment and materials.

4.1.3 Easy to Reconfigure, Modify and Dismantle

One of the major environmental and economic impacts of conventional dams is that they become nearly permanent structures that are difficult and costly to dismantle. In cellular cofferdams, the construction can be carried out rapidly, and the completed structure can be suitably modified during their lifetime and easily removed after completion of its intended lifetime. Cellular cofferdams can be easily configured to different arrangements by using combinations of several interconnected cells. Steel sheet piles are easily installed and removed. (Gilbert, 2011). All of these factors and benefits make a huge difference between construction costs of traditional dams and cellular cofferdams. Figure 4.5 is a representative example to show the difficulties existed in removing and dismantling the traditional dams. The removal process for the small dam on the Elwha River lasted more than eight months and cost a lot of money. Removal of the Elwha Dam began in September 2011 and was fully complete by March 2012 (Warrick et al., 2015).



Figure 4.5. Dam Removal on the Elwha River in the Olympic Peninsula, Washington. U.S.

Dismantling usually entails a major operation requiring: 1) re-diversion of the water, 2) destruction of the dam by explosives, and 3) disposal of the dam material. In order to achieve minimal economic and environmental impacts, removal of the cellular cofferdams can be planned

and executed with the same degree of care as its installation. This is achieved by leaving the cellular cofferdam as the last structure to remove, then allowing the water to flood the downstream side leaving the main cellular cofferdam submerged in water. The granular fill inside the cellular cofferdams can be removed while the steel piles forming the cells are left standing. Steel sheet piles extending below the permanent structure can be cut off and left in place, where their environmental impact on the foundation soil will be minimal (Bulletin, 2011).

4.1.4 Recycling of Construction Materials

For the construction of dams, natural materials such as soils and rocks are required and must be extracted from surrounding areas. This material extraction can cause damage to the environment. In cellular cofferdams, the construction cost and extraction expected to be much less than conventional earthfill or concrete hydropower dams due to reduced work on the foundation and the main structure. Construction materials of cellular cofferdams also can be local filling material or construction wastes. Moreover, steel templates used in the construction of one cell can be recycled and re-used in the entire construction. There is a long industry track record in the construction and use of cellular cofferdams as temporary water exclusion structure in a wide range of conditions and applications that can show how to recycle and reuse the cofferdam material (Texas, 2009). Therefore, using cellular cofferdam as the core structure will maintain the adaptability to local conditions while maintaining low construction cost.

4.1.5 Reducing Footprint

For the construction of the earth dam a large base is required. The huge base has to be evacuated and major modification takes place. All this disrupts the ecological balance and results in adverse effects. Back waters are also a potential disaster for human life and property. This should be taken care of very well to avoid any harm. Big dams accumulate a large volume of water that can lead to an outbreak of water resulting in floods and a huge damage to life and property. Moreover, the building of large dams can cause serious geological damage as well as expensive construction cost (Gui and Han, 2009). For example, the building of the Hoover Dam (Figure 4.6) in the U.S. triggered a number of earth quakes and has depressed the earth's surface at its location.



Figure 4.6. Hoover Dam in Utah, U.S.

In cellular cofferdams, external forces and water pressures are resisted by the weight of the cofferdam and by embedment of the sheet piles into the ground. In general, cellular cofferdams will have smaller footprint than conventional concrete or earthfill dams which results in reducing environmental and economic impacts.

4.2 General Benefits of Cofferdams

In addition to contributing to reduced environmental impact, cellular cofferdams retain many of the advantages and benefits of dams. These are listed and discussed below.

4.2.1 Less Impacts on Climate Change

Hydropower is considered clean because it does not contribute to global warming, air pollution, acid rain, or ozone depletion. However, hydropower earth dams impact on environment of a region with increasing global population, global economy, electricity demand, renewable energy source and decreasing electricity gap, and climate change. In the proposed design concept, cellular cofferdam has less impact on climate change based on smaller construction and footprint. Developing technologies, tools, and strategies to evaluate and address environmental impacts are different solutions to increase resilience to climate change. The world's needs for water and energy are rising but unless these needs are met sustainably, social or environmental impacts will be huge.

Using cellular cofferdams instead of large dams helps to minimize environmental and social impacts.

4.2.2 Decreasing River Fragmentation

The environmental consequences of large dams include direct impacts to the biological and physical properties of rivers and environments. Most of the world's large rivers are fragmented by dams that alter migration patterns among fish populations and convert free flowing river to reservoir habitat (Tockner et al., 2014). The fragmentation alters the balance of plant and animal populations mainly because invasive species occupy disturbed ecologies and endanger native species. As a result, 40% of future dams will need to be constructed in regions that are either not impacted or moderately impacted in order to have less river fragmentation. In the case of cellular cofferdams, river fragmentation does not happen in a large scale because they do not have same impacts as large earth dams have. One reason is that the dams will be smaller and will be used only in smaller river channels, and other is that river diversion will not be required during construction.

The construction of dams is one of the major factors that is contributing to the loss of fish species worldwide. Some species are completely separated from their spawning habitats because the wall of the dam blocks fish migrations. That is why species become extinct and endangered. The alteration in fish migration can also affect plant and animal species that are dependent on their interaction with fish from the river system. Moreover, local fish species will not be adapted to the new environment that is present after a dam is built and do not survive, leading to the decreasing of local populations. This happens because of changes in river's flow, temperature, and local plant life. Smaller dams such as cellular cofferdams have less impacts on fish population, and eventually on surrounding ecosystems.

4.2.3 Recreation

In addition to benefits from hydropower generation, flood control and providing water supply for residential, industrial and agricultural uses, dams create artificial lakes that can be used for a variety of recreational purposes. Dams provide prime recreational facilities throughout the world. Boating, skiing, fishing, camping, swimming, picnic areas, and boat launch facilities are all

supported by dams (Figure 4.7). The lake that forms behind the dam can be used for water sports and leisure activities. Often large dams become tourist attractions in their own right. Recreational activities can be another benefit of cellular cofferdam for hydropower.



Figure 4.7. Recreational facilities of dams.

4.2.4 Flood Control and Destruction

Dams help prevent the loss of life and property caused by flooding. Flood control dams impound floodwaters and then either release them under control to the river below the dam or store the water for other uses. The flood control is an important benefit of cellular cofferdam as well. On the other hand, the flooding of large areas of land means that the natural environment is destroyed, because flooding can displace many different organisms such as plants, and wildlife. Also, people living in villages and towns that are in the valley to be flooded, must move out. This means that they lose their farms and businesses. In some countries, people are forcibly removed so that hydropower schemes can go ahead. Having less volume of water in upstream of the cellular cofferdams can be an advantage since flooding is less likely to happen (Jansen, 1983).

4.2.5 Water Storage

Another aspect of dam construction is its social impacts on the environment by increasing the water storages. Dams and cellular cofferdams create reservoir that supply water for many uses, including industrial, municipal, and agricultural. The lake's water can be used for irrigation

purposes and the percent of the world is irrigated using water stores behind dams. Thousands of jobs are tied to producing crops grown with irrigated water.

Hydropower which is generated with the help of dams gives electricity to a huge population of the world and if electricity is not needed, the sluice gates can be shut, stopping electricity generation. The water can be saved for use another time when electricity demand is high. The buildup of water in the lake means that energy can be stored until needed, when the water is released to produce electricity. For the cellular cofferdams, the volume of water can be used when there is the lack of available water resources to meet the demands of water usage within a region.

4.2.6 Sediment and Erosion Control

One of the first problems with dams is the erosion of land. Dams hold back the sediment load normally found in a river flow. After that the downstream water erodes its channels and banks. This lowering of the riverbed threatens vegetation and river wildlife. Dammed rivers also lack the natural transport of sediment crucial to maintaining healthy organic riparian channels. A major example of soil erosion problems is the Aswan Dam (Figure 4.8).



Figure 4.8. Aswan Dam, Egypt.

The effects of dams on rivers can have consequences both upstream and downstream as the natural flow and drainage of the land are altered. These changes in sedimentation can lead to alterations in plant life and animal life and how they are distributed. These disadvantages apply

for cellular cofferdam as well, but as said before they have less impacts on environment based on their smaller constructions and footprints.

4.3 Hydropower Cellular Cofferdam Construction Procedure

In order to assess the cost of cellular dam construction, the steps in its construction need to be delineated and analyzed. There are several design issues during construction and implementation of proposed design concept #1 of hydropower cellular cofferdams that were explained in chapter 2. All of these studies showed that safety is a paramount concern during construction, since workers will be exposed to the hazard of flooding and collapse. Safety requires: good design, proper construction, verification that the structure is being constructed as planned, monitoring the behavior of the cofferdam and surrounding area, provision of adequate access, light and ventilation, and attention to safe practices on the part of all workers and supervisors (Nemati, 2005). All of above requirements should be taken into consideration to avoid the additional costs during construction and operation of the hydropower cellular cofferdams. Figure 4.9 shows the Austin dam failure that killed several dozen people in 1911. Poor design of dam caused the failure during construction of Austin dam. The destruction of the dam drained the Lake McDonald reservoir and left the city of Austin without electrical power for a number of months (Rose, 2013).



Figure 4.9. Austin Dam failure in Texas, 1911.

Reduction of economic and environmental impacts of proposed design concept #1 emphasizes that the cellular cofferdams can be adapted for more permanent use as hydropower

dams. Knowing the construction procedure of the proposed design concept #1 which is listed below is essential to analyze the economic gains/losses of hydropower cellular cofferdams.

4.3.1 Pre-Dredging

The first step in construction of cellular cofferdams is to pre-dredge the dam foundation in order to prepare requirements for in-water construction. Pre-dredging is necessary to remove soil or soft sediments from the base of cofferdam and level the area of construction.

Once the project starts, one or more specialized dredgers should be assigned to the cofferdam. The number of dredgers depends on size of the cofferdam, degree and cohesiveness of silt present, time set for operational results, and budget of the client. Operational planning and set-up is relatively quick, as is the effect on dam storage levels. There are several variables that determine the dredging cost of a dam foundation. The most important ones are the amount and the nature of the material that should be dredged (Mohan, 2016).

4.3.2 Cell Template

Pre-constructed templates are used to ensure accurate positioning of interlocking steel sheet-piles, which are driven into the foundation to form individual cells. To reduce construction time and cost, multiple reusable templates are assembled to enable simultaneous construction of several cells across the river. The interlocking steel sheet piles and templates are arranged in cellular configurations including circular or diaphragm shapes (Figure 4.10), and are supported by wales, and internal and cross braces.

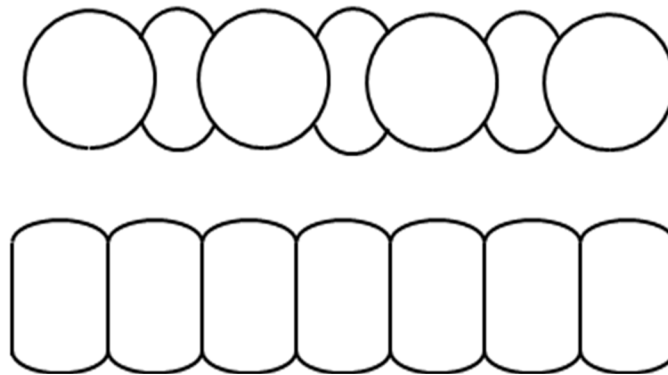


Figure 4.10. Plan views of cofferdam structures formed with circular cells (Top), and diaphragm cells (Bottom).

The cell template should be positioned within about 150 to 300 mm of alignment for circular cells. Closer tolerance is not usually possible and necessary as it may results in cell distortion during filling.

4.3.3 Sheet Pile Driving

The typical cofferdam consists of sheet piles set around a bracing frame and driven into the soil sufficiently far to develop vertical and lateral support and to cut off the flow of soil and, in some cases the flow of water (Bowles, 1996).

Sheet piling is a manufactured construction product with a mechanical connection “interlock” that forms a continuous wall of sheeting. Sheet pile applications are typically designed to create a rigid cell, while resisting the lateral pressures of bending forces. In addition, the sheet pile which is driven into the soil has numerous mechanical properties that can affect the performance (Nemati, 2005). The properties used for the steel sheet pile, which is modeled as a beam, were given in Table 2.2. Figure 4.11 shows the installation of wale and strut system for cell template and driving the sheet piles for cellular cofferdam.



Figure 4.11. Installation of wale and strut system and driving the sheet piles (Nemati, 2005).

During driving sheet piles, the base of each cell should be excavated down to the desired level to allow for placement of tremie concrete that will form the foundation of the cell to prevent seepage from underneath the base. When founded on soft soils, the sheet piles making up the cells

are embedded deep into the foundation to provide stability and reduce seepage. The final result is a massive, stable, self-standing and efficient structure of multiple interacting cells spanning the width of the river. The cost of driving sheet pile during construction depends on the number of cells and sheet piles that are required to construct the cellular cofferdam.

4.3.4 Concrete Seal

As explained in Chapter 2 and 3, dry construction can be achieved by adding a waterproof seal inside the cell, at the bottom of the cell, and on the top of the cell to encapsulate the cellular fill material.

The structure inside cellular cofferdams may be founded directly on rock or soil or may require pile foundations. These generally extend well below the cofferdam. Inside excavation is usually done using clam shell buckets. In order to dewater the cofferdam, the bottom must be stable and able to resist hydrostatic uplift (Nemati, 2005). Placement of an underwater concrete seal course is the fastest and most common affordable method. An underwater concrete seal course should then be placed prior to dewatering in order to seal off the water, resist its pressure, and also to act as a slab to brace against the inward movement of the sheet piles in order to mobilize their resistance to uplift under the hydrostatic pressure (Gilbert, 2011).

The seal inside the cell will prevent seepage and keep the cellular soil fill dry. It should be noted that the liner is not supposed to provide structural support as its main purpose is to provide an impermeable barrier for the cofferdam cell. One potential seal material is concrete, which is highly impermeable. Once the concrete is poured into the cells, the cells are stable and self-sustaining.

Moreover, top of the cells should be covered with concrete or asphalt cap to keep the cell dry in the case that overtopping occurs. Figure 4.12 shows cap concrete placement of Kentucky cofferdam that was placed after filling the cells. Concrete cap keeps the cell and filling material dry when overtopping happens, so the cofferdam will be more stable against structural failure.



Figure 4.12. Kentucky River Lock and Dam (Gilbert, 2011).

4.3.5 Cell Filling and Berm

Steel sheet piling is one of the widely used method to construct cellular water retaining structures that are typically filled with granular fill. During cell filling, the sheet pile interlocks are loaded by hoop tensions as the cell fill pushes radially against the sheet piles.

There are three ways to fill the cells by the use of hydraulic dredging, conveyors and clamshell buckets. Hydraulic dredging does not work properly for circular cofferdams because a huge amount of water enters the sheet piling cells during filling, while the water level would reach to that outside of the cells. On the contrary, clamshell buckets and conveyor belts do not significantly raise cell water levels and generate less radial pressure. During hydraulic filling, the tensions resulting from the filling itself (i.e., clamshell-filled tension, if applicable), soil compaction (if applicable) and lateral loading need to be taken into account.

The best cell fill materials for circular cellular cofferdams should have the following specific characteristics: 1) have a large degree of permeability; 2) have a high angle of internal friction; 3) contain small amounts, preferably less than 5% by weight, of materials passing the # 200 (i.e., silt and clay), and 4) be resistant to scour which requires presence of some gravel (Bowles, 1996). As explained in chapter 2, the main material used in the construction of the

Kentucky cellular cofferdam is granular sand. Cell filling cost depends mostly on the volume of required cell fill, and filling equipment price.

4.3.6 Hydropower Generation

Once dams are built, hydroelectricity is cheap to produce. The cost of power production from hydropower can vary widely depending on project details, but usually fall into a range of US\$ 50 to 100/MWh. Upgrading existing hydropower plant projects offers further options for cost-effective increases in generation capacity. Hydropower generation by the top ten countries accounted for about two-thirds of the world's hydropower generation in 2008 (Tockner et al., 2014).

The components of hydroelectric power production is shown in figure 4.13. It is in the generator where the electricity is produced and the shaft of the water turbine rotates which produces alternating current in the coils of the generator. Hence, the rotation of the shaft of the turbine is crucial for the production of electricity. Thus, potential energy of water is converted into electricity in hydroelectricity power plants (Chen et al., 2015).

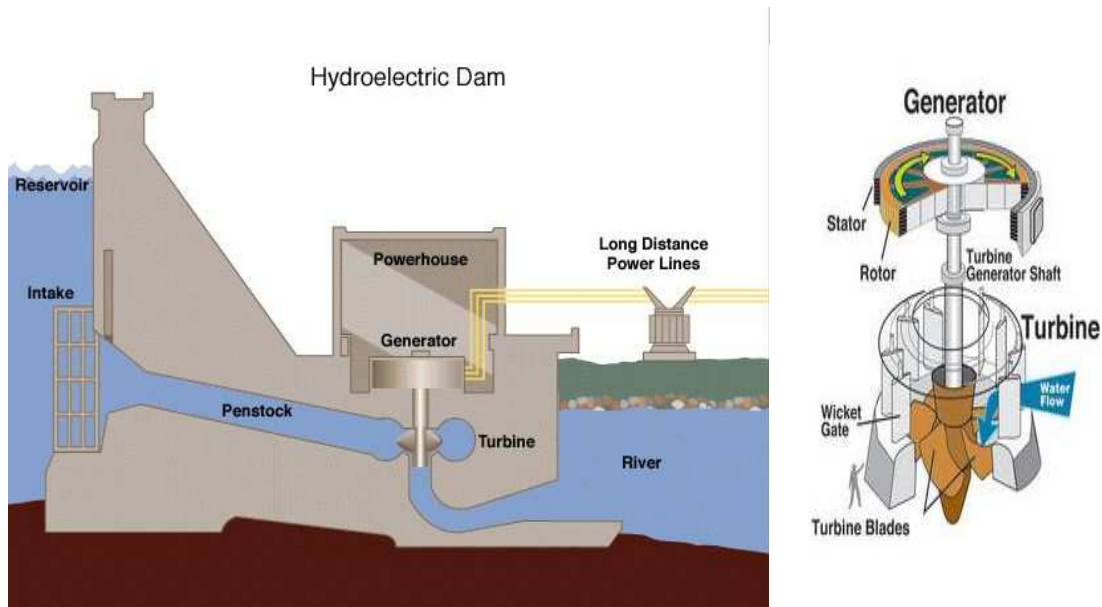


Figure 4.13. Components of Hydroelectric Power Plant (Irena, 2012).

Hydropower construction cost depends on the size of hydropower generation which are divided into Large, Medium, Small, Mini, Micro, and Pico. These different sizes range from 5 Kilowatt to 100 Megawatt (Irena, 2012). Since the construction cost of hydropower generation is expected to be same for all dams, the cost analysis of hydropower production for cellular cofferdam is not considered in the next section. Moreover, it cannot be possible to make general conclusions about the impact and cost of building hydropower systems due to difference in river conditions (e.g., water head and flow rates).

4.4 Construction Cost Analysis

Construction site conditions of dams can strongly influence the extent and cost of civil engineering work. However, for the same projects, it is possible to obtain reasonable estimates of the potential cost savings and benefits of the proposed scheme in comparison to traditional dam constructions. The costing of the dam can go ahead, with estimates based on either costs for dams already constructed in the same locality or rates provided by local contractors and or government departments. For each case, the survey must be sufficiently accurate and detailed to enable comparative estimates to be made for various heights of dam.

The estimates shown in Table 4.1 are obtained in terms of unit cost of construction to enable applications of the estimated savings to different sizes of dam construction. The objective is to get approximate ballpark estimates of the ranges of cost savings possible if cellular cofferdams were to become more viable for long-term use. The approximate per unit costs of three different hydropower dams are based on the information and guidelines of Hill et al. (2014), U.S. Society of Dams (2012), United Nations (2011), Gilbert (2011), and dam construction companies. The earth dam and concrete dam cost approximations are based on the Brown Hill Creek Dam as reported in Hill et al. (2014) and the cellular cofferdam cost analysis is based on the Kentucky cellular cofferdam. Note that in Table 4.1, the filling materials are assumed to be granular sand for cellular cofferdam and gravel for earth and concrete dams. Also, the economic analysis of steel sheet piles is based on sheet pile number A31 that was selected for the proposed design concept #1 in chapter 2.

Table 4.1. Per unit cost analysis of different hydropower dams.

Description	Unit	Cellular Cofferdam	Earth Dam	Concrete Dam
Foundation Preparation	US\$/ft ²	0.45	7,061	7,061
Drainage	US\$/ft	--	15,845	15,845
Sheet Pile	US\$/Pile	43	--	--
Concrete (Tremie, seal, core wall or backfill)	US\$/ft ³	41	85	11.7
Filling Material	US\$/ft ³	0.36	0.42	0.42
Construction Cost	US\$/ft ²	7	18,581	16,252
Total	US\$	93.81	41,573.7	39,171.4

As can be seen in Table 4.1, there is a huge difference between the per unit cost of cellular cofferdam and the traditional hydropower dams. Again, the hydropower construction cost of dams is not considered in the table because it is assumed that hydropower production cost is same for all dams depending on the size of hydropower generation. It also should be noted that Table 4.1 just show the cost analysis of labor, earth preparation, construction, and materials of dams and thus exclude, client cost, maintenance cost, and risk allocation.

After estimating the unit cost of each parameter in construction procedures, it is time to calculate the approximate construction cost of these three dams with similar height and width of the dam structures. This calculation is required in order to compare various hydropower dam construction costs with the same unit volume of water behind the dams. The geometry and dimension shown in Table 2.3, are used for the total construction cost of Kentucky cellular cofferdam.

Obtaining an approximate cost of Kentucky Cellular Cofferdam construction requires estimating several properties such as foundation preparation cost, total number of sheet piles, and total volume of filling material and concrete seal. Table 4.2 demonstrates the total construction

costs of the cellular cofferdam, earth dam, and concrete dam with the same height and width as shown in Table 2.3.

Table 4.2. Detailed approximation construction costs of different hydropower dams with same height and width.

Description	Unit	Cellular Cofferdam	Earth Dam	Concrete Dam
Foundation Preparation	US\$	35,469	508,160	508,160
Drainage	US\$	--	741,000	741,000
Sheet Pile	US\$	283,649	--	--
Concrete	US\$	1,034,102	1,254,000	2,434,698
Filling Material	US\$	1,669,233.96	1,347,500	302,150
Construction Cost	US\$	546,245	5,496,240	4,296,200
Total	US\$	3,568,698.96	9,346,900	8,282,208

In Table 4.2, the foundation preparation of Kentucky cofferdam is calculated using the pre-dredge unit cost of cofferdam multiplied by the total area of the cells (A_{soil}). The total costs of filling material and concrete construction for Kentucky cellular cofferdam are also estimated using the required volume of cell fill and concrete structure multiplied by the unit costs shown in table 4.1.

In order to find the total sheet piles price, the total number of piles for the Kentucky cellular cofferdam is determined using below equation:

$$N_s \times N = 226 \times 29 = 6554 \quad (4.1)$$

where N_s is the number of piles for each cell as shown in Table 2.4 and N is the total number of cells used in construction of Kentucky cellular cofferdam as shown in Table 2.3.

Since, the total number of sheet piles are estimated, the cost of sheet pile structures is determined using the per unit cost of steel sheet pile as shown in Table 4.1. The construction cost of Kentucky cofferdam is approximated based on the information provided in Gilbert (2011), and U.S. Society of Dams (2012). Construction costs of cellular cofferdam include barge(s) that will be used for placement of the cells, crane(s) to construct the cells, pile driving, underwater work for foundation preparation (pre-dredge), filling the cells with materials, tremie concreting, and labor.

The total construction costs of Brown Hill Creek Earth Dam and Concrete Dam for the same height and width are approximated using the detailed construction cost analysis listed in Hill et al. (2014).

As can be seen in Table 4.2, filling material price of Kentucky cellular cofferdam is expensive and costs more than 1.6 million dollars. If the local filling material can be used for construction of dam, the total construction cost of cofferdam will be around 2 million dollars. Also, using used sheet piles (instead of new ones) for cell construction can significantly reduce the construction cost.

CHAPTER 5

GENERAL CONCLUSION

5.1 Research Originality

The proposed work is a research study to develop engineering designs that extend the capabilities of cellular cofferdam construction to more permanent implementation as hydropower dams. Using sound engineering analysis, modeling and design practices, the study proposes and investigates new design to mitigate the shortcomings of cellular cofferdams and make them more suitable for hydropower use. In addition to developing enhanced configurations, a manual for the design and construction of more permanent cellular cofferdams for hydropower use is developed by improving current methodologies. Finally, the environmental and economic impacts of the proposed scheme is studied in relation to traditional hydropower dams.

Using cellular cofferdams, it is envisioned that hydropower dams can be rapidly built and deployed in a maximum of two years, conveniently replaced or modified when necessary, and decommissioned without difficulty after completion of their intended use. It is projected that hydropower dams based on cellular cofferdam design and construction will be versatile, and have less impact on the environment and will cost less to build than conventional hydropower dams.

The results of the project are of interest to: 1) Federal agencies (U.S. Army Corps of Engineers, Bureau of Reclamation, and the Tennessee Valley Authority) which own nearly half of the installed hydropower capacity in the U.S. The 176 plants owned by these federal agencies account for 49% of the hydropower generating capacity, 2) Publicly owned utilities, state agencies, and electric cooperatives which own an additional 24% of capacity, and 3) Construction and Civil Engineering companies who can pursue further development and marketing of the design concept #1 from the project.

5.2 Summary of Accomplishments

There are different procedures available, which have been in practice, and these all are used with due diligence to check adequacy of the different proposed design concepts of Kentucky cellular cofferdam. A particular feature of the new design is the “wet construction” resulting from

the in-water construction of the cofferdam. The “wet construction” eventually allows for seepage to occur through the cellular fill material from upstream to downstream. Though this seepage is allowed for temporary use of cellular cofferdam due to cost savings and shorter construction times, the “wet construction” may not be suited for the use of cellular cofferdam for more permanent and more long-term use. In order to address the deficiencies of the “wet construction” method for cellular cofferdam, a new design concept called “dry construction” was proposed. This can be achieved by adding a waterproof seal inside the cell to encapsulate the cellular fill material. The seal will prevent seepage and keep the cellular soil fill dry.

In chapter two of this dissertation, the procedures for the design of cellular cofferdam are presented covering determination of cell geometries including the main and cells, and the connections. It also covers, determination of earth pressure distribution on the wall which determines maximum pile and interlock tensions, which, in turn, determines the required pile type and sectional properties as well as the types and properties of joints. Numerical modeling of Kentucky Cofferdam shows linear earth pressure distribution with depth. However, the earth pressure distribution may deviate from linear depending on the properties of the foundation, thus, it is essential to check for pile tensile capacity based on different appropriate earth pressure scenarios. Of the different methods to calculate earth pressure coefficients, the methods of Maitland and Schroeder (1979), and Wissmann et al. (1995) are recommended. The former accounts for soil-pile interface behavior, and the latter are based on extensive scale model testing. The linear distribution of earth pressure suggests that the depth of maximum earth pressure should be located one-third of the cell height from the mudline as suggested by Schroeder and Maitland (1979). As for the depth of pile fixity and required penetration, the Matlock and Rees (1969) procedure, which accounts for soil-structure interaction such, appear to be in better accord with numerical results. However, the Schroeder and Maitland (1979) should be used as well to check the depth of fixity. Because cellular cofferdam design eventually involves complicated soil-structure interaction that cannot be accurately captured by manual design procedures, numerical modeling such as that carried out for Kentucky Cofferdam is carried out to verify design concept #1 for Kentucky cofferdam.

This dissertation presents design procedures for the operation of cellular cofferdams for permanent hydropower use. To establish the design procedures, a review of the main design issues

for the operation of cellular cofferdams for permanent hydropower use is first conducted. New design procedures are developed or existing manual/analytical design procedures are adapted for cellular cofferdams for permanent hydropower use. Finally, the proposed design procedures are validated using results of computational model, and example calculations are provided for structural and geotechnical analysis and design of cellular cofferdams for permanent hydropower use as can be seen in Appendix B. The design procedures cover geotechnical aspects including stability due to sliding, overturning, bearing capacity failure and seepage induced failure. For designs that use downstream berm, stability of the berm slope is also considered. The main structural design issue is safety against failure of sheet piles forming the cofferdam walls. Geological hazards include extreme flooding leading to overtopping of the dam, and earthquakes. The design procedures are illustrated and validated using the Kentucky cofferdam to provide realistic conditions and parameters using data and information from a cofferdam that has already been designed and built. By showing the validity of the methodologies used in the study to an actual case, it can be argued that the methodology can be applied to other conditions and situations in the field. Validation of the manual/analytical design procedures shows good agreement with predicted design performance against computational modeling and analysis. Significant increases in factor of safety are obtained when seepage is prevented and the cellular fill material and the downstream berm are kept dry. At the same time, re-analysis of the Kentucky cofferdam showed the improved performance of the “dry construction” of cellular cofferdam, and thus, demonstrating that with the “dry construction” modification, cellular cofferdams can be potentially used as more permanent structures for hydropower use.

In terms of designing cellular cofferdam against flooding-induced overtopping, various solutions are proposed including the addition of emergency spillway. Stability analysis against earthquake failure of cofferdams is done based on the modified Mononobe-Okabe procedure. It shows how to use manual calculations of earth pressure forces and earth pressure coefficients to make the cellular cofferdam stable against earthquake hazards. In addition to validate analytical and numerical results, manual calculations of slope stability of the berm based on Improved Ordinary Method of Slices (IOMS) procedure are compared with good agreements with computational results of FS_{slope} . In addition, earth pressure and bending moment diagrams of steel sheet piles are plotted based on manual calculations and compared with those computational results.

The dissertation carefully delineates the environmental and economic benefits of cellular cofferdam construction for permanent hydropower use compared to conventional concrete and earth dam constructions. Hydropower dams are usually very expensive and complex structures that require major investments and several years to plan and construct. However, their construction causes changes in the environment including fragmentation of river, which prevents free movement of migrating organisms. Large dams also result in modification of flow, reduction in sediment transport, direct habitat alterations up and downstream the river, and decline in native freshwater biodiversity. The major environmental and economic impacts of the proposed scheme is expected to be less than those for traditional hydropower dam constructions. Reduced construction cost and environmental impact come from: the ability to construct in water avoiding the need to divert water flow during construction, the dam can be decommissioned more easily than conventional dams and while the main cofferdam structure remains in water, the ability to completely remove the dam from the site, shorter construction time and ease of removal, lower price of material, standard construction technologies and equipment, and smaller cofferdam base resulting in reduced permanent impacts. The design also comes with several major benefits in addition to hydropower generation in terms of water supply, flood control, recreation and aquaculture. All these advantages indicate that, with appropriate design, cellular cofferdams can have many positive advantages in terms of environmental and economic impacts.

In order to do the construction cost analysis, the construction procedures of cellular cofferdams are analyzed and explained step by step. Using different sources, construction costs for hydropower cellular cofferdams are estimated in chapter 4. Costs and construction steps reductions and increases in using cellular cofferdams for hydropower use are identified and listed together with estimates of the amounts of potential monetary and construction time gains in comparison to traditional hydropower dam constructions. The cost analysis proves that cellular cofferdams are cost-effective structures.

Next generation of hydropower dams should be more sustainable than traditional dams. The cellular cofferdams can be a massive, stable, self-standing and efficient structure of multiple interacting cells spanning the width of the river. With their versatility in terms of applicability to a wide range of conditions, cellular cofferdams have the potential to be adapted and used as the main component for the construction of future innovative hydropower dams.

REFERENCES

- Bowles, J.E. (1996), "Foundation Analysis and Design. Chapter 15: Cellular Cofferdams," New York: McGraw-Hill, pp. 828-866.
- Mahan, C.J. (2007), "Kentucky Dam Lock Addition: Upstream Cofferdam," Paducah, Kentucky <http://www.cjmahan.com/static/upstream.php>, Accessed October 10, 2016.
- Pile Buck (1990). *Cellular Cofferdams*. Jupiter, FL: Pile Buck, Inc.
- Iqbal, Q. (2009), "The Performance of Diaphragm Type Cellular Cofferdams," Ph.D. Thesis, University of Southampton, 142 pp.
- Mosher, R.L. (1992), "Three-Dimensional Finite Element Analysis of Sheet-Pile Cellular Cofferdams," US Army Corps of Engineers, Report No. ITL-9201, 464 pp.
- Meier, P., Blaszczyk, P., Harris, C. and Gilbert, K. (2010), "Project Development: From Concept to Construction: Steps to Developing a Hydro Project," Hydro World, April 2010, vol. 29, No. 3.
- Weinmann, T., Nyren, R. and Marr, W.A. (2015). "Exposure of Deep Foundations for the Kentucky Lock Addition Project," Proceedings of IFCEE 2015, March 17–21, 2015, San Antonio, Texas.
- Bittner, R. and Kirk, N. (2014), "Cofferdam Solution for Steeply Sloping Rock Using Flat-Sheet Piles," Proceedings of the 39th Annual Conference on Deep Foundations, October 21-24, 2014, Atlanta, GA.
- Tennessee Valley Authority (1957), "Steel Sheet Piling Cellular Cofferdam on Rock," TVA Technical Monograph No. 75, vol. 1, pp. 61-69.
- Terzaghi, K. (1945), "Stability and Stiffness of Cellular Cofferdams," Transactions of the American Society of Civil Engineers, vol. 110, no. 1, pp. 1083-1119
- Sheppard, J. (2010), "St Germans Pumping Station Lifts Storm Water and Land Drainage to the River Ouse," Wastewater Treatment and Sewerage, pp. 79-81.
- Cummins, E.M. (1957), "Cellular Cofferdams and Docks," Journal of Waterways and Harbors Division, ASCE, vol. 83, no. WW3, pp. 13-45.
- Hansen, J.B. (1953). *Earth Pressure Calculations*, Danish Technical Press, Institution of Danish Civil Engineers, Copenhagen.
- ITASCA (2016), "FLAC: Fast Lagrangian Analysis of Continua," Itasca Consulting Co., Minneapolis, MN.
- Matlock, H. and Reese, L. (1969), "Moment and Deflection Coefficients for Long Piles," Handbook of Ocean and Underwater Engineering, J.J. Myers, C.H. Holm and R.F. McAllister (eds.), McGraw-Hill, New York.
- Schroeder, W.I. and Maitland, J.K. (1979). "Model Study of Circular Sheetpile Cell," Journal of Geotechnical Engineering Division, ASCE, vol. 105, no. GT7, pp. 805-821.
- Swatek, E.P. Jr. (1967), "Cellular Cofferdam Design and Practice," Journal of the Waterways and Harbors Division, 1967, Vol. 93, Issue 3, pp. 109-132.

- Wissmann, K., Filz, G., Mosher, R. and Martin, J.R. (2003), "Sheet Pile Tension in Cellular Structures," *Journal of Geotechnical Geoenvironmental Engineering*, ASCE, vol. 129 no. 3, pp. 224-233.
- Coetzee, M.J., Hart, R.D., Varona, P.M., and Cundall, P.A. (1998), "FLAC Basics," Minneapolis, MN. pp 1-5.
- Changnon, S.A., 2005: Economic impacts of climate conditions in the United States: past, present, and future – an editorial essay. *Climatic Change*, 68, 1- 9.
- Schlenker, W., W.M. Hanemann and A.C. Fisher, 2005: Will U.S. agriculture really benefit from global warming? Accounting for irrigation in the hedonic approach. *Am. Econ. Rev.*, 95, 395-406
- Young, R.A., 2005: Determining the Economic Value of Water: Concepts and Methods. Resources for the Future Press, Washington, District of Columbia, 300 pp.
- Duncan, J.M., Horz, R.C. and Yang, T.L. (1987). "Shear Strength Correlations for Geotechnical Engineering." Center for Geotechnical Practice and Research.
- Virginia Department of Transportation (2013). "Geotechnical Design Parameters for Retaining Walls, Sound Barrier Walls and Non-Critical Slopes." Staunton Materials Section, VDOT Staunton District.
- U.S. Army Corps of Engineers (1989). "Design of Sheet Pile Cellular Structures Cofferdams and Retaining Structures," Engineering Manual EM 1110-2-2503, US Army, Washington D.C.
- Ciammaichella, M. and Tantalla, J. (2014), "Temporary Cellular Cofferdam Design, Installation and Removal at Willow Island Hydroelectric Project," In *Proceedings of HydroVision 2014*, Nashville, TN, pp 2-7.
- Costa, J. E. (1985). *Floods from dam failures* (Open-File Report 85-560). Denver, CO: U.S. Geological Survey.
- Foster, M., Fell, R., & Spannagle, M. (2000). The statistics of embankment dam failures and accidents. *Canadian Geotechnical Journal*, 37(5), 1000–1024.
- Jandora, J., & Říha, J. (2008). *The failure of embankment dams due to overtopping*. Brno, Czech Republic: Brno University of Technology.
- USBR. (2012). Flood overtopping failure of dams and levees. Retrieved May 20, 2017, from <https://www.usbr.gov/ssle/damsafety/risk/methodology.html>.
- Martin II, J., & Clough, G. (1990). *A study of the effect of differential loadings on cofferdams* (Technical Report ITL-90-1). Vicksburg, MS: USAE Waterways Experiment Station.
- Larese, A., Rossi, R., & Nate, E. O. (2009). Analysis of stability of earth dams in overtopping scenarios with the particle. In *Particles 2009: International Conference on Particle-Based Methods* (pp. 1–4). Barcelona, Spain: European Community on Computational Methods in Applied Sciences.
- Acharya, K. P., Bhandary, N. P., Dahal, R. K., & Yatabe, R. (2016). Seepage and slope stability modelling of rainfall-induced slope failures in topographic hollows. *Geomatics, Natural Hazards and Risk*, 7(2), 721–746.

- Wu, C., & Xia, Y. (2014). Seepage response and stability variation during a rainfall in soil landslide. *Electronic Journal of Geotechnical Engineering*, 19, 17885–17893.
- Yazdani, M., Azad, A., Farshi, A., H., & Talatahari, S. (2013). Extended “Mononobe-Okabe” Method for Seismic Design of Retaining Walls. *Journal of Applied Mathematics*, 10, from <http://dx.doi.org/10.1155/2013/136132>.
- Iqbal, Q. (2009). “The Performance of Diaphragm Type Cellular Cofferdams,” University of Southampton, School of Civil Engineering and the Environment, Ph.D. Thesis, pp 136-138.
- Kramer, S. L. (1996). *Geotechnical Earthquake Engineering*. New York, USA: Prentice-Hall.
- Mononobe, N., & Matsuo, H. (1929). On the determination of earth pressures during earthquakes. In *World Engineering Congress* (p.9). Tokyo, Japan.
- Okabe, S. (1926). General theory of earth pressures. *Journal of the Japan Society of Civil Engineering*, 12(1).
- Itasca. (2011a). *Fast lagrangian analysis of continua: FISH in FLAC*. Minneapolis, MN: Itasca Consulting Group.
- Itasca. (2011b). *Fast lagrangian analysis of continua (version 7.00): User’s guide*. Minneapolis, MN: Itasca Consulting Group.
- Clough, G.W., and Hansen, L.A. (1977), A Finite Element Study of the Behavior of the Willow Island Cofferdam. Technical Report No. CE-218, Department of Civil Engineering, Stanford University, Stansfield. C.A.
- KDNG. (2007). Damming the Irrawaddy. Retrieved from <http://burmacampaign.org.uk/media/DammingtheIrr.pdf>
- Baba, K., & Hirose, T. (1998). Environmental Impact Assessment for Dams and Reservoir. *Encyclopedia of Life Support Systems (EOLSS)*. Retrieved from <http://www.eolss.net/Sample-Chapters/C07/E2-12-02-01.pdf>
- Bulletin, T. (2011). Dam Decommissioning and Removal, (August).
- Gilbert, D. A. (2011). Kentucky River Lock and Dam Projects, (1).
- Gui, M. W., & Han, K. K. (2009). An investigation on a failed double-wall cofferdam during construction. *Engineering Failure Analysis*, 16(1), 421–432. <https://doi.org/10.1016/j.engfailanal.2008.06.004>
- Jansen, R. B. (1983). Dams and Public Safety: A Water Resources Technical Publication, 332.
- Kundzewicz, Z. W., Mata, L. J., Arnell, N. W., Döll, P., Kabat, B., Jimenez, B., ... Editors, R. (2007). Freshwater resources and their management. *World Water*, 173–210. <https://doi.org/10.1017/CBO9781107415324.004>
- States, U., & Accountability, G. (2017). ARMY CORPS OF Factors Contributing to Cost Increases and Schedule Delays in the Olmsted Locks and Dam Project, (February).
- Texas, S. O. (2009). Design and Construction Guidelines for Dams in Texas. *Program*, (August).
- Schneider, Keith (August 18, 2014). "On Books Since 1988, Ohio River Dam Project Keeps Rolling Along". The New York Times. Retrieved December 30, 2016.

- Warrick, J. A., Bountry, J. A., East, A. E., Magirl, C. S., Randle, T. J., Gelfenbaum, G., ... Duda, J. J. (2015). Large-scale dam removal on the Elwha River, Washington, USA: Source-to-sink sediment budget and synthesis. *Geomorphology*, 246, 729–750. <https://doi.org/10.1016/j.geomorph.2015.01.010>
- Tockner, K., Zarfl, C., Alex, E., Berlekamp, J., & Tydecks, L. (2014). Future boom in hydropower dam construction will change the global map (Slides). *17th International Riversymposium : Excellence-Collaboration-Integration. Canberra, Australia, 15-18 September 2014*, 1–8.
- Nemati, K. (2005). Cofferdams. *Advanced Topics in Civil Engineering*, 1–15.
- Rose, A. T. (2013). Using the 1911 Austin Dam Failure Case History in Undergraduate Teaching.
- Mohan, Ram, et al. "Review of environmental dredging in North America: current practice and lessons learned." *Journal of Dredging* 15.2 (2016): 29.
- IRENA. (2012). Hydropower. *Renewable Energy Technologies: Cost Analysis Series, 1: Power s(3/5)*, 44. https://doi.org/10.1007/978-3-319-08512-8_7
- Chen, S., Chen, B., & Fath, B. D. (2015). Assessing the cumulative environmental impact of hydropower construction on river systems based on energy network model. *Renewable and Sustainable Energy Reviews*, 42(19), 78–92. <https://doi.org/10.1016/j.rser.2014.10.017>
- WEDA. (2016). WEDA Journal of Dredging, Vol. 15, No. 2. *Journal of Dredging*, 15(2). Retrieved from [https://www.westerndredging.org/phocadownload/WEDA Journal Vol 15 No 2.pdf#page=31](https://www.westerndredging.org/phocadownload/WEDA%20Journal%20Vol%2015%20No%202.pdf#page=31)
- "Factors Contributing to Cost Increases and Schedule Delays in the Olmsted Locks and Dam Project". Government Accountability Office. February 2017.
- Hill, B., Creek, K., & Management, S. (2014). Appendix 15 Estimated costs of dams, (September).
- United States Society on Dams. (2012). *Guidelines for Construction Cost Estimating for Dam Engineers and Owners*.
- United Nations. (2011). Dam Construction Alternatives. Retrieved from http://www.amppartners.org/docs/default-source/brochures/hydro_brochure.pdf?sfvrsn=2
- Leps, T. M. (1970). Review of shearing strength of rockfill. *Journal of the Soil Mechanics and Foundation Division, SM 4*, 7394–1170.
- Chinkulkijniwat, A., Yubonchit, S., Horpibulsuk, S., Jothityangkoon, C., Jeeptaku, C., & Arulrajah, A. (2016). Hydrological responses and stability analysis of shallow slopes with cohesionless soil subjected to continuous rainfall. *Canadian Geotechnical Journal*, 53(12), 2001–2013.
- Marold, W.J. (2012). "Construction of a 100-Foot Deep Cofferdam in the Ohio River," In 32nd Annual USSD Conference, New Orleans, Louisiana, pp. 1129–1144.
- Pile Buck (1990), "Sheet Pile Design. Chapter 2: Structural Design of Sheet Pile Walls," <http://www.pilebuck.com/sheet-pile-design-manual/chapter-2-structural-design-sheet-pile-walls/>, Accessed September 30, 2016.

Yao, S.X., Berner, D.E. and Gerwick, B.C. (1999). Assessment of Underwater Concrete Technologies for In-the-Wet Construction of Navigation Structures. Tech. no. INP-SL-1. Washington, DC: U.S. Army Corps of Engineers, 1999.

Sheppard, J. (2010), "St Germans Pumping Station Lifts Storm Water and Land Drainage to the River Ouse," Wastewater Treatment and Sewerage, pp. 79-81.

APPENDIX A

BASIC EQUATIONS USED IN THE MANUAL STABILITY CALCULATION OF CELLULAR COFFERDAM

The Appendix includes the manual stability calculations against sliding, overturning, cell shear, cell bursting, and bearing capacity failure. Figure A.1 shows the corresponding type of failures along with terminology used in the calculation as summarized from Bowles (1996), and Rossow and Mosher (1992). Figure A.2 shows cell pressure profiles for stability analysis against cell shear.

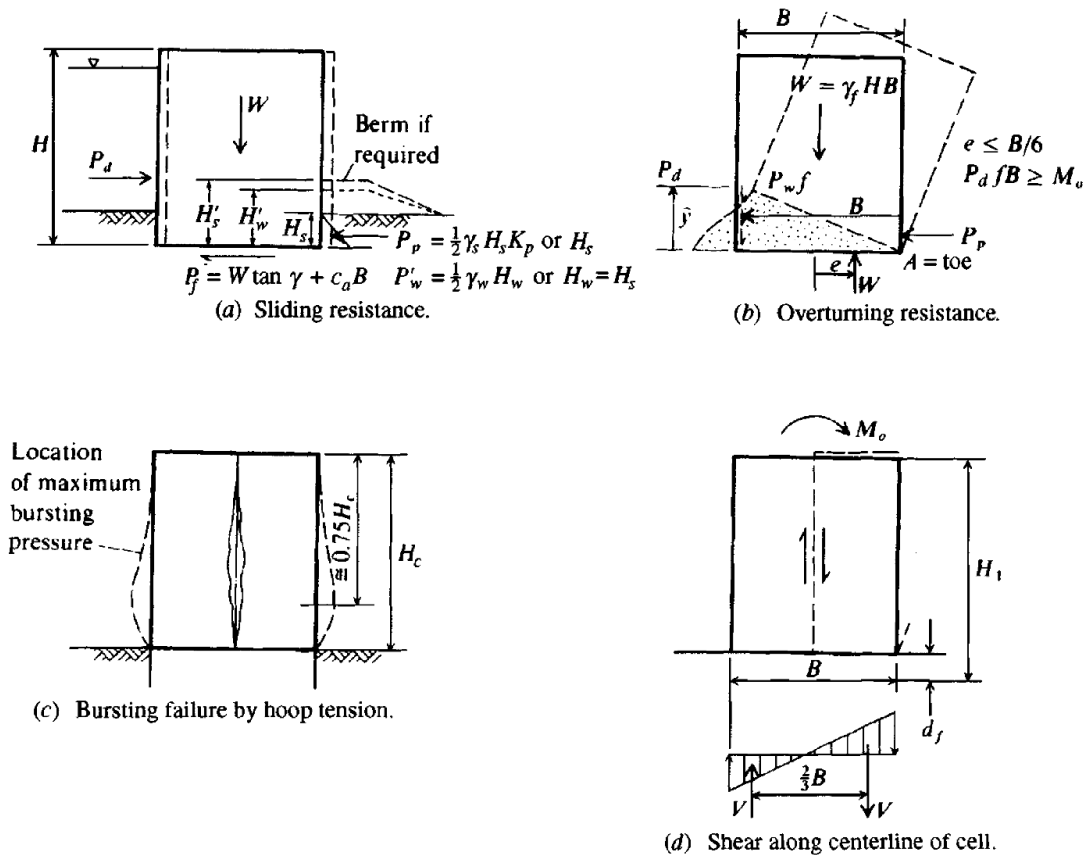


Figure A.1. Type of cofferdam failures for stability analysis (Bowles, 1996).

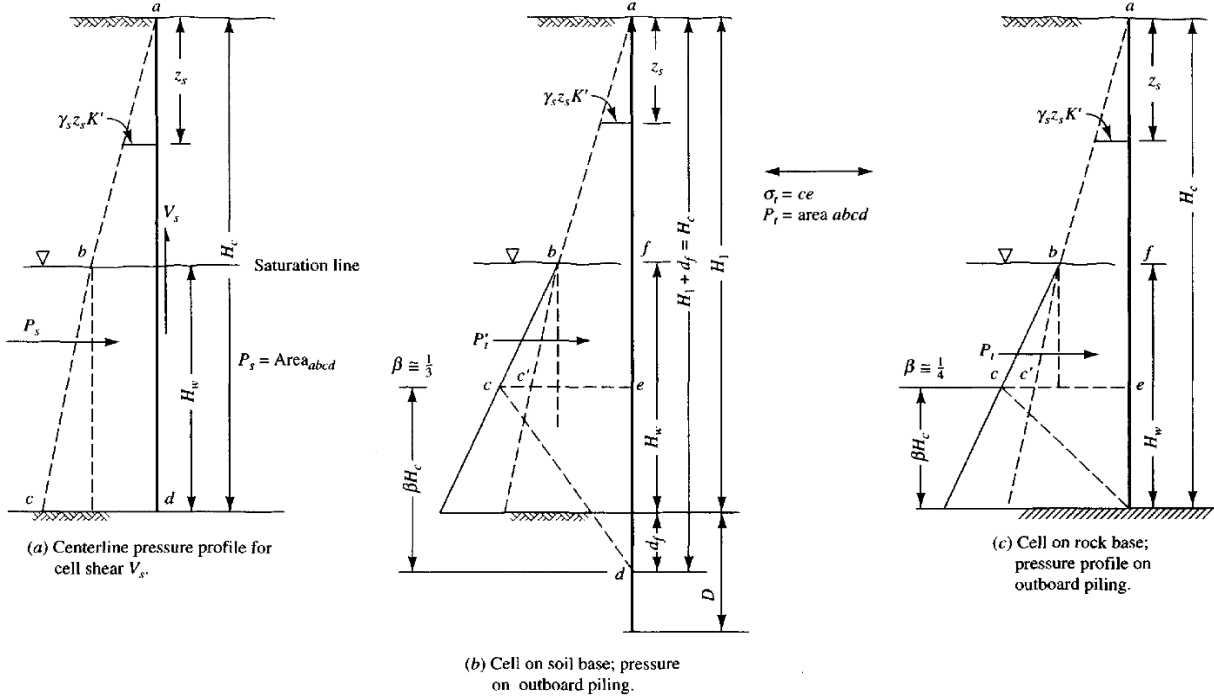


Figure A.2. Cell pressure profiles for stability analysis against cell shear (Bowles, 1996).

- **Stability against sliding**

$$FS_{sliding} = \frac{P_p + P_f + P'_w}{P_d} \quad (A.1)$$

where P_f is the friction on the base as $W \tan \delta + c_0 B$, P_d is the driving force (usually outside water with $P_w = 0.5 \gamma_w H_w^2$), and P_p is the passive resistance ($0.5 \gamma'_s H_s^2 K_p$) but may include a berm.

- **Stability against overturning**

The resultant weight W must lie within the middle one-third of the base which gives:

$$e = \frac{P_d \bar{y}}{\gamma H B} = \frac{P_d \bar{y}}{W} \quad (A.2)$$

$$FS_{overturning} = \frac{B \tan \delta}{y} \quad (A.3)$$

- **Stability against cell shear**

$$FS_{cell\ shear} = \frac{P_s \tan \delta + P_t f_i}{1.5 M_o / B} \quad (A.4)$$

- **Stability against cell bursting**

$$FS_{cell\ bursting} = \frac{t_u C_1}{q_t r} \quad (A.5)$$

where q_t is the pressure intensity, C_1 is the constant, and t_u is the ultimate interlock value.

- **Stability against bearing capacity failure**

$$FS_{bearing\ capacity} = \frac{q_{ult}}{q} = \frac{\bar{q}N_q d_q i_q + \frac{1}{2} \gamma' BN_{\gamma} i_{\gamma}}{q} \quad (A.6)$$

APPENDIX B

MANUAL STABILITY CALCULATIONS BASED ON BOWLES, J.E. (1996)

With using the equations in Appendix A, Factors of Safety against different failures are determined in Appendix B.

Properties	Symbol	Value	Unit
Unit weight of water	γ_w	9.8	kN/m ³
Active earth-pressure coefficient for water	K_a	1.0	
Interlock friction	f_i	0.3	
Base soil			
Saturated unit weight	γ_{sat}	19.2	kN/m ³
Friction angle	ϕ	34.0	deg
Overburden (upstream side)			
Height towards cell heel	H	4.0	m
Friction angle	ϕ	34.0	deg
Rankine active earth-pressure coefficient	K_a	0.3	
Effective unit weight	γ'	9.4	kN/m ³
Berm (Downstream side)			
Height towards cell heel	H	4.0	m
Height below water		3.0	m
Friction angle	ϕ	34.0	deg
Rankine passive earth-pressure coefficient	K_p	3.5	
Effective unit weight	γ'	9.4	kN/m ³
Cell			
Height above saturation line		10.0	m
Height between saturation line and DL		8.5	m

Embedment depth	H_s	4.0	m
Cell height	H_c	22.5	m
Cell width	B	27.3	m
Fill material			
Dry unit weight	γ_s	17.0	kN/m ³
Effective unit weight	γ'	9.0	kN/m ³
Friction angle	ϕ	32.0	deg
Friction angle between fill and sheet pile at upstream side	δ	32.0	deg
Rankine active earth-pressure coefficient	K_a	0.3	
Stability against cell sliding			
Driving force (upstream side)			
Water force	P_w	2482.4	kN/m
Active earth pressure	P_a	21.3	kN/m
	y_w	7.5	m
	y_a	1.3	m
Resisting force (downstream side)			
Water force	P'_w	44.1	kN/m
Passive earth pressure	P_p	265.7	kN/m
	y'_w	1.0	m
	y_p	1.3	m
Net force			
	P_{net}	2193.8	kN/m
Weight of a unit width slice x B	W	7755.2	kN/m
Resisting force	P_r	5230.9	kN/m
Driving force	P_d	2193.8	kN/m
Factor of safety against sliding	$FS_{sliding}$	2.38	

Stability against cell overturning			
Driving moment (upstream side)			
Moment from water		18618.0	kN.m/m
Moment from overburden		28.4	kN.m/m
Resisting moment (downstream side)			
Moment from water		44.1	kN.m/m
Moment from overburden		354.2	kN.m/m
Net overturning moment about cell base at point O	M_o	18248.0	kN.m/m
Eccentricity within the middle one-third of the base	e	4.6	m
Resisting moment	$W.e$	35286.0	kN.m
Factor of safety against overturning	$FS_{\text{overturning}}$	1.93	
Stability against cell shear			
Earth pressure coefficient	K'	0.56	
		0.6	
Area of pressure profile for shear force	P_s	1572.1	kN/m
Area above saturation line		510.0	kN/m
Area between saturation line and DL		1062.1	kN/m
Soil shear resistance	V_s	982.3	kN/m
Area of pressure profile for lateral force	P'_t	906.8	kN/m
Lateral earth pressure	P_a	69.8	kN/m
Depth of fixity	d_f	2.3	m
Total effective pile depth	H_1	20.8	m
Location of the maximum stress		6.9	m
Height of area between saturation line and maximum stress		3.9	
Pressure intensity	q_t	101.1	kN/m
Area above saturation line		261.0	kN/m

Area between saturation line and maximum stress		295.6	kN/m
Area within d_f		350.3	kN/m
Interlock resistance	R_{il}	272.0	kN/m
Total cell shear resistance	V_r	1254.4	kN/m
Vertical shear force	V	1002.6	kN/m
Factor of safety against cell shear	$FS_{\text{cell shear}}$	1.25	
Stability against cell bursting			
Constant	C_1	1.0	
Radius of cell	r	15.6	m
Critical interlock tension	t_i	1577.6	kN/m
Ultimate interlock tension	t_u	2800.0	kN/m
Factor of safety against cell bursting	$FS_{\text{cell bursting}}$	1.77	
Stability against bearing capacity failure			
Coefficient N	N_q	29.4	
	N_γ	28.7	
Depth factor		0.3	
	H	2193.8	kN/m
	V	7755.2	kN/m
The base eccentricity	e	2.4	m
	B'	22.6	
	L	1.0	
	d_q	1.0	
	i_q	0.68	
	i_γ	0.46	
The ultimate bearing capacity (cohesionless soil)		783.4	
		62.3	

The ultimate bearing capacity (cohesionless soil)		845.7	
The actual bearing pressure		284.1	
Factor of safety against bearing capacity failure	$FS_{bearing}$	2.98	